



Kingdom of Saudi Arabia
Ministry of Education
Jazan University



JAZAN UNIVERSITY

JOURNAL OF
JAZAN UNIVERSITY
For
Applied Sciences

A Refereed Scientific Periodical

ISSN:1658-6913

Supplement To Vol. 11 No 2 November 2023 (Jumada al-Awwal)



Kingdom of Saudi Arabia

Publication Rules Education

Jazan University

The University of Jazan provides an opportunity for scholars to publish their scholarly work on research. The editorial board will consider manuscripts from all fields of knowledge. Manuscripts submitted in either Arabic or English, and if the due accepted for publication, may not be published elsewhere, without permission of the Editor-in-Chief. The journal issues one volume per year. The types of manuscript classification used by the Editorial Board run as follows:

1. Article:

An author's original work contributing new knowledge to the field in which research was conducted.

2. Review Article:

A critical synthesis of the current literature in a particular field, or a synthesis of the literature in a particular field during an explicit period of time.

3. Brief Article:

A short article (note) with the characteristics of an article.

4. Book Reviews

5. Forum:

Letters to the editor, comments, responses, preliminary results or findings, and miscellany

General Instructions for

1. Submission of manuscripts:

Original manuscripts should be typewritten (one side only), using an A4 size paper, double spaced along with 3 copies. All pages are to be numbered consecutively, including tables and graphs. Tables, other illustrations, and references should be presented on separate sheets with their proper text position indicated.

2. Abstracts:

Manuscripts for articles, review articles, and brief articles require both Arabic and English abstracts, using no more than 200 words, in single column (13cm wide), for each version.

3. Tables and other illustrations:

Tables, charts, figures, and plates should fit the journal's page size (12.5 cm x 18cm). All inner drawings must be presented on high quality. Tracing paper is necessary, using black Indian ink as well. Photographs may be submitted, but on glossy print paper in either black or color.

4. Abbreviations and Units:

A4 sizes and quantities should be expressed according to international standards. Standardized abbreviation should only be used. The names of periodicals should be abbreviated in accordance with the words of scientific periodicals.

5. Title Page:

Should contain the title, name of the authors, name and address of the institution, where the work was carried out. The title should be brief and use strong keywords. Scientific names of organism should be clearly stated and should be typed italic.

6. Text:

The organization of the manuscript should be as follows: Introduction, materials, results, discussion, and references. Results and discussions can be combined in one section. Acknowledgement (if needed) should be brief and added before the reference sections.

A Refereed Scientific Periodical

1. References:

Citation of the references (within the text) should be indicated by author. Date, style, and references should be listed in an alphabetical order and conform to the following examples: Periodical citations in the text are to be enclosed in one line brackets, e.g.(6).

Periodical references are to be presented in the following form:

References number in line brackets (), author's name followed by a given name and/or initials, the title of an article or periodical (italicized), volume number, year of publication (in parentheses) and pages e.g.

Basahy, A.Y. (1992). Protein and Amino Acid contents in seeds of some soybean cultivate (Glycin Max 1) Arab Gulf J. Sci. Res. 11(2), 221-228.

Book Citation:

Book references should include the following:

Reference number (), author's surname followed by a given name and/or title of the book (italicized), place of publication, publisher, and year of publication.

Example:

Lehman. H.C. (1953). Age and Achievement. Princeton: Princeton University Press.

2. Content Notes:

Content notes are to be presented on separate sheets. They will be printed below

a solid line separating the content notes from the text.

9. The manuscripts and forum items submitted to the journal for publication contain the author's conclusions and opinions, and if published they do no bear a conclusion or opinion of the Editorial Board.

10. Authors will be provided with 20 reprints free of charge, along with two issues of the journal. Additional copies could be purchased, if ordered when the proofs are returned. Price will be shown on the order form.

11. It is the responsibility of the researcher to make sure that the manuscript is free of linguistic, grammatical and typo errors.

12. The editors' board has the right to set priorities of publishing the research.

13. The journal is not obligated to repeat the research it reaches, whether it was approved for publication or not.

14. All the received research is subject to primary examination by the editorial board in order to determine their eligibility for arbitration. The editorial board is entitled to excusing itself from accepting the research without giving reasons.

15. The journal is published twice a year.

Kingdom of Saudi Arabia
Ministry of Education
Jazan University

**JOURNAL OF
JAZAN UNIVERSITY**
For
Applied Sciences

A Refereed Scientific Periodical

Supplement To Vol. 11 No 2 November 2023 (Jumada al-Awwal)

ISSN:1658-6913

Journal Jazan University

for applied sciences

General Supervisor

Prof. Mari Hussain Al-Qahtani

Deputy General Supervisor

Prof. Mohammed Hassan Aburasain

Managing Editor

Mr. abdulrahman Hassan Hobani

Editor-in-chief

Prof. Ahmed abdulrahman Al-barraq

Editorial Board

Prof. Muhammad Ali Mubarak

Prof. Gasem Mohammad Abu-Taweel

Dr. Zaki Weli Hakami

Dr. Mohammed Abdulraheem Akeel

Dr. Basem Ibrahim Assiri

Dr. Nouf Hussain Abuhadi

Administrative and technical staff

Mr. Ahmad Mohammad Al-Hazmi

Mr. Ali Mohammad Qabi

Mr. Bandar Ali Wasli

Correspondence

All correspondence should be directed to:
Editor-in-chief of Jazan University Journal of Applied Sciences, Jazan - University City
Administrative Tower - PO Box 114 - Zip Code 4514, Kingdom of Saudi Arabia
jas@jazanu.edu.sa

(1445) Jazan University

All copyrights reserved. No part of the magazine may be reproduced or copied in any form or by any means

Electronic or mechanical, including photocopying, recording, or entering into any information storage or retrieval system without obtaining

On the written approval of the editor-in-chief of the magazine.



فهرس المحتويات

الموضوع

صفحة

- ٤-١ علي حافظ حكمي
The Uniform Distribution of Quasi-lattices in the Real Space R^2
Ali H. Hakami
- ٢٦-٥ عبدالرحمن أحمد الصايغ وآخرون
Assessment of dietary patterns among students at Jazan University, Saudi Arabia: A cross-sectional study
Abdulrahman A. Alsayegh and ather
- ٤٧-٢٧ عبده محمد جباري
Blockchain Empowered IoT Security Framework: Challenges and Opportunities
Abdoh Jabbari
- ٦٠-٤٨ عمرو شحاته محمد فايد
A review of the key energy-based criteria under mixed mode I-II loading for brittle materials
A. S. Fayed
- ٧١-٦١ وليد عبده زعقان
A hybrid ROA-KNN approach for botnet detection in IoT networks
Waleed Abdu Zogaan
- ٨٣-٧٢ أحلام علي الزهراني
A review on Plackett-Burman Design
Ahlam Ali Alzharani
- ٩٢-٨٤ أحمد محمد فتحي
Studying of Solar radiation components over Jazan the Kingdom of Saudi Arabia
A. M. Fathy

- تأثير تلوث التربة بالرصاص والكاديوم على نشأة عزلات بكتيرية مقاومة للعناصر الثقيلة في منطقة
جازان، المملكة العربية السعودية
أزهار يحيى النعمي و محمد نصر الليثي.....
١١١-٩٣
**Effect of Soil Pollution with Lead and Cadmium on the Development of
Heavy Metal-Tolerant Bacterial Isolates in Jazan Region, KSA**
Azhar Y. Al-Nuaimi and Mohamed N. Al-Leithy
- التعرف في الوقت الفعلي على مستخدمي النظام في البيئات المعقدة باستخدام التعلم الآلي
يحيى محمد القحطاني.....
١٢٨-١١٢
**Real-Time Identification of System Users in Complex Settings using
Machine Learning**
Yahya Muhammed Alqahtani
- تشخيص الانتباز البطاني الرحمي من ندبة قيصرية بواسطة الرنين المغناطيسي: تقرير حالة
ساره علي.....
١٤٠-١٢٩
**MRI Diagnosis of Endometriosis Fungating Out of a Caesarean Scar: A
Case Report**
Sara Ali
- انتشار الملاريا وفيروس تي اللفاوي البشري والزهري في المتبرعين بالدم من الأصحاء بمنطقة
جازان بالمملكة العربية السعودية خلال الفترة ٢٠١٩-٢٠٢٠
أيمن محمد مدخلي.....
١٥٢-١٤١
**Prevalence of malaria, human T lymphotropic virus, and syphilis in
healthy blood donors from Jazan region, Saudi Arabia during
2019-2020**
Aymen M Madkhali

The Uniform Distribution of Quasi-lattices in the Real Space \mathbb{R}^2

Ali H. Hakami¹

¹Department of Mathematics, Faculty of Science, Jazan University, Saudi Arabia

Abstract

In this small note we employ the *cut-and-project* technique to obtain the uniform distribution of quasi-lattices in the real space \mathbb{R}^2 .

AMS Subject Classification: Primary 37B50, 05B25, 06B25, 05B07, 03G10 .

Keywords: Quasi-lattice; lattice, cut-and-project; uniformly distribution.

1. Introduction and main result

In this paper we interested to see how the quasi-lattice are uniformly distributed in \mathbb{R}^2 using the method of *cut-and-project* . For history and explanation of this method, see refences Hof [7] (a proof using Weyl equidistribution on the torus \mathbb{T}^n) and the work of Marklof and Strömbergsson [10, Prop.3.2]. Also see de Bruijn [2], [3] who developed the cut-and-project technique for creating icosahedral Penrose tilings and other tilings with symmetry.

Our main result is

Theorem 1. *Let ψ_1, ψ_2 be the coordinate projections from \mathbb{R}^2 to \mathbb{R} , i.e. $\psi_j((v_1, v_2)) = v_j$, and let $\beta^{(1)}, \beta^{(2)} \in \mathbb{R}^2$ be a basis of \mathbb{R}^2 such that the two real numbers $\psi_2(\beta^{(1)}), \psi_2(\beta^{(2)})$ are linearly independent over \mathbb{Q} . Let $\mathcal{L} \subseteq \mathbb{R}^2$ be the lattice spanned by $\beta^{(1)}, \beta^{(2)}$, i.e.*

$$\begin{aligned} \mathcal{L} &= \mathbb{Z}\beta^{(1)} + \mathbb{Z}\beta^{(2)} \\ &= \{j_1\beta^{(1)} + j_2\beta^{(2)} : j_1, j_2 \in \mathbb{Z}\}. \end{aligned}$$

Then for any fixed bounded open interval $\mathcal{J} \subset \mathbb{R}$,

$$\begin{aligned} \lim_{T \rightarrow \infty} \frac{1}{2T} \#([[-T, T] \times \mathcal{J}) \cap \mathcal{L}) \\ = m(\mathcal{J}) \left| \det \begin{pmatrix} \beta_1^{(1)} & \beta_2^{(1)} \\ \beta_1^{(2)} & \beta_2^{(2)} \end{pmatrix} \right|, \end{aligned}$$

where $m(\mathcal{J}) :=$ Lebesgue measure of the interval \mathcal{J} .

We are going to allocate Section 2 to providing Theorem 1's proof. We make the assumption that the reader is familiar with some fundamental concepts in number theory (see, for example, books by Einsiedler and Ward [4] and Hardy and Wright [6], Niven and Zuckerman and Montgomery [12], and Stark [15]), ergodic theory, and analysis and measure theory (see books by Rudin[13,14] and G.B. Folland [5]). Simple information about Euclidean lattices, see [9, Section 2], and Lebesgue measure concepts are also required (see, for instance, Einsiedler and Ward [4]).

2. Proof of the main result

We shall give a direct proof this theorem.

Let us write $\mathcal{J} = (a, b)$. Then

$$\begin{aligned} \#([[-T, T] \times \mathcal{J}) \cap \mathcal{L}) &= \\ \sum_{j_1 \in \mathbb{Z}} \# \{j_2 \in \mathbb{Z} : j_1\beta^{(1)} + j_2\beta^{(2)} \in [-T, T] \times \\ &(a, b)\}. \quad (2.1) \end{aligned}$$

Given $j_1 \in \mathbb{Z}$, the line $j_1\beta^{(1)} + \mathbb{R}\beta^{(2)}$ intersects the line $v_2 = a$ at the point

$$j_1\beta^{(1)} + \frac{a - j_1\beta_1^{(2)}}{\beta_2^{(2)}}\beta^{(2)} = \left(\frac{j_1\Delta + a\beta_1^{(2)}}{\beta_2^{(2)}}, a \right),$$

where

$$\Delta := \det \begin{pmatrix} \beta_1^{(1)} & \beta_2^{(1)} \\ \beta_1^{(2)} & \beta_2^{(2)} \end{pmatrix} = \beta_1^{(1)} \beta_2^{(2)} - \beta_2^{(1)} \beta_1^{(2)}.$$

(Note here that $\beta_1^{(2)} \neq 0$, since $\beta_2^{(1)}$ and $\beta_2^{(2)}$ are linearly independent over \mathbb{Q} by assumption.)

This point belongs to the boundary of the rectangle $[-T, T] \times (a, b)$ if and only if

$$-T \left| \frac{\beta_2^{(2)}}{\Delta} \right| - \frac{a\beta_1^{(2)}}{\Delta} \leq j_1 \leq T \left| \frac{\beta_2^{(2)}}{\Delta} \right| - \frac{a\beta_1^{(2)}}{\Delta}.$$

Similarly the point where $j_1\beta^{(1)} + \mathbb{R}\beta^{(2)}$ intersects $v_2 = b$ belongs to $\partial[-T, T] \times (a, b)$ if and only if

$$-T \left| \frac{\beta_2^{(2)}}{\Delta} \right| - \frac{b\beta_1^{(2)}}{\Delta} \leq j_1 \leq T \left| \frac{\beta_2^{(2)}}{\Delta} \right| - \frac{b\beta_1^{(2)}}{\Delta}.$$

Hence, for any given $T > 0$, there exist integer $\kappa \leq \acute{\kappa}$ satisfying

$$\kappa = -T \left| \frac{\beta_2^{(2)}}{\Delta} \right| + O(1) \quad \text{and} \quad \acute{\kappa} = T \left| \frac{\beta_2^{(2)}}{\Delta} \right| + O(1), \quad (2.2)$$

such that line segment $(j_1\beta^{(1)} + \mathbb{R}\beta^{(2)}) \cap \{a < v_2 < b\}$ is contained in the rectangle $[-T, T] \times (a, b)$ exactly for the integers $j_1 \in \mathbb{Z} \cap [\kappa, \acute{\kappa})$, and furthermore there are at most $O(1)$ other integers j_1 for which $(j_1\beta^{(1)} + \mathbb{R}\beta^{(2)}) \cap \{a < v_2 < b\}$ is not disjoint from $[-T, T] \times (a, b)$. Hence we conclude that (2.1) is

$$O(1) + \sum_{j_1=\kappa}^{\acute{\kappa}-1} \#\{j_2 \in \mathbb{Z}: j_1\beta_2^{(1)} + j_2\beta_2^{(2)} \in (a, b)\} \quad (2.3)$$

Let us write

$$\lambda = (b - a) |\beta_2^{(2)}|^{-1} > 0 \quad \text{and} \quad r_j = (a - j\beta_2^{(1)}) |\beta_2^{(2)}|^{-1};$$

then for every $j_1 \in \mathbb{Z}$ we have

$$\begin{aligned} \#\{j_2 \in \mathbb{Z}: j_1\beta_2^{(1)} + j_2\beta_2^{(2)} \in (a, b)\} &= \#(\mathbb{Z} \cap (r_{j_1}, r_{j_1} + \lambda)) \\ &= \lfloor \lambda \rfloor + \#(\mathbb{Z} \cap (r_{j_1}, r_{j_1} + \lambda - \lfloor \lambda \rfloor)) \\ &= \lfloor \lambda \rfloor + \begin{cases} 1 & \text{if } \{r_{j_1}\} + \{\lambda\} > 1 \\ 0 & \text{otherwise,} \end{cases} \end{aligned}$$

where we write $\{v\} := v - \lfloor v \rfloor \in [0, 1)$, $\forall v \in \mathbb{R}$. Recalling the definition of r_j we see that $\{r_{j_1}\} + \{\lambda\} > 1$ holds if and only if $j_1\beta_2^{(1)} |\beta_2^{(2)}|^{-1}$ lies in $I = a |\beta_2^{(2)}|^{-1} + (0, \{\lambda\}) + \mathbb{Z}$. (Note that I is an open "interval" on the torus \mathbb{T}^1 , of length $\{\lambda\}$.) Hence we conclude that (2.3) is

$$= O(1) + (\acute{\kappa} - \kappa) \lfloor \lambda \rfloor + \sum_{j_1=\kappa}^{\acute{\kappa}-1} \#\{j_1 \frac{\beta_2^{(1)}}{\beta_2^{(2)}} \in I\}. \quad (2.4)$$

By assumption, $\beta_2^{(1)}v + \beta_2^{(2)}u \neq 0$ for all $\langle v, u \rangle \in \mathbb{Z}^2 \setminus \{(0, 0)\}$; thus $\beta_2^{(1)} |\beta_2^{(2)}|^{-1}$ is irrational. Hence by Weyl equidistribution,

$$\lim_{n \rightarrow +\infty} \frac{1}{N} \#\left\{j_1 \in \{1, \dots, N\}: j_1 \frac{\beta_2^{(1)}}{\beta_2^{(2)}} \in I\right\} \rightarrow \{\lambda\}.$$

(see Einsiedler and Ward [4], Theorem 4.10, Lemma 4.17). Similarly

$$\lim_{n \rightarrow +\infty} \frac{1}{N} \#\left\{j_1 \in \{0, -1, -2, \dots, 1 - N\}: j_1 \frac{\beta_2^{(1)}}{\beta_2^{(2)}} \in I\right\} \rightarrow \{\lambda\}.$$

Now recall (2.2), where in particular we note that $\kappa \rightarrow -\infty$ and $\acute{\kappa} \rightarrow \infty$ as $T \rightarrow \infty$. It follows that as $T \rightarrow \infty$ (2.4) is

$$\begin{aligned} &= O(1) + (\acute{\kappa} - \kappa) \lfloor \lambda \rfloor + (\acute{\kappa} - \kappa) (\{\lambda\} + o(1)) \\ &= O(1) + (\acute{\kappa} - \kappa) + (\lambda + o(1)) \end{aligned}$$

$$\begin{aligned}
&= O(1) + \left(2T \left| \frac{\beta_2^{(2)}}{\Delta} \right| + O(1) \right) (\lambda + o(1)) \\
&= 2T \left| \frac{\beta_2^{(2)}}{\Delta} \right| \lambda + o(T) \\
&= 2T \frac{b-a}{\Delta} + o(T).
\end{aligned}$$

We have thus proved:

$$\#([-T, T] \times J) \cap \mathcal{L} = 2T \frac{b-a}{\Delta} + o(T) \quad \text{as } T \rightarrow \infty.$$

This is equivalent with the desired formula. ■

References

- [1] Z. I. Borevich and I.R. Shafarevich, *Number Theory*, Academic Press, Vol. 20 in Series on Pure and Applied Mathematics, New York, 1966.
- [2] N. G. de Bruijn, *Algebraic theory of Penrose's non-periodic tilings of the plane. I*, Kon. Nederl. Akad. Wetesch. Proc Ser. A. (= Indag. Math.) (1981), 39–52.
- [3] N. G. de Bruijn, *Algebraic theory of Penrose's non-periodic tilings of the plane. II*, Kon. Nederl. Akad. Wetesch. Proc Ser. A. (= Indag. Math.) (1981), 53–66.
- [4] M. Einsiedler and T. Ward, *Ergodic Theory with a view towards Number Theory*, Springer Graduate Text in Mathematics, Vol. 259, Springer-Verlag London Ltd., London, 2011.
- [5] G. B. Folland, *Real Analysis: Modern Techniques and Their Applications*, 2nd edn, John Wiley & Sons, 1999.
- [6] G. H. Hardy and E. M. Wright, *An Introduction to the Theory of Numbers*, Oxford Science Publications, Clarendon Press, Oxford, 1998.
- [7] A. Hof, *Uniform distribution and the projection method, Quasicrystals and discrete geometry* (Toronto, ON, 1995), Fields Inst. Monogr., vol. 10, Amer. Math. Soc., Providence, RI, 1998, pp. 201–206.
- [8] L. Hörmander, *The analysis of linear partial differential operators i*, SpringerVerlag, 1990.
- [9] J. Marklof and A. Strömbergsson, *The distribution of free path lengths in the periodic Lorentz gas and related lattice point problems*, Annals of Math. 172 (2010), 1949–2033.
- [10] J. Marklof and A. Strömbergsson, *Free path lengths in quasicrystals*, Comm. Math. Phys. DOI 10.1007/s00220-014-2011-3, arXiv:1304.2044.
- [11] V. H. Moll, *Number and functions*, Student Mathematical Library. American Mathematical Society, Providence, RI, 2012. Special Functions for Undergraduates.
- [12] I. Niven, H. S. Zuckerman and H. L. Montgomery, *An introduction to the Theory of Numbers*, John Wiley & Sons, New Yourk, 1991.
- [13] W. Rudin, *Principles of Mathematical Analysis*, 3rd edn, McGraw-Hill, 1976.
- [14] W. Rudin, *Real and Complex Analysis*, 3rd edn, McGraw-Hill, 1987.
- [15] H. M. Stark, *An Introduction to Number Theory*, Markham Publishing Company, Chicago, 1970.

في مسألة التوزيع المنتظم لأشباه شبكة الأعداد الصحيحة في فضاء الأعداد الحقيقية \mathbb{R}^2

علي حافظ حكيم

قسم الرياضيات كلية العلوم - جامعة جازان

المخلص

في هذا البحث نستخدم ما يسمى طريقة القطع والمسقط (قطع واسقاط) cut-and-project للحصول على توزيع منتظم لأشباه شبكة الأعداد الصحيحة في الفضاء الحقيقي \mathbb{R}^2 (مستوى الأعداد الحقيقية الثنائي).

الكلمات المفتاحية: أشباه شبكة الأعداد الصحيحة، شبكة الأعداد الصحيحة، يسمى طريقة القطع والمسقط (قطع واسقاط)، توزيع منتظم.

Assessment of dietary patterns among students at Jazan University, Saudi Arabia: A cross-sectional study

Abdulrahman A. Alsayegh PhD^a, Rama M. Chandika PhD^a, Husameldin E. Khalafalla FCM, MHPE^b, Fatima A. Elfaki M.Sc^a, Khaled M. Dhamry Student^a, Meshal A. Alharby Student^a, Shadi A. Bosily Student^a and Abdulrahman H. Ahmed Student^a.

^a Department of Clinical Nutrition, College of Applied Medical Sciences, Jazan University, Jazan, Kingdom of Saudi Arabia

^b Department of Family and Community Medicine, College of Medicine, Jazan University, Jazan, Kingdom of Saudi Arabia

Abstract

Background: University life is a crucial stage for transforming adolescents to early adulthood and experience numerous health-related behavioral changes. These changes include unhealthy dietary habits, which are the major risk factors for developing chronic diseases. This study aimed to identify dietary patterns among Jazan University students in Saudi Arabia. **Methods:** A cross-sectional study was conducted from December 2022 to February 2023 at the Clinical Nutrition Department, Jazan University. Based on their characteristics, 103 of Saudi's common food items were categorized into 18 food groups. A self-designed questionnaire was distributed online to students to collect data on their food intake. Data were coded, validated, and analyzed using IBM SPSS statistics version 27.0. A Scree plot was constructed at more than 1.1 to select the optimal number of dietary patterns. Exploratory factor analysis with varimax rotation was applied to determine the highest factor loading of food groups. A P-value less than 0.05 was set as significant. **Results:** A principal component analysis identified four dietary patterns among university students: 1) a Westernized pattern that includes food items rich in sugar and refined grains; 2) a traditional pattern that includes milk, milk products, and traditional Saudi foods; 3) a prudent pattern that includes vegetables, legumes, nuts, and fruits; and 4) a protein pattern that includes meat, fish and seafood, and poultry.

Conclusion: Four dietary patterns were identified by the study. To establish relevant strategies and interventions, the results of this study can be used to further explore the relationship between these patterns and different cultural, demographic, environmental, and lifestyle variables.

Keywords: Dietary pattern, food frequency, university students, factor analysis.

1. Introduction

The effect of individual food items on health outcomes has been studied using traditional study approaches. However, individuals consume combinations of foods that are complex and interrelated (Newby et al., 2004). Single food items might interact in a way that even a sophisticated statistical analysis cannot resolve (Hu, 2002; Schwerin et al., 1982). Schwerin et al. (1982) started the trend of studying “foods as they are actually consumed,” i.e., in different and complex combinations. Hence, the terms “dietary patterns” and “eating patterns” gained popularity in areas where statistical manipulation created groups of nutritional variables and labeled them according to the food items that strongly correlated with their

relevant patterns (Kesse-Guyot et al., 2009). Despite some controversy around grouping and labeling (Hu 2002; Schwerin et al., 1982), researchers constructed food groupings for healthy eating, in general, such as the Mediterranean dietary pattern (Bach-Faig et al., 2011), or for specific health conditions, such as the Dietary Approaches to Stop Hypertension (DASH) (Campbell, 2017) and Mediterranean-DASH Intervention for Neurodegenerative Delay diets (MIND) (Marcason, 2015). This approach assesses the overall quality of diets (Newby et al., 2004), which is closer to the daily practice of people determined by complex cultural, economic, environmental, and other factors, rather than individual food items.

For youths, the university lifestyle is a transition period from the protection of family supervision to self-dependency (Cheema et al., 2021). Specifically, first-year students may exhibit changes in personality, viewpoint, and conduct as a result of being in the new environment at the university (Elneim, 2013). University students' diets have also changed as a result of technology, fast food, and social factors (Sogari et al., 2018a).

Habits that are instilled in early university life will probably persist throughout a person's life. Universally, studies conducted during the past 20 years have consistently demonstrated that university students tend to develop an unhealthy diet (Dodd et al., 2010; Kang et al., 2014; Keller et al., 2008; Kritsotakis et al., 2016; Steptoe et al., 2002). This could be caused by many factors, such as culture, behavior, environment, and work atmosphere (Dodd et al., 2010; Kang et al., 2014; Keller et al.,

2008; Kritsotakis et al., 2016; Sogari et al., 2018b).

Several studies have documented the dietary habits of university students. Studies from Saudi Arabia reported that fast food dominated unhealthy eating practices (Al-Gelban, 2008; Khabaz et al., 2017). A study has found that United Arab Emirates students consumed fewer than recommended vegetables and fruits and more dairy products and meat (Cooper & Al-Alami, 2011).

Identification of dietary patterns enables researchers to investigate the relationship between dietary patterns and nutrition-related diseases, which can assist in developing well-balanced dietary strategies (Schoenaker et al., 2013). Factor analysis is a widely used technique for discovering dietary patterns (Marchioni et al., 2005). Accumulated evidence has confirmed that many studies use factor analysis to identify dietary patterns (Agodi et al., 2018; Asadi et al., 2019; Shab-Bidar et al., 2018;

Syauqy et al., 2018). One of the focuses of public health is the assessment of eating patterns to help establish associations with health outcomes (Cespedes & Hu, 2015).

Diet is a crucial risk factor for chronic diseases. Determining dietary patterns might help to formulate strategies that can improve healthy eating behavior and decrease the onset of the diseases (Ambrosini et al., 2010). Dietary pattern analysis suggests that it is useful to evaluate the association between the quality of diet and its impact on health outcomes (Pan et al., 2021).

The outcomes of dietary pattern analysis would be sufficient if the overall diet was taken under consideration rather than the health effects of an individual food or nutrient (Hu, 2002). Studies of dietary habits among university students from Saudi Arabia and the associated health outcomes have discussed the results based on individual food items (Alsayegh et al., 2022; Alshammari et al., 2017;

Gosadi et al., 2017; Khabaz et al., 2017; Shahatah et al., 2021; Syed et al., 2020). Therefore, the current study aimed to use a factor analysis approach, concentrating on the overall dietary pattern rather than individual food items, to investigate university students' dietary patterns.

2. Methods

2.1. Study design

A cross-sectional study was conducted from December 2022 to February 2023 at the Clinical Nutrition Department of Jazan University in Saudi Arabia. A self-administered and structured questionnaire was sent online to the university students. The questionnaire was piloted to minimize possible errors. All currently enrolled male and female university students were included, except pregnant students. Well-trained volunteer students, supervised by the Clinical Nutrition Department staff, recruited participants. The study was approved by the ethics committee—Standing Committee for Scientific

Research, Jazan University (REC-44/06/470). Participants signed an informed consent form before filling out the questionnaire.

2.2. Dietary data

Food intake data were collected using a self-designed and pretested online questionnaire. Based on the characteristics of food items, 103 common Saudi food items were categorized into 18 food groups. Participants were asked to select any one from eight options that reflected their patterns: 6+ times daily, 5–6 times daily, 2–4 times daily, once daily, 5–6 times weekly, 2–4 times weekly, once weekly, and 1–3 times monthly for the consumption each food item. The frequency of each food item was converted into weekly frequencies (Alsayegh et al., 2022).

Sample size

The total number of enrolled students at Jazan University in the 2021 academic year was 24,968. The required size to provide a representative sample from the Jazan University student population was

calculated at 648 participants to be sufficient with the formula below:

$$n = N * X / (X + N - 1), \text{ where, } X = Z_{\alpha/2}^2 * p * (1-p) / \text{MOE}^2$$

Where: N (Population size) = 24,968, P (Response distribution) = 50%, $Z_{\alpha/2}$ (critical value at 1% level of significance) = 2.58, and MOE (Margin of error) = 5% (Atuhaire et al., 2021).

2.3. Statistical Analysis

Dietary patterns were identified using principal component analysis for the selected 18 food groups. The Cronbach's alpha index was calculated to evaluate the internal consistency of the data. The connection structure of the food groups with the least diagonal coefficient was prepared to evaluate the relationships within the food groups. Kaiser-Meyer-Olkin (KMO) measurement of sample advocacy and Bartlett's Test of Sphericity (BTS) were calculated to confirm the appropriateness of using factor analysis. Factors were considered with an eigenvalue greater than 1.1.

A Scree plot was also constructed to obtain the optimal number of factors. In the principal component analysis, the first extracted factor illustrated the highest quantity of variances, and it decreased gradually, followed by other factors in the data set. Data were coded, validated, and analyzed using IBM SPSS software, version 27.0 for Windows, Chicago, Illinois, USA.

The P-value was considered to denote significance at less than 0.05.

3. Results

Table-1 shows the demographic characteristics of participants. There is a balanced distribution of gender: three-quarters are urban dwellers and earn less than 4,000 Saudi Riyals (about 1,000 USD), half are of average BMI, and the remainder are equally above or below that.

Table-1: Demographic characteristics of the participants

Characteristics	Frequencies (%) n = 648
Age in years (Mean \pm SD) (22.64 \pm 3.52)	
Gender	
Male	348 (53.7%)
Female	300 (46.3%)
Residence	
Urban	491 (75.8%)
Rural	157 (24.2%)
Marital status	
Single	568 (87.7%)
Married	74 (11.4%)
Divorced	6 (0.9%)
Monthly income (SAR)	
<4,000	488 (75.3%)
4,000-10,000	106 (16.4%)
>10,000	54 (8.3%)
Body Mass Index (Wt. in Kg/ Ht. in m ²)	
Under weight	156 (24.3%)
Normal weight	317 (48.8%)
Overweight	97 (14.9%)
Obesity Class I	53 (8.2%)
Obesity Class II	17 (2.6%)
Obesity Class III	8 (1.2%)

Table-2 shows the 18 groups of food items. Principal component analysis was used on the reported 18 food groups to identify the four distinct dietary patterns among university students, which are: 1) Westernized pattern: fried foods, drinks and juices, soda drinks, cake/biscuits/sweets, salty snacks and

chips, and pastries/pizza; 2) traditional pattern: milk and milk products, breakfast cereal and bread, rice/pasta/potatoes, and traditional foods; 3) prudent pattern: vegetables (fresh and cooked), legumes, nuts, and fruits; 4) protein pattern: meat and chicken, processed meat, fish and seafood, and eggs.

Table-2: Food groups intake

Sl. No	Food Group	Food Items
1	Fried foods	Fast foods (all types), mayonnaise, salad dressing
2	Drinks and juices	Juices (all types), coffee, tea, Arabic coffee
3	Soda drinks	Soft drinks, energy drinks.
4	Cake, biscuits, sweets	Cake, biscuits (all types), pancakes, waffles, honey, jam, cream, caramel, Arabic desserts, maamool dates, cinnamon, doughnut, ice cream, chocolate
5	Salty snacks and chips	Crackers, chips (all types), popcorn
6	Pastries and pizza	Pizza, sambosa, fatayer, croissants
7	Milk and milk products	Milk, yogurt, cheese (all types), labenah, laban
8	Breakfast cereal and bread	Bread (all types), shaborah, cornflakes, breakfast
9	Rice, pasta, potato	Rice (all types), pasta (all types), potatoes (all types)
10	Tradition foods	Kabsa, gareesh, haress, qursan, mashghotha, areka, manto, yagmush, maasoob, mohala, aseeditamerr-gareesh soup
11	Vegetables (fresh and cooked)	Tomatoes, onion, cucumber, carrot, cauliflower, lettuce, watercress, celery, cabbage, cooked mixed vegetables, cooked pumpkin, cooked okra, cooked peas, cooked green beans, cooked molokhiyah, cooked spinach, vegetable soup
12	Legumes	Lentils, chickpeas, beans, peas soup, soy products
13	Nuts	Nuts (all types)
14	Fruits	Melon, watermelon, apple, orange, mandarin, banana, grapes, pears, apricot, peach, strawberry, dates, dried fruit
15	Meats and chicken	Chicken (all types), beef (all types), lamb, goat, camel
16	Processed meat	Sausage, hot dogs, pepperoni, martedella
17	Fish and seafood	Fried fish, grilled fish, tuna (all types), seafood, shrimp
18	Eggs	Eggs (all types)

Foods consumed by study participants were categorized into 18 food groups. *Food intake data were collected using a 103-item semi-quantitative Food Frequency Questionnaire.

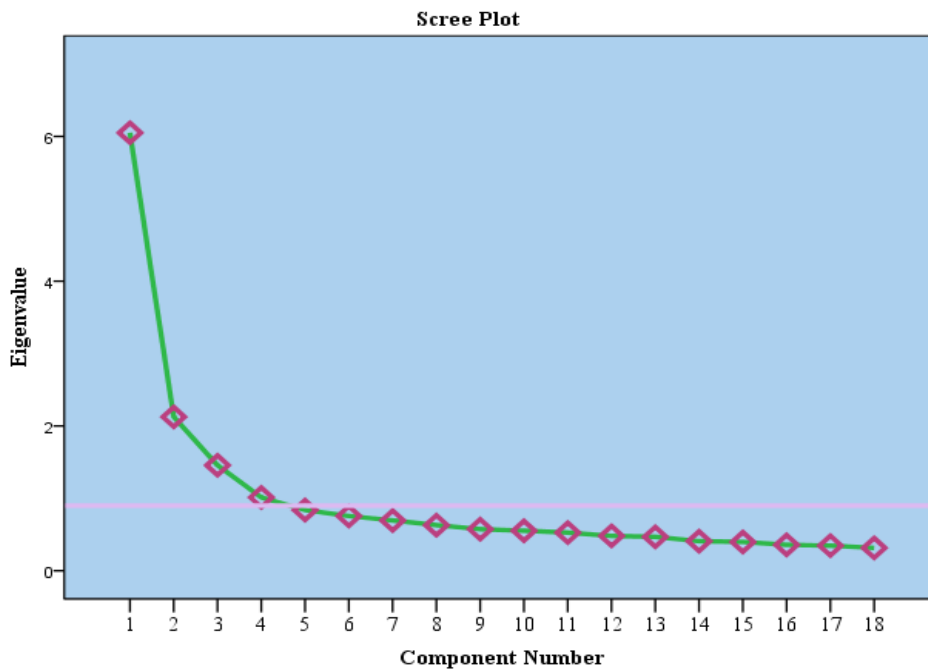
The four major patterns—Westernized, traditional, prudent, and protein—explained 20.020%, 17.672%, 12.556%, and 8.900% of the total variance, respectively, and as a whole, the model explained 59.419% of the total variance [Table-3].

Table-3: Food group factor loadings for the four dietary patterns

	Component or food pattern			
	Westernized	Traditional	Prudent	Protein
Fried foods	0.736			
Drinks and juices	0.597			
Soda drinks	0.721			
Cake, biscuits, sweets	0.730			
Salty snacks and chips	0.751			
Pastries and pizza	0.638			
Milk and milk products		0.588		
Breakfast cereal and bread		0.737		
Rice/pasta/potatoes		0.669		
Traditional foods		0.598		
Vegetable (fresh & cooked)			0.528	
Legumes			0.504	
Nuts			0.717	
Fruits			0.733	
Meats and chicken				0.331
Processed meat				0.781
Fish and seafood				0.684
Egg				0.311
% Explained Variance	20.020	17.672	12.556	8.900
% Cumulative Variance	20.020	37.693	50.249	59.419

Extraction Method: Principal Component Analysis, Rotation Method: Varimax with Kaiser Normalization.

The factor analysis was significant as a whole. Kaiser-Meyer-Olkin test showed the sample adequacy of 0.892 and the Bartlett test of sphericity ($P < 0.01$). Four factors were above the eigenvalue 1.1, and all the remaining factors were below the absolute line of the eigenvalue 1.1 [Figure-1].

Figure-1: Scree plot

4. Discussion

The current study aimed to explore the dietary patterns among students at Jazan University using factor analysis. Four dietary patterns—Westernized, traditional, prudent, and protein—were identified. Likewise, previous studies characterized a number of patterns ranging between three to seven (Kesse-Guyot et al., 2009; Naja et al., 2011, 2012, 2013; Park et al., 2005). In fact, these factors represented around 54.89% of the variances in dietary intake, where the majority of variances were interpreted to be the sweet and

starch pattern (20.68%). The current study showed similar results: Westernized food patterns contributed to 20.020% of the total variance. (Naja et al., 2011, 2012, 2013).

The Westernized dietary pattern is composed of fried foods, drinks and juices, soda drinks, cake, biscuits, sweets, salty snacks and chips, and pastries and pizza, which demonstrate its strongest association with energy intake. This pattern is packed with items with added sugars and starchy foods of refined grains, indicating a high energy intake at the expense of meeting the

recommended levels of other food items (Jomaa et al., 2016). The Westernized pattern can be found in many other studies, though its composition might differ. A systematic review study uses the same label to denote patterns containing products of refined grains consistent with our labeling; however, they also include refined meat in this category, which is included in our protein pattern (Hu, 2002). High caloric intake coupled with an inadequate intake of fruits and vegetables is found to contribute to higher rates of diabetes and obesity (Ledikwe et al., 2006).

The traditional pattern in this study is categorized by traditional Saudi dishes, such as harees, maasoob, and gerish, as well as milk and milk products, breakfast cereal and bread, and rice/pasta/potatoes (Table 1). Studies on food intake among the Saudi population are limited (Ahmed, Salih, and Khan, 2014; Al-Assaf and Al-Numair, 2007; Moradi-Lakeh et al., 2017). Studies have shown that the typical

Saudi diet consists of white rice, wheat bread, dates, and Arabic coffee (Al-Assaf and Al-Numair, 2007; Bawazeer, Al-Qahtani, and Alzaben, 2021),

Diet with high fat and high simple carbohydrates causes to increase the BMI. In contrast, compared to a Western diet, traditional diets are usually lower in fat and higher in complex carbohydrates. However, it does not seem to cause people of normal weight to gain weight, which suggests that limiting carbohydrate intake may not be universally effective in reducing obesity and cardiovascular risk (Cena and Calder, 2020; Wan et al., 2017). The expected effect of high carbohydrate intake is probably offset by the fact that traditional food has less total energy and possesses more dietary fiber than non-traditional foods, which improves insulin resistance and protects from many chronic diseases (Esmailzadeh & Azadbakht, 2008; Kerver et al., 2003).

The prudent pattern includes fruits, vegetables (fresh and cooked), legumes, and nuts. This is another popular label in research involving dietary patterns and is reported in other studies (Ambrosini et al., 2014; Hu, 2002; Slagter et al., 2018) and, in other research, is labeled as a “healthy” pattern. The protein pattern is composed of a high intake of meat and chicken, processed meat, fish and seafood, and eggs. This pattern could be associated with central obesity and hypertension (Haidari et al., 2014).

5. Limitations

The study population was restricted to university students, who share some important characteristics that could have an influence on the patterns selected (e.g., age and education) that might not represent the proportions in the general population. The number of patterns obtained by factor analysis and their labeling might not be applicable in other settings.

6. Conclusion

This study identified four dietary patterns of Saudi University students. The composition and labeling of those groups are found to resemble those outlined in many other studies. The results of this study can be useful for further investigations to find the relationship between the patterns and the different factors, such as culture, demographic, environment, and lifestyle variables, in order to build relevant strategies and interventions.

Acknowledgement

We are grateful to Jazan university students for their time and cooperation to participate in this study.

Conflicts of interest

Authors declare that they have no conflicts of interest.

Funding

This research received no specific grants from any funding agency in the public, commercial, or non-profit sector.

Institutional Review Board Statement:

The study was conducted in accordance with the Declaration of Helsinki, and approved by the Standing Committee for Scientific Research at Jazan University (REC-44/06/470).

Authors contributions:

Conceptualization: Abdulrahman A. Alsayegh, Rama M. Chandika, Fatima A. Elfaki, Khaled M. Dhamry, Meshal A. Alharby, Shadi A. Bosily and Abdulrahman H. Ahmed.

Methodology: Fatima A Elfaki and Rama M. Chandika.

Data curation: Fatima A Elfaki and Rama M. Chandika.

Validation: Husameldin E. Khalafalla.

Data Analysis: Rama M. Chandika.

Supervision: Rama M. Chandika, Fatima A Elfaki and Abdulrahman A. Alsayegh.

Writing – original draft: Abdulrahman A. Alsayegh, Rama M. Chandika, Husameldin E.

Khalafalla, Fatima A. Elfaki, Khaled M. Dhamry, Meshal A. Alharby, Shadi A. Bosily and Abdulrahman H. Ahmed.

Review & Editing: Abdulrahman A. Alsayegh, Rama M. Chandika, Husameldin E. Khalafalla, Fatima A. Elfaki, Khaled M. Dhamry, Meshal A. Alharby, Shadi A. Bosily and Abdulrahman H. Ahmed.

References

- Agodi, Antonella, Andrea Maugeri, Sarka Kunzova, Ondrej Sochor, Hana Bauerova, Nikola Kiacova, Martina Barchitta, and Manlio Vinciguerra. 2018. 'Association of Dietary Patterns with Metabolic Syndrome: Results from the Kardiovize Brno 2030 Study'. *Nutrients* 10(7):898. doi: 10.3390/nu10070898.
- Ahmed, Adam, Osama Salih, and Muhammad Ibrar Khan. 2014. 'Nutrition and Food Consumption Patterns in the Kingdom of Saudi Arabia'. *Pakistan Journal of Nutrition* 13:181–190. doi:10.3923/pjn.2014.181.190.

- Al-Assaf, Abdullah, and Khalid Al-Numair. 2007. 'Body Mass Index and Dietary Intake of Saudi Adult Males in the Riyadh Region-Saudi Arabia'. *Pakistan Journal of Nutrition* 6.doi:10.3923/pjn.2007.414.4 18.
- Al-Gelban, Khalid S. 2008. 'Dietary Habits and Exercise Practices among the Students of a Saudi Teachers' Training College'. *Saudi Medical Journal* 29(5):754-59.
- Alsayegh, Abdulrahman A., Rama M. Chandika, Amal A. Tubaigi, Abdulrahman M. Majrashi, Wedad A. Meree, and Abdulmajeed A. Asiri. 2022. 'Factor Analysis - Eating Patterns among Khat Chewers'. *Journal of Family Medicine and Primary Care* 11(6):2774-79. doi: 10.4103/jfmpc.jfmpc_1924_2 1.
- Alshammari, Eyad, Epuru Suneetha, Mohd Adnan, Saif Khan, and Awfa Alazzeah. 2017. 'Growth Profile and Its Association with Nutrient Intake and Dietary Patterns among Children and Adolescents in Hail Region of Saudi Arabia'. *BioMed Research International* 2017:1-9. doi: 10.1155/2017/5740851.
- Ambrosini, G. L., R. C. Huang, T. A. Mori, B. P. Hands, T. A. O'Sullivan, N. H. de Klerk, L. J. Beilin, and W. H. Oddy. 2010. 'Dietary Patterns and Markers for the Metabolic Syndrome in Australian Adolescents'. *Nutrition, Metabolism, and Cardiovascular Diseases: NMCD* 20(4):274-83. doi: 10.1016/j.numecd.2009.03.024.
- Ambrosini, Gina L., Pauline M. Emmett, Kate Northstone, and Susan A. Jebb. 2014. 'Tracking a Dietary Pattern Associated with Increased Adiposity in Childhood and Adolescence'. *Obesity (Silver Spring, Md.)* 22(2):458-65. doi: 10.1002/oby.20542.
- Asadi, Zahra, Mojtaba Shafiee, Fatemeh Sadabadi, Maryam Saberi-Karimian, Susan Darroudi, Maryam Tayefi, Hamideh Ghazizadeh, Alireza Heidari Bakavoli, Mohsen Moohebaty, Habibollah Esmaeily, Gordon A. Ferns, and Majid Ghayour-Mobarhan. 2019. 'Association Between Dietary Patterns and the Risk of Metabolic Syndrome among Iranian Population: A Cross-Sectional Study'. *Diabetes & Metabolic Syndrome* 13(1):858-65. doi: 10.1016/j.dsx.2018.11.059.

- Atuhaire, Catherine, Godfrey Zari Rukundo, Grace Nambozi, Joseph Ngonzi, Daniel Atwine, Samuel Nambile Cumber, and Laura Brennaman. 2021. 'Prevalence of Postpartum Depression and Associated Factors among Women in Mbarara and Rwampara Districts of South-Western Uganda'. *BMC Pregnancy and Childbirth* 21(1):503. doi: 10.1186/s12884-021-03967-3.
- Bach-Faig, Anna, Elliot M. Berry, Denis Lairon, Joan Reguant, Antonia Trichopoulou, Sandro Dernini, F. Xavier Medina, Maurizio Battino, Rekia Belahsen, Gemma Miranda, Lluís Serra-Majem, and Mediterranean Diet Foundation Expert Group. 2011. 'Mediterranean Diet Pyramid Today. Science and Cultural Updates'. *Public Health Nutrition* 14(12A):2274–84. doi: 10.1017/S1368980011002515
- Bawazeer, Nahla Mohammad, Seham Jubran Al-Qahtani, and Abeer Salman Alzaben. 2021. 'The Association Between Dietary Patterns and Socio-Demographic and Lifestyle Characteristics: A Sample of Saudi Arabia'. *Current Research in Nutrition and Food Science Journal* 9(3):1046–57.
- Campbell, Amy P. 2017. 'DASH Eating Plan: An Eating Pattern for Diabetes Management'. *Diabetes Spectrum: A Publication of the American Diabetes Association* 30(2):76–81. doi: 10.2337/ds16-0084.
- Cena, Hellas, and Philip C. Calder. 2020. 'Defining a Healthy Diet: Evidence for The Role of Contemporary Dietary Patterns in Health and Disease'. *Nutrients* 12(2):334. doi: 10.3390/nu12020334.
- Cespedes, Elizabeth M., and Frank B. Hu. 2015. 'Dietary Patterns: From Nutritional Epidemiologic Analysis to National Guidelines'. *The American Journal of Clinical Nutrition* 101(5):899–900. doi: 10.3945/ajcn.115.110213.
- Cheema, Sohaila, Patrick Maisonneuve, Amit Abraham, Karima Chaabna, Wajiha Yousuf, Tasnim Mushannen, Hania Ibrahim, Abdallah Tom, Albert B. Lowenfels, and Ravinder Mamtani. 2021. 'Dietary Patterns and Associated Lifestyle Factors among University Students in Qatar'. *Journal of American College Health: J of ACH* 1–9. doi: 10.1080/07448481.2021.1996374.

- Cooper, R. G., and U. Al-Alami. 2011. 'Food Consumption Patterns of Female Undergraduate Students in the United Arab Emirates'. *West African Journal of Medicine* 30(1):42–46. doi: 10.4314/wajm.v30i1.69915.
- Dodd, Lorna J., Yahya Al-Nakeeb, Alan Nevill, and Mark J. Forshaw. 2010. 'Lifestyle Risk Factors of Students: A Cluster Analytical Approach'. *Preventive Medicine* 51(1):73–77. doi: 10.1016/j.ypmed.2010.04.005.
- Elneim, Eshraga Abdallah Ali. 2013. 'Dietary Patterns of University Students: A Case Study of the University of Sennar'.
- Esmailzadeh, Ahmad, and Leila Azadbakht. 2008. 'Major Dietary Patterns in Relation to General Obesity and Central Adiposity among Iranian Women'. *The Journal of Nutrition* 138(2):358–63. doi: 10.1093/jn/138.2.358.
- Gosadi, Ibrahim M., Abdullah A. Alatar, Mojahed M. Otayf, Dhaerah M. AlJahani, Hisham M. Ghabbani, Waleed A. AlRajban, Abdullah M. Alrsheed, and Khalid A. Al-Nasser. 2017. 'Development of a Saudi Food Frequency Questionnaire and Testing Its Reliability and Validity'. *Saudi Medical Journal* 38(6):636–41. doi: 10.15537/smj.2017.6.20055.
- Haidari, Fatemeh, Esmat Shirbeigi, Makan Cheraghpour, and Majid Mohammadshahi. 2014. 'Association of Dietary Patterns with Body Mass Index, Waist Circumference, and Blood Pressure in an Adult Population in Ahvaz, Iran'. *Saudi Medical Journal* 35(9):967–74.
- Hu, Frank B. 2002. 'Dietary Pattern Analysis: A New Direction in Nutritional Epidemiology'. *Current Opinion in Lipidology* 13(1):3–9. doi: 10.1097/00041433-200202000-00002.
- Jomaa, Lamis, Nahla Hwalla, Leila Itani, Marie Claire Chamieh, Abla Mehio-Sibai, and Farah Naja. 2016. 'A Lebanese Dietary Pattern Promotes Better Diet Quality among Older Adults: Findings from a National Cross-Sectional Study'. *BMC Geriatrics* 16:85. doi: 10.1186/s12877-016-0258-6.

- Kang, Joseph, Christina Czart Ciecierski, Emily L. Malin, Allison J. Carroll, Marian Gidea, Lynette L. Craft, Bonnie Spring, and Brian Hitsman. 2014. 'A Latent Class Analysis of Cancer Risk Behaviors among U.S. College Students'. *Preventive Medicine* 64:121–25. doi: 10.1016/j.ypmed.2014.03.023.
- Keller, Stefan, Jason E. Maddock, Wolfgang Hannover, J. René Thyrian, and Heinz-Dieter Basler. 2008. 'Multiple Health Risk Behaviors in German First Year University Students'. *Preventive Medicine* 46(3):189–95. doi: 10.1016/j.ypmed.2007.09.008.
- Kerver, Jean M., Eun Ju Yang, Leonard Bianchi, and Won O. Song. 2003. 'Dietary Patterns Associated with Risk Factors for Cardiovascular Disease in Healthy US Adults'. *The American Journal of Clinical Nutrition* 78(6):1103–10. doi: 10.1093/ajcn/78.6.1103.
- Kesse-Guyot, E., S. Bertrais, S. Péneau, C. Estaquio, L. Dauchet, A. C. Vergnaud, S. Czernichow, P. Galan, S. Hercberg, and F. Bellisle. 2009. 'Dietary Patterns and Their Sociodemographic and Behavioural Correlates in French Middle-Aged Adults from the SU.VI.MAX Cohort'. *European Journal of Clinical Nutrition* 63(4):521–28. doi:10.1038/sj.ejcn.1602978.
- Khabaz, Mohamad Nidal, Marwan Abdulrahman Bakarman, Mukhtiar Baig, Tawfik Mohammed Ghabrah, Mamdouh Abdullah Gari, Nadeem Shafiq Butt, Faisal Alghanmi, Abdulaziz Balubaid, Ahmed Alzahrani, and Safwan Hamouh. 2017. 'Dietary Habits, Lifestyle Pattern and Obesity among Young Saudi University Students'. *JPMA. The Journal of the Pakistan Medical Association* 67(10):1541–46.
- Kritsotakis, George, Maria Psarrou, Maria Vassilaki, Zacharenia Androulaki, and Anastas E. Philalithis. 2016. 'Gender Differences in the Prevalence and Clustering of Multiple Health Risk Behaviours in Young Adults'. *Journal of Advanced Nursing* 72(9):2098–2113. doi:10.1111/jan.12981.

- Ledikwe, Jenny H., Heidi M. Blanck, Laura Kettel Khan, Mary K. Serdula, Jennifer D. Seymour, Beth C. Tohill, and Barbara J. Rolls. 2006. 'Dietary Energy Density Is Associated with Energy Intake and Weight Status in US Adults'. *The American Journal of Clinical Nutrition* 83(6):1362–68. doi: 10.1093/ajcn/83.6.1362.
- Marcason, Wendy. 2015. 'What Are the Components to the MIND Diet?' *Journal of the Academy of Nutrition and Dietetics* 115(10):1744. doi:10.1016/j.jand.2015.08.002.
- Marchioni, Dirce Maria Lobo, Maria do Rosário Dias de Oliveira Latorre, José Eluf-Neto, Victor Wünsch-Filho, and Regina Mara Fisberg. 2005. 'Identification of Dietary Patterns Using Factor Analysis in an Epidemiological Study in São Paulo'. *Sao Paulo Medical Journal = Revista Paulista De Medicina* 123(3):124–27. doi: 10.1590/s1516-31802005000300007.
- Moradi-Lakeh, Maziar, Charbel El Bcheraoui, Ashkan Afshin, Farah Daoud, Mohammad A. AlMazroa, Mohammad Al Saeedi, Mohammed Basulaiman, Ziad A. Memish, Abdullah A. Al Rabeeah, and Ali H. Mokdad. 2017. 'Diet in Saudi Arabia: Findings from a Nationally Representative Survey'. *Public Health Nutrition* 20(6):1075–81. doi: 10.1017/S1368980016003141
- Naja, F., L. Nasreddine, L. Itani, N. Adra, A. M. Sibai, and N. Hwalla. 2013. 'Association between Dietary Patterns and the Risk of Metabolic Syndrome among Lebanese Adults'. *European Journal of Nutrition* 52(1):97–105. doi: 10.1007/s00394-011-0291-3.
- Naja, Farah, Nahla Hwalla, Leila Itani, Maya Salem, Sami T. Azar, Maya Nabhani Zeidan, and Lara Nasreddine. 2012. 'Dietary Patterns and Odds of Type 2 Diabetes in Beirut, Lebanon: A Case-Control Study'. *Nutrition & Metabolism* 9(1):111. doi: 10.1186/1743-7075-9-111.

- Naja, Farah, Lara Nasreddine, Leila Itani, Marie Claire Chamieh, Nada Adra, Abla Mehio Sibai, and Nahla Hwalla. 2011. 'Dietary Patterns and Their Association with Obesity and Sociodemographic Factors in a National Sample of Lebanese Adults'. *Public Health Nutrition* 14(9):1570–78.doi:10.1017/S136898001100070X.
- Newby, P. K., Denis Muller, Judith Hallfrisch, Reubin Andres, and Katherine L. Tucker. 2004. 'Food Patterns Measured by Factor Analysis and Anthropometric Changes in Adults'. *The American Journal of Clinical Nutrition* 80(2):504–13.doi:10.1093/ajcn/80.2.504.
- Pan, Kathy, Aaron K. Aragaki, Marian L. Neuhouser, Michael S. Simon, Juhua Luo, Bette Caan, Linda Snetselaar, Joanne E. Mortimer, JoAnn E. Manson, Candyce Kroenke, Dorothy Lane, Kerry Reding, Thomas E. Rohan, and Rowan T. Chlebowski. 2021. 'Low-Fat Dietary Pattern and Breast Cancer Mortality by Metabolic Syndrome Components: A Secondary Analysis of the Women's Health Initiative (WHI) Randomised Trial'. *British Journal of Cancer* 125(3):372–79.doi:10.1038/s41416-021-01379-w.
- Park, Song-Yi, Suzanne P. Murphy, Lynne R. Wilkens, Jennifer F. Yamamoto, Sangita Sharma, Jean H. Hankin, Brian E. Henderson, and Laurence N. Kolonel. 2005. 'Dietary Patterns Using the Food Guide Pyramid Groups Are Associated with Sociodemographic and Lifestyle Factors: The Multiethnic Cohort Study'. *The Journal of Nutrition* 135(4):843–49.doi:10.1093/jn/135.4.843.

- Schoenaker, Danielle A. J. M., Annette J. Dobson, Sabita S. Soedamah-Muthu, and Gita D. Mishra. 2013. 'Factor Analysis Is More Appropriate to Identify Overall Dietary Patterns Associated with Diabetes When Compared with Treelet Transform Analysis'. *The Journal of Nutrition* 143(3):392–98. doi: 10.3945/jn.112.169011.
- Schwerin, H. S., J. L. Stanton, J. L. Smith, A. M. Riley, and B. E. Brett. 1982. 'Food, Eating Habits, and Health: A Further Examination of the Relationship between Food Eating Patterns and Nutritional Health'. *The American Journal of Clinical Nutrition* 35(5Suppl):1319–25. doi:10.1093/ajcn/35.5.1319
- Shab-Bidar, Sakineh, Mahdieh Golzarand, Mina Hajimohammadi, and Sara Mansouri. 2018. 'A Posteriori Dietary Patterns and Metabolic Syndrome in Adults: A Systematic Review and Meta-Analysis of Observational Studies'. *Public Health Nutrition* 21(9):1681–92. doi:10.1017/S1368980018000216.
- Shahatah, Mashael, Alaa Jadkarim, Revan Banjar, Yousof Kabli, Asmaa Milyani, and Abdulmoein Al-Agha. 2021. 'The Relationship between Body Weight and Dietary Habits with Respect to the Timing of Puberty among Saudi Children and Adolescents'. *Annals of African Medicine* 20(3):193–97. doi:10.4103/aam.aam_41_20.
- Slagter, Sandra N., Eva Corpeleijn, Melanie M. van der Klauw, Anna Sijtsma, Linda G. Swart-Busscher, Corine W. M. Perenboom, Jeanne H. M. de Vries, Edith J. M. Feskens, Bruce H. R. Wolffenbuttel, Daan Kromhout, and Jana V. van Vliet-Ostaptchouk. 2018. 'Dietary Patterns and Physical Activity in the Metabolically (Un)Healthy Obese: The Dutch Lifelines Cohort Study'. *Nutrition Journal* 17(1):18. doi: 10.1186/s12937-018-0319-0.
- Sogari, Giovanni, Catalina Velez-Argumedo, Miguel I. Gómez, and Cristina Mora. 2018a. 'College Students and Eating Habits: A Study Using An Ecological Model for Healthy Behavior'. *Nutrients* 10(12):1823. doi:10.3390/nu10121823.

- Sogari, Giovanni, Catalina Velez-Argumedo, Miguel I. Gómez, and Cristina Mora. 2018b. 'College Students and Eating Habits: A Study Using An Ecological Model for Healthy Behavior'. *Nutrients* 10(12):1823. doi: 10.3390/nu10121823.
- Steptoe, Andrew, Jane Wardle, Weiwei Cui, France Bellisle, Anna-Maria Zotti, Reka Baranyai, and Robert Sanderman. 2002. 'Trends in Smoking, Diet, Physical Exercise, and Attitudes toward Health in European University Students from 13 Countries, 1990-2000'. *Preventive Medicine* 35(2):97-104. doi:10.1006/pmed.2002.1048.
- Syauqy, Ahmad, Chien-Yeh Hsu, Hsiao-Hsien Rau, and Jane C. J. Chao. 2018. 'Association of Dietary Patterns with Components of Metabolic Syndrome and Inflammation among Middle-Aged and Older Adults with Metabolic Syndrome in Taiwan'. *Nutrients* 10(2):143. doi: 10.3390/nu10020143.
- Syed, Nabeel Kashan, Mamoon Hussain Syed, Abdulkarim M. Meraya, Ahmed A. Albarraq, Mohamed Ahmed Al-kasim, Saad Alqahtani, Hafiz Antar Makeen, Ayesha Yasmeen, Otilia J. F. Banji, and Mohamed Hassan Elnaem. 2020. 'The Association of Dietary Behaviors and Practices with Overweight and Obesity Parameters among Saudi University Students'. *PLoS ONE* 15(9):1-15. doi: 10.1371/journal.pone.0238458.
- Wan, Yi, Fenglei Wang, Jihong Yuan, Jie Li, Dandan Jiang, Jingjing Zhang, Tao Huang, Jusheng Zheng, Jim Mann, and Duo Li. 2017. 'Effects of Macronutrient Distribution on Weight and Related Cardiometabolic Profile in Healthy Non-Obese Chinese: A 6-Month, Randomized Controlled-Feeding Trial'. *EBioMedicine* 22:200-207. doi:10.1016/j.ebiom.2017.06.017.

تقييم النمط الغذائي لطلاب جامعة جازان، المملكة العربية السعودية: دراسة مقطعية

عبدالرحمن بن أحمد الصايغ^a، راما موهان شانديكا^a، حسام الدين الصاوي خلف الله خالد^b، فاطمة عوض الكريم الفكي محمد^a، خالد محمد جبران ظامري^a، مشعل علي احمد الحربي^a، شادي احمد علي بصيلي^a، عبد الرحمن حارث سالم احمد^a

^aقسم التغذية الاكلينيكية – كلية العلوم الطبية التطبيقية – جامعة جازان – المملكة العربية السعودية

^bقسم الاسرة وطب المجتمع – كلية الطب – جامعة جازان – المملكة العربية السعودية

الملخص

الخلفية: تعد الحياة الجامعية مرحلة حاسمة لتحويل المراهقين إلى مرحلة البلوغ المبكرة وتجربة العديد من التغييرات السلوكية المتعلقة بالصحة. وتشمل هذه التغييرات العادات الغذائية غير الصحية، وهي من عوامل الخطر الرئيسية للإصابة بالأمراض المزمنة. تهدف هذه الدراسة إلى التعرف على أنماط الغذاء لدى طلاب جامعة جازان بالمملكة العربية السعودية. **منهجية البحث:** دراسة مقطعية أجريت في الفترة من ديسمبر ٢٠٢٢ إلى فبراير ٢٠٢٣ في قسم التغذية الإكلينيكية بجامعة جازان. تم تصنيف 103 مادة غذائية شائعة بالمملكة العربية السعودية إلى ١٨ مجموعة غذائية بناءً على خصائص المواد الغذائية. تم توزيع استبيان مصمم ذاتياً تم اختباره مسبقاً عبر الإنترنت على طلاب الجامعة لجمع الطعام المتكرر على هذه المجموعات الغذائية الثمانية عشر. تم ترميز البيانات والتحقق من صحتها وتحليلها باستخدام إحصائيات IBM SPSS الإصدار ٢٧,٠. تم إنشاء مخطط (سكري) Scree بأكثر من ١,١ لتحديد العدد الأمثل للأنماط الغذائية. تم تطبيق تحليل العامل الاستكشافي مع دوران فارماكس varimax لتحديد أعلى عامل تحميل للمجموعات الغذائية للأنماط الغذائية التي تم الحصول عليها. تم تعيين قيمة P أقل من ٠,٠٥ باعتبارها ذات دلالة مهمة. **النتائج:** حدد تحليل المكون الرئيسي أربعة أنماط غذائية بين طلاب الجامعات: (1) "النمط الغربي" الذي يشمل المواد الغذائية الغنية بالسكريات والحبوب المكررة؛ (٢) "النمط التقليدي": ويشمل الألبان ومنتجات الألبان والأغذية السعودية التقليدية؛ (٣) "النمط الحكيم": الخضار والبقوليات والمكسرات والفواكه؛ (٤) "نمط البروتين": اللحوم والأسماك والدواجن. **الخلاصة:** تم تحديد أربعة أنماط غذائية من خلال الدراسة. يمكن أن تكون نتائج هذه الدراسة مفيدة لمزيد من استكشاف العلاقة بين هذه الأنماط والمتغيرات الثقافية والديموغرافية والبيئية وكذلك نمط الحياة، من أجل بناء الاستراتيجيات والتدخلات ذات الصلة.

الكلمات المفتاحية: النمط الغذائي، معدل تكرار الطعام، طلاب الجامعة، تحليل العوامل.

Blockchain Empowered IoT Security Framework: Challenges and Opportunities

Abdoh Jabbari¹

College of Computer Science and Information technology, Jazan University, Jazan

Abstract.

The rapid proliferation of Internet of Things (IoT) devices has brought forth numerous security challenges, necessitating the development of robust frameworks. In this study, we explore the application of blockchain technology to enhance IoT security, focusing on its challenges and opportunities. The goal of this research is to investigate the feasibility and effectiveness of integrating blockchain into IoT security frameworks, with a particular emphasis on addressing key security concerns. By utilizing a blockchain model, multiple entities can manage their identities securely, enabling efficient authentication and authorization for IoT devices. Our study reveals several significant findings. Firstly, the integration of blockchain technology in IoT security frameworks offers enhanced security through the utilization of digital signatures. This ensures that only authorized entities can access the system, mitigating the risk of unauthorized access and potential security breaches. Furthermore, the use of a blockchain model demonstrates improved efficiency in terms of authentication and authorization processes. By streamlining verification and permission-granting mechanisms, entities in the network can quickly and securely authenticate themselves and access required resources or services without the need for time-consuming manual procedures. This research underscores the significance of a blockchain-based IoT security framework in addressing the challenges faced by IoT systems. By leveraging blockchain technology, we provide a robust solution that enhances security, efficiency, and distributed consensus among multiple trusted entities.

Keywords: Internet of Things (IoT), blockchain, Security.

1. Introduction

The Internet of Things (IoT) has transformed the way we interact with our physical environment. The proliferation of smart devices and sensors has enabled a wide range of applications, from home automation and energy management to transportation and healthcare. However, the rapid growth of IoT also poses significant security risks. IoT devices are vulnerable to attacks such as data breaches, identity theft, and device hijacking, which can compromise the privacy, safety, and functionality of these systems. Moreover, the centralized architecture of traditional IoT systems creates a single point of failure, making them susceptible to hacking and data manipulation[1].

Distributed ledger technology, also known as blockchain, has emerged as a promising solution to enhance the security of IoT systems. Blockchain is a decentralized, distributed database that enables secure and transparent transactions without the need for intermediaries. Blockchain technology provides several key features, including decentralization, immutability, and consensus mechanisms that can address the security challenges of IoT systems. The integration of blockchain in IoT systems can enable secure data sharing, identity management, and device authentication, among other applications[2].

Blockchain technology has received immense attention in recent years because of its distinct ability to transform the financial business landscape. The area of blockchain technology has been actively explored to analyze its importance in improving business data and security aspects [3]. Internet of Things primarily is the interconnection of the various smart devices to essentially perform the task of gathering relevant data with the sole objective of demonstrating enhanced and intelligent decision-making. The IoT is considered to be a ubiquitous platform that has turned the physical world into a gigantic information system. The prevalence of IoT technologies can be gauged from the fact that it was stated around 95 percent of the products

pooled in world markets in 2020 will witness the IoT technology embedded in them. However, with this rising popularity of the IoT platform amongst the masses, it has been observed that the lack of intrinsic security options makes the entire IoT platform prone to security and privacy threats. Considering

the performance-driven capabilities of the Blockchain technology comprising of transparency, robust data encryption, and operational resilience can serve to play a critical role in strengthening the performance of the IoT platform thereby appropriately overcoming its security and privacy problems[4].

1.1 Blockchain: According to the study, the well-known innovation known as blockchain is gaining a lot of attention and producing a lot of initiatives in a variety of industries. The financial industry is the one that employs the blockchain concept more than any other. As a result, the financial industry is regarded as the blockchains principal user. Though one of blockchains most well-known features is its application in the crypto-currency Bitcoin, it has also been effectively employed to improve substantial process inefficiencies and a major "cost-base issue" unique to this industry. Figure 1 is presented as an illustration of blockchain to make it

more understandable. It is understood that blockchain is made up of data sets that are made up of a chain of data packages known as blocks, each of which contains several operations/ transactions (TX1-n). Its expansion of more blocks reflects an entire transaction record ledger. The blockchain concept is used to save data from fraud and this idea guarantees the blockchains validity all the way starting to form the first block which is named genesis (figure 1). Hash values are distinctive and because of their uniqueness forgery can be successfully blocked because modification to a block in the chain changes the hash value instantly [5]

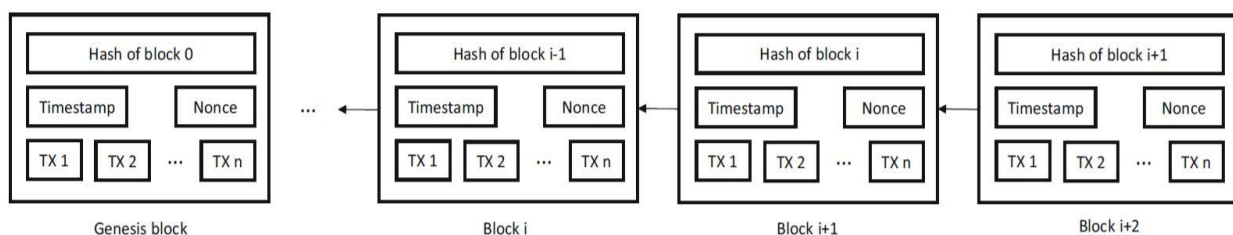


Fig.1. Blockchain

Because of the importance of data and the rise in fraud, blockchain is becoming increasingly relevant in IoT (internet of things) security. Due to the obvious rise in data fraud, industries are increasingly implementing the concept of blockchain, which aids in the authentication and tracking of multistep operations that demand confirmation and traceability. It can deliver data security, reduced regulatory costs, and fast data transfers. Contract administration and auditing departments both can be aided by blockchain technology. It can also be used to manage designations and activities, as well as voting platforms [6]. One popular example for this case is that Americans are having a hard time

trusting their government and the number of people who have trust in its government, unfortunately, the percentage is very low. According to the survey, only 18% of the population of Washington Dc believe that the government will do the right thing. In this case, it was advised to the government to opt for the Blockchain concept, as the blockchain-based application will be able to benefit the government by increasing transparency through decentralization, enabling information to be viewed and verified by participants. Furthermore, blockchain has the potential to enable verifiable proof of official assertions [7] , Figure 2 shows various properties of blockchain[8].

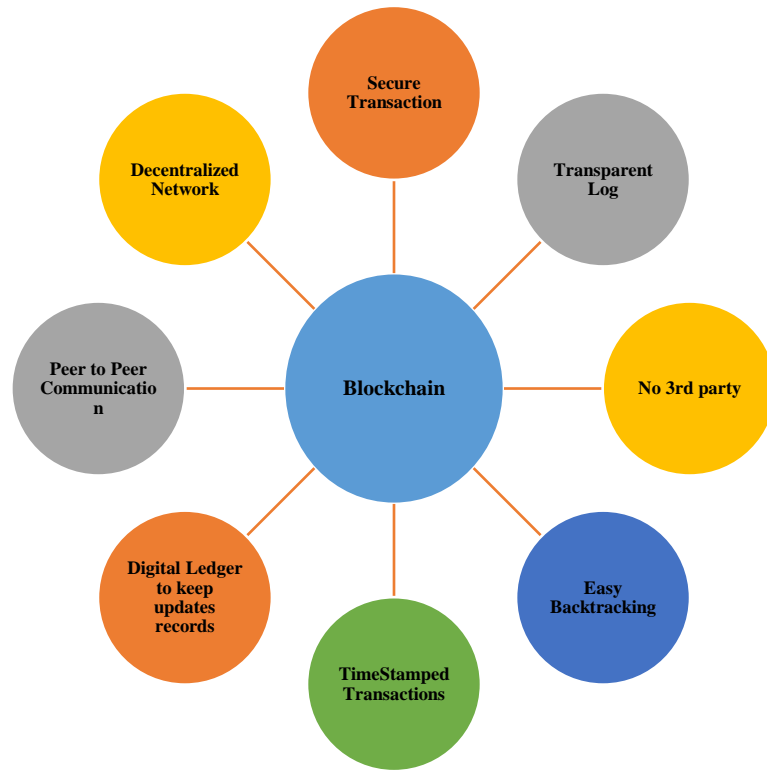


Fig.2. Blockchain Properties

This article offers a thorough evaluation of the current research on the application of distributed ledger technology for bolstering the security of IoT systems. The authors delve into the main characteristics of blockchain technology and how they can improve IoT security. Moreover, they analyze the current progress of research on blockchains role in IoT security, inclusive of practical examples. Lastly, the authors pinpoint the major obstacles and research areas that require attention for the integration of distributed ledger technology into IoT security.

2. Literature Review

Several research studies have explored the potential of blockchain for IoT security, and proposed various architectures and protocols for integrating blockchain into IoT systems. For example, in a study by Conoscenti et al. (2016), a blockchain-based architecture for IoT security was proposed, which aimed to provide secure and tamper-proof data sharing among IoT devices. The study utilized smart contracts to manage access control and data sharing, and demonstrated the feasibility of the proposed

architecture through a proof-of-concept implementation[9].

Another study by Tanweer Alam (2023) proposed a blockchain-based identity management system for IoT devices, where devices can securely and efficiently manage their identities and authenticate themselves to other devices on the network using digital signatures. The study also proposed a consensus mechanism based on proof-of-work and proof-of-stake, to ensure secure and efficient data exchange[4].

Other research studies have focused on the scalability and efficiency of blockchain-based IoT systems. For example, in a study by Syed Mujtaba Hosseini et al. (2020), a lightweight blockchain protocol for IoT devices was proposed, which uses a consensus mechanism based on proof-of-stake to ensure secure and efficient data exchange. The study demonstrated the feasibility of the proposed protocol through a simulation-based evaluation, and showed that the proposed protocol can achieve high throughput and low latency in IoT networks[10].

Moreover, a study by Wang et al. (2019) proposed a hybrid blockchain architecture for IoT networks, which combines the benefits of public and private

blockchains to achieve scalability and privacy. The study utilized a hierarchical architecture, where private blockchains are deployed at the edge of the network, and a public blockchain is used to validate transactions and maintain global consensus. The study demonstrated the feasibility of the proposed architecture through a proof-of-concept implementation and showed that the proposed architecture can provide high scalability and privacy in IoT networks[11].

Several pilot projects and experimental evaluations have also been conducted to assess the feasibility and effectiveness of blockchain for IoT security. For example, in a pilot project by Xu et al. (2018), the use of blockchain for secure and auditable energy transactions between IoT devices in a microgrid was demonstrated. The pilot project utilized a consortium blockchain, where multiple entities in the microgrid can securely and transparently exchange energy tokens using smart contracts. The pilot project demonstrated the feasibility of the proposed architecture and showed that blockchain can provide secure and auditable energy transactions in IoT networks.

Another experimental evaluation by Kshetri et al. (2018) showed that a blockchain-based identity management

system can provide secure and efficient authentication and authorization for IoT devices. The evaluation utilized a consortium blockchain, where multiple entities in the network can manage their identities and authenticate themselves to other entities using digital signatures. The evaluation demonstrated the feasibility of the proposed system and showed that it can provide secure and efficient authorization and authentication mechanism.

3. IoT Security

The internet of things (IoT) concept and application, providing numerous application scenarios for blockchain utility. This allows end-user to connect their devices directly with one another which minimizes the time of database or service connections and enhances the efficiency for devices to be more incorporated completely and comprehensively with each other, irrespective of system scale. This also helps to lessen the potential risks connected with any kind of gadget which is being connected by decreasing the probability of data loss by incorporating it across the program's operating system [12]. The IoT environment

or ecosystem consists of internet electronic objects or devices, that gather information or data, communicate within the system, and respond to the collected information from their surroundings using embedded systems such as CPUs, sensors, and different hardware.

According to [13] internet of things (IoT) will be considered a game-changer, it will involve millions and billions of smart devices that will be incorporated with processing, sensing, and actuating capabilities that will enable them to stay connected to the internet. In today's world incorporating social networking concepts into the internet of things has given birth to a new concept known as social IoT (SIoT), this concept allows people and smart systems to communicate and share information more rapidly. Though security challenge issues are increasing day by day because as the internet and software are getting smarter people are getting smarter too and they are finding ways to hack data or any other sensitive information. This is where blockchain comes in. figure 2 represents 3 different layers of the IoT Model

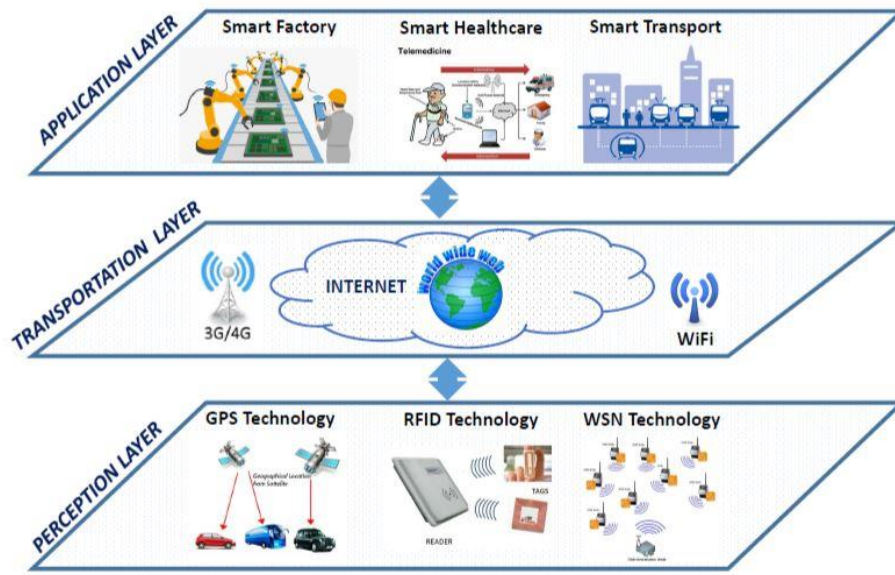


Fig. ٣. IoT Model

All of these layers have their own unique set of challenges. The perception layer is the initial layer that deals with physical sensors used in IoT. These sensors utilize different standard technologies like RFID, wireless sensor networks (WSN), and GPS to facilitate data collection and processing. The sensors and actuators in this layer are responsible for measuring various environmental factors such as temperature, humidity, and so on. The transportation layer, on the other hand, provides universal access to the perception layer by transmitting information to a specific information system. This is accomplished through various means such as 3G, wireless fidelity (Wi-Fi), ad hoc networks, and core networks like the internet. Finally, the

application layer is responsible for providing customer service. This layer's value is high as it can offer high-quality smart devices to meet customer demands, which are critical in various IoT settings such as smart cities, healthcare, and transportation[14].

4. IoT Security Issues

Internet of things spread so fast that people who were responsible for security data had to keep up with IoT spread to make sure the data is secured. But still, some problems cannot be resolved without a specific product. The "things" in the IoT devices, because the diversification of IoT devices broadens the range of the IoT and makes cybersecurity difficult. Below we will discuss current IoT issues.

Table 1.IoT Issues

Levels	Threats	
Application Level Threats	Data leakage	The unlawful way of communicating or passing data within an organization to external destination. Data leakage threats are most commonly transmitted over web, mobile, USB devices, and laptops [15]
	Dos-Attack	Dos stands for denial of service attacks [16]flooding the user (target) with traffic of requests or sending information which will crash the system.
	Malicious-Code Injection	Attackers can attack with malicious codes and inject them in the system.
Transportation Level	Routing-Attack	Entering of wrong routing table and data will cause problems.
	Dos-Attack	Denial of service attacks also present in transportation level.
	Data-Transit-Attack	Movement of data increase security problem and attackers can attack data in the middle of transmission.
Perception Level	Physical-Attack	Hardware focused attacks, fake identity attacks to enter the environment, attacking the ability of Nodes and making them unavailable, and attacks on confidential data.
	Impersonation	
	DoS-Attacks	
	Routing-Attack	
	Data Transit Attack	
Development of various technologies for monitoring network activities, Security tools and their administration, IoT network maintenance is difficult due to software problems, and Concerns about IoT network security [17]		

5. Blockchain to Mitigate These Issues Related to IoT Security

Blockchain technology can be used to improve the security of IoT systems in a variety of ways. Secure data sharing is a key application. IoT devices can securely share data with other devices or parties using

blockchain, eliminating the need for intermediaries or centrally hosted servers. This approach can enhance the privacy and confidentiality of the data and reduce the risk of data breaches. Another application is identity management. By using blockchain-based identity management systems, IoT

devices can securely and autonomously manage their identities and authenticate themselves to other devices on the network. This approach can prevent unauthorized access and device spoofing. A third application is device authentication and authorization. By using blockchain-based

digital signatures, IoT devices can verify their authenticity and authorization to perform specific actions on the network, such as data transmission or device control. This approach can prevent device hijacking and unauthorized actions.

Table 2. Solutions

Issues	Solutions
Network Breaches – Application level Several devices, interfaces, and continual processes leave gaps [18]	Blockchain is the solution to block attackers who can exploit the data and hack into the system to gather information [19]
Software attacks	Internet of things is 24/7 connected to the internet and lack of security might welcome malware and other virus attacks which lock data and ask for ransoms. Blockchain encrypts the data being shared [20]
Data security[21]	Blockchain provides traceability and security related to finance and other transactions. It has the ability to capture the data in a block while transferring which secures data from attacks and fraud.
Human errors[22]	Data is stored by humans and there is always a chance of humans making an error. Blockchain eliminates these errors by issuing encrypted identities such as SSL certificates for future verifications.
Data Storage	With implementation of Blockchain – it generates decentralized ledger for data recording. This protects and controls the communication and other activities within the system [23]
Iot devices and networks: secure with Blockchain.	Blockchain has the ability to monitor and record communication between all devices which are linked to the network, it allows organizations to access data available on activity logs, suspect login information [24]

BLOCKCHAIN MAKING IOT SECURE

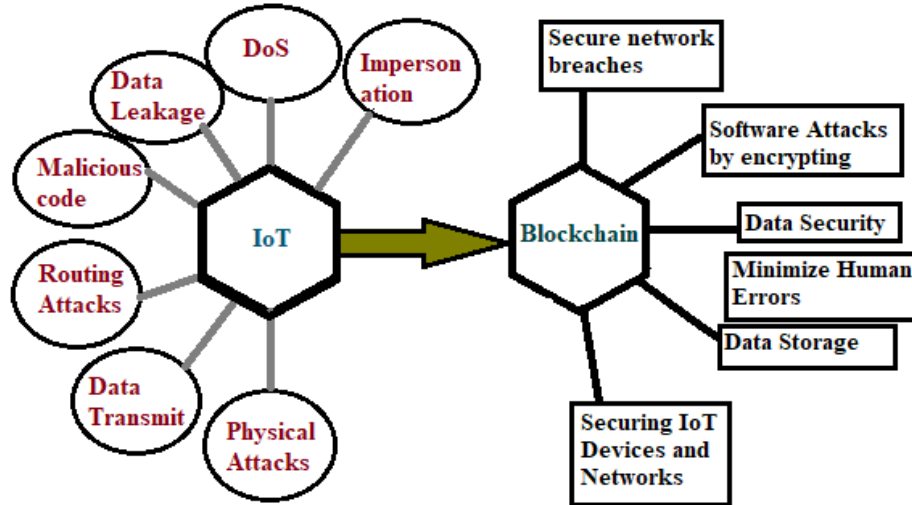


Fig. 4. IoT with Blockchain

6. Blockchain Based Framework To Mitigate IoT Security Issues

One of the key advantages of blockchain technology is that it can enhance the security of IoT systems by providing various essential features. Firstly, blockchain is a distributed and decentralized ledger, meaning that there is no single entity or authority that controls the network. Instead, all participants collectively maintain the ledger, reducing the risk of a single point of failure or attack. Additionally, the immutability of blockchain ensures that once a transaction is recorded on the ledger, it cannot be changed or deleted, thus

protecting the integrity of the data and preventing any unauthorized changes. Another benefit of blockchain is that it uses consensus mechanisms, such as proof-of-work or proof-of-stake, to ensure that all network participants agree on the state of the ledger. This helps to enhance the trust and transparency of the system and prevent any malicious actors from tampering with the data. From Fig.5 It is evident that the utilization of blockchain technology is employed in tracking potential threats associated with IoT devices. This involves monitoring the communication between IoT

devices and network transmission, as well as between IoT devices and the cloud.

The use of blockchain technology can address various security concerns in IoT systems, such as identifying malicious activities in network transmission and achieving identity authentication between IoT devices and the cloud. However, traditional security measures that require trusted third parties can lead to resource consumption. With blockchain technology, security policies can be implemented without the need for third parties. For

instance, the identity authentication mechanism between IoT devices and the cloud can be achieved without third-party key distribution. This approach can save time and improve user experience. This paper proposes the use of blockchain technology to establish a comprehensive security system for IoT devices throughout their entire life cycles. By leveraging the blockchain technology as the primary method and IoT as the support, a platform layer can be created that manages massive IoT devices in the asset database.

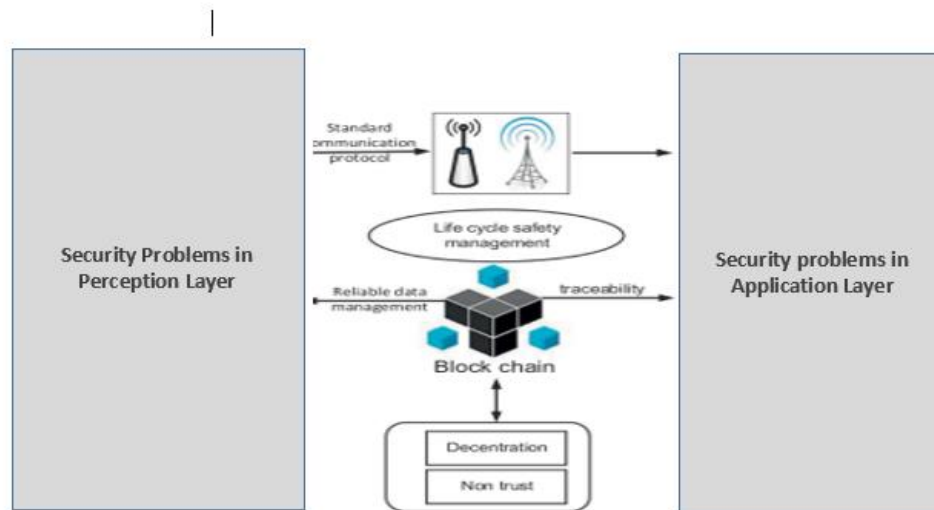


Fig.5 Blockchain based framework for IoT security

By adding blockchain to the existing IoT-based framework, several problems can be addressed, leading to various benefits. Table 3 shows comparison of existing frameworks and blockchain based framework.

Table 3: Comparison of existing frameworks and blockchain based framework

Existing IoT-based Framework Problems	Blockchain Based IoT Security framework
Lack of data integrity and trust	Enhanced data integrity and immutability through blockchain's distributed ledger technology
Inadequate security and privacy	Improved security and privacy protection through blockchain's cryptographic techniques
Centralized architecture	Decentralized architecture with blockchains distributed consensus mechanism
Limited interoperability	Enhanced interoperability through standardized protocols and smart contracts on the blockchain
Single point of failure	Redundancy and fault tolerance with blockchain's distributed nature
Lack of auditability and transparency	Transparent and auditable transactions and data provenance on the blockchain
Issues with data provenance	Reliable data provenance and traceability with blockchain's immutable ledger
Inefficient and costly intermediaries	Reduction of intermediaries and streamlined processes through smart contracts on the blockchain
Trust issues among stakeholders	Increased trust among stakeholders due to blockchain's consensus and transparency features
Data tampering and manipulation	Protection against data tampering and manipulation through blockchain's consensus algorithms

In summary, the key features mentioned in Table 4 of blockchain framework such as decentralization, immutability, and consensus mechanism, can help solve many of the security challenges faced by IoT systems. By leveraging these features, blockchain can provide a more secure and reliable foundation for IoT applications and services.

Table 4: Key features of Distributed Ledger system

Feature	Description
Decentralization	The ledger is not controlled by a single entity, reducing the risk of a single point of failure or attack
Immutability	Once a transaction is recorded on the ledger, it cannot be changed or deleted, protecting the data's integrity
Consensus mechanisms	Network participants must agree on the state of the ledger through consensus mechanisms such as proof-of-work or proof-of-stake, enhancing trust and transparency and preventing malicious actors from manipulating the data
Encryption	Blockchain uses advanced cryptographic techniques to ensure secure data transmission and storage
Smart contracts	Smart contracts can be used to automate transactions and enforce business logic, reducing the risk of human error or fraud
Transparency	All network participants have access to the same ledger, providing transparency and accountability
Traceability	Each transaction is recorded on the ledger with a unique identifier, allowing for easy traceability and auditability

7. Conclusion

Internet of things is a wide range of internet devices connected to Wi-Fi and another form of internet service to transfer data from one end to another. While transferring data there is a chance that the data might get hacked in middle by attackers or it can attach the virus to itself. In this case, scenario blockchain is the best solution to protect data from attackers and viruses. Implementation of blockchain framework provide a stable and secure environment for companies. As companies are now more digitally connected with their consumers and other shareholders because of which a lot of information shared on cloud based systems

with the help of internet. Internet of things challenges privacy of data, security concerns, and durability of the data. Blockchain is successfully used in crypto currency transactions which does not mean that it is not for other businesses. It can successfully be used for other businesses like agriculture, product management etc. it give validation of data, monitor data continuously, records threats coming it way, and can easily address IoT issues by providing best solutions and creating secure environment for fearless transactions and information sharing. In conclusion, the integration of distributed ledger technology, or blockchain, in IoT systems has the

potential to enhance the security, privacy, and trust of these systems. Blockchain offers several key features, such as decentralization, immutability, and consensus mechanisms, that can address the security challenges of IoT systems. However, there are several challenges and open research questions that need to be addressed to enable the practical adoption of blockchain in IoT security. Future research efforts should focus on developing scalable and efficient blockchain-based IoT systems, exploring novel consensus and incentive mechanisms, and conducting real-world case studies and evaluations.

8. Challenges and Future Research Directions

While blockchain has the potential to improve IoT security, there are several challenges that must be addressed to fully realize its benefits. One major challenge is the scalability and efficiency of blockchain-based IoT systems. As IoT networks grow in size and complexity, the capacity of the blockchain to handle the increased volume of transactions and data becomes a critical issue.

Another challenge is the integration of blockchain with existing IoT infrastructure and standards. Many IoT

devices and platforms may not be designed to work with blockchain, and retrofitting them to support blockchain can be a significant challenge. Moreover, the lack of common standards for IoT security and blockchain implementation can create interoperability issues and complicate the integration process.

Another significant challenge is the energy consumption of blockchain-based systems, especially those that rely on resource-intensive consensus mechanisms like proof-of-work. This issue is particularly important for IoT devices that have limited battery life and processing power.

In terms of future research directions, there is a need for more comprehensive studies on the performance and effectiveness of blockchain-based IoT security solutions. This research should focus on identifying the optimal blockchain configurations and consensus mechanisms for different types of IoT applications. Additionally, there is a need for the development of standards and best practices for the integration of blockchain with IoT devices and platforms.

Furthermore, the development of privacy-preserving blockchain solutions can also be an area of future research. This

would enable secure data sharing among IoT devices and systems without compromising user privacy. Finally, research should also focus on developing effective governance mechanisms for blockchain-based IoT systems to ensure their long-term sustainability and stability. This would

involve identifying the appropriate roles and responsibilities for different stakeholders and establishing mechanisms for resolving disputes and addressing security incidents. Table 5, shows research Gaps or shortcoming's that needs more research.

Table 5: Research Gaps and shortcomings

Key Findings	Research Gaps and Shortcomings
Scalability and Performance	Existing studies often acknowledge the scalability and performance challenges associated with implementing blockchain in IoT environments. However, specific solutions and techniques to address these challenges are limited, necessitating further research and development of optimized blockchain architectures for IoT devices. The resource limitations and high-volume data transactions in IoT environments require tailored scalability solutions.
Privacy and Confidentiality	While blockchain technology offers enhanced security, ensuring privacy and confidentiality in blockchain-empowered IoT security frameworks remains a critical concern. Existing studies provide limited insight into effective techniques for preserving privacy in these frameworks. Future research should focus on developing robust privacy-preserving mechanisms, such as zero-knowledge proofs or secure data sharing protocols, to address privacy concerns effectively.
Interoperability and Standards	The lack of standardized protocols and interoperability between different blockchain and IoT platforms is a significant obstacle to seamless integration. While this challenge is often acknowledged in previous studies, comprehensive solutions and frameworks for achieving interoperability are lacking. Further research is needed to develop standardized protocols, frameworks, and interoperability mechanisms that facilitate seamless integration between diverse blockchain and IoT systems, promoting interoperability and compatibility.
Trust and Governance	While blockchain technology inherently promotes trust among IoT entities through its decentralized nature, studies often overlook the governance mechanisms required for effective implementation. Future research should focus on exploring and developing governance models and frameworks specific to blockchain-empowered IoT security frameworks. These governance mechanisms will ensure transparent and accountable decision-making processes, establishing trust and effective implementation of such frameworks.
Real-world Implementation and Case Studies	Despite the theoretical insights provided by existing literature, practical implementation and real-world case studies of blockchain-empowered IoT security frameworks are limited. Future research should emphasize real-world deployments, assessing the feasibility, performance, and effectiveness of these frameworks in various IoT application domains. This research will provide valuable insights into the practical implications, challenges, and successes of implementing blockchain-empowered IoT security frameworks in real-world scenarios.

By addressing these research gaps and shortcomings, researchers can further advance the development of robust and comprehensive blockchain-empowered IoT security frameworks. These frameworks will overcome scalability challenges, enhance privacy preservation techniques, establish interoperability standards, incorporate effective governance mechanisms, and validate their practical applicability through real-world implementation and case studies.

References

- [1] M. Ghiasi, T. Niknam, Z. Wang, M. Mehrandezh, M. Dehghani, and N. Ghadimi, "A comprehensive review of cyber-attacks and defense mechanisms for improving security in smart grid energy systems: Past, present and future," *Electr. Power Syst. Res.*, vol. 215, no. July 2022, 2023, doi: 10.1016/j.epsr.2022.108975.
- [2] S. N. G. Aryavalli and H. Kumar, "Top 12 layer-wise security challenges and a secure architectural solution for Internet of Things," *Comput. Electr. Eng.*, vol. 105, no. November 2022, p. 108487, 2023, doi: 10.1016/j.compeleceng.2022.108487.
- [3] F. A. Reegu, M. O. Al-Khateeb, W. A. Zogaan, M. R. Al-Mousa, S. Alam, and I. Al-Shourbaji, "Blockchain-Based Framework for Interoperable Electronic Health Record," *Ann. Rom. Soc. Cell Biol.*, pp. 6486–6495, 2021.
- [4] T. Alam, "Blockchain-Based Internet of Things: Review, Current Trends, Applications, and Future Challenges," *Computers*, vol. 12, no. 1, 2023, doi: 10.3390/computers12010006.
- [5] S. A. Faheem Reegu, Salwani Mohd Daud, "Interoperability Challenges in Healthcare Blockchain System - A Systematic Review," *Ann. RSCB*, vol. 25, no. 4, 2021.
- [6] Reegu Faheem, Zada Khan Wazir, Mohd Daud Salwani, Arshad Quratulain, and Armi Nasrullah, "A Reliable Public Safety Framework for Industrial Internet of Things (IIoT)," *Proceeding - 2020 Int. Conf. Radar, Antenna, Microwave, Electron. Telecommun. ICRAMET 2020*, pp. 189–193, Nov. 2020, doi: 10.1109/ICRAMET51080.2020.9298690
- [7] shadab alam faheem reegu, salwani daud, zaid hakami, Kaiser kareem reegu, "Towards Trustworthiness of Electronic Health Record system using Blockchain," *Ann. RSCB*, vol. 25, no. 6, 2021.
- [8] S. Katsikeas, P. Johnson, M. Ekstedt, and R. Lagerström, "Research communities in cyber security: A comprehensive literature review," *Comput. Sci. Rev.*, vol. 42, p. 100551, 2021, doi: 10.1016/j.cosrev.2021.100431.
- [9] M. S. Mahmood and N. B. Al Dabagh, "Blockchain technology and internet of things: review, challenge and security concern," *Int. J. Electr. Comput. Eng.*, vol. 13, no. 1, pp. 718–735, 2023, doi: 10.11591/ijece.v13i1.pp718-735.
- [10] S. M. H. Bamakan, A. Motavali, and A. Babaei Bondarti, "A survey of blockchain consensus algorithms performance evaluation criteria," *Expert Syst. Appl.*, vol. 154, 2020, doi: 10.1016/j.eswa.2020.113385.

- [11] Y. Xiaodong *et al.*, “Blockchain-Based Secure and Searchable EHR Sharing Scheme,” *ieeexplore.ieee.org*, pp. 822–825, 2019, doi: 10.1109/ICMCCE48743.2019.00188.
- [12] S. Roy, M. Ashaduzzaman, M. Hassan, and A. R. Chowdhury, “BlockChain for IoT security and management: Current prospects, challenges and future directions,” *Proc. 2018 5th Int. Conf. Networking, Syst. Secur. NSysS 2018*, 2019, doi: 10.1109/NSysS.2018.8631365.
- [13] A. Dorri, S. S. Kanhere, R. Jurdak, and P. Gauravaram, “Blockchain for IoT security and privacy: The case study of a smart home,” *2017 IEEE Int. Conf. Pervasive Comput. Commun. Work. PerCom Work. 2017*, no. March, pp. 618–623, 2017, doi: 10.1109/PERCOMW.2017.7917634.
- [14] S. Badr, I. Goma, and E. Abd-Elrahman, “Multi-tier blockchain framework for IoT-EHRs systems,” in *Procedia Computer Science*, 2018, vol. 141, pp. 159–166, doi: 10.1016/j.procs.2018.10.162.
- [15] I. Lee, “Internet of Things (IoT) Cybersecurity: Literature Review and IoT Cyber Risk Management,” *Futur. Internet*, vol. 12, no. 9, p. 157, 2020, doi: 10.3390/fi12090157.
- [16] S. Badr, I. Goma, and E. Abd-Elrahman, “Multi-tier blockchain framework for IoT-EHRs systems,” *Procedia Comput. Sci.*, vol. 141, pp. 159–166, 2018, doi: 10.1016/j.procs.2018.10.162.
- [17] M. Alamri, N. Jhanjhi, M. Humayun, and S. Arabia, “Blockchain for Internet of Things (IoT) Research Issues Challenges & Future Directions: A Review,” 2019.
- [18] Henry hillford, “How to Secure the Internet of Things (IoT) with Blockchain - Best Security Place,” 2018. [Online]. Available: <https://www.bestsecurityplace.com/secure-internet-things-iot-blockchain/>. [Accessed: 27-Oct-2020].
- [19] J. Sengupta, S. Ruj, and S. Das Bit, “A Comprehensive Survey on Attacks, Security Issues and Blockchain Solutions for IoT and IIoT,” *J. Netw. Comput. Appl.*, vol. 149, no. September 2019, p. 102481, 2020, doi: 10.1016/j.jnca.2019.102481.
- [20] A. Sultan, M. A. Mushtaq, and M. Abubakar, “IoT security issues via blockchain: A review paper,” in *ACM International Conference Proceeding Series*, 2019, vol. Part F148153, pp. 60–65, doi: 10.1145/3320154.3320163.

- [21] S. Alam, S. T. Siddiqui, and F. Masoodi, "SECURITY& PRIVACY THREATS, ATTACKS AND COUNTERMEASURES IN INTERNET OF THINGS," *Int. J. Netw. Secur. Its Appl.*, vol. 11, no. 2, 2019, doi: 10.5121/ijnsa.2019.11205.
- [22] D. Hawig, C. Zhou, S. Fuhrhop, A. S. Fialho, and N. Ramachandran, "Designing a distributed ledger technology system for interoperable and general data protection regulation-compliant health data exchange: A use case in blood glucose data," *J. Med. Internet Res.*, vol. 21, no. 6, pp. 1-13, 2019, doi: 10.2196/13665.
- [23] E. F. Jesus, V. R. L. Chicarino, C. V. N. De Albuquerque, and A. A. D. A. Rocha, "A Survey of How to Use Blockchain to Secure Internet of Things and the Stalker Attack," *Secur. Commun. Networks*, vol. 2018, 2018, doi: 10.1155/2018/9675050.
- [24] F. Aliyu, T. Sheltami, and E. M. Shakshuki, "A detection and prevention technique for man in the middle attack in fog computing," *Procedia Comput. Sci.*, vol. 141, pp. 24-31, 2018, doi: 10.1016/j.procs.2018.10.125.

إطار عمل أمن إنترنت الأشياء المعزز بتقنية البلوكشين: التحديات و الفرص

عبد محمد جباري

كلية علوم الحاسب وتقنية المعلومات، جامعة جازان، المملكة العربية السعودية

الملخص

في الأونة الأخيرة ، كان هناك اهتمام كبير بتقنية البلوكشين نظرًا لإمكاناتها المميزة لتحويل النظرة العامة للقطاع المالي. تزداد شعبية الاختراق المعروف والمعروف باسم البلوكشين. الصناعة المالية هي التي تستخدم الفكرة أكثر من غيرها. وقد تم استخدامه بنجاح لتحسين أوجه القصور الكبيرة في العمليات والمخاوف المتعلقة بقاعدة التكلفة. يسهل المصادقة وتتبع الإجراءات متعددة الخطوات التي تتطلب التأكيد والتتبع. يمكن استخدامه أيضًا لإدارة منصات التصويت ، بالإضافة إلى التعيينات والأنشطة نظرًا لقدرته على توفير تحقق يمكن التحقق منه من التأكيدات الرسمية. نظرًا لحقيقة أنه يتضمن عددًا لا يحصى من الأجهزة الذكية ذات إمكانات المعالجة والاستشعار والتشغيل ، فإن إنترنت الأشياء (IoT) يعتبر بمثابة تقنية لتغيير قواعد اللعبة. أدى دمج مبادئ الشبكات الاجتماعية في إنترنت الأشياء في مجتمع اليوم إلى ولادة مفهوم جديد يُعرف باسم إنترنت الأشياء الاجتماعي. يهتم إنترنت الأشياء في المقام الأول بالربط البيئي لمختلف الأدوات الذكية. نظرًا لنقص خيارات الأمان الأساسية ، فإن البنية التحتية لإنترنت الأشياء بأكملها معرضة لمخاوف تتعلق بالأمان والخصوصية. سيبحث هذا البحث في المشكلات الموجودة في أطر عمل IoT و البلوكشين للتخفيف من هذه المشكلات.

الكلمات المفتاحية: انترنت الأشياء، الامن السيبراني، البلوكشين (Blockchain).

A review of the key energy-based criteria under mixed mode I-II loading for brittle materials

A. S. Fayed

Department of Mechanical Engineering, College of Engineering, Jazan University, Saudi Arabia

Abstract

The propagation of a crack along two or more different fractured modes is an important topic of research within the field of structural integrity and fracture mechanics. As cracks exert a substantial influence on the performance and safety of any structure, it is vital to identify the appropriate criteria to expect crack propagation due to mixed mode loading. Many investigators have conducted several mixed-mode fracture experiments to determine several fracture parameters for brittle materials. These tests have been focused on fracture toughness, stress intensity factor and direction of crack advance. The results acquired from these tests have been theoretically validated using several mixed-mode fracture criteria. Many investigators have even developed empirical relations to approximate results that were not possible with existing famous fracture criteria. This paper will provide an overview of current energy-based criteria used to predict mixed mode crack propagation, including relevant studies. These criteria are vital in enhancing our understanding of fracture mechanics and will help in the development of safer and more reliable structures and components in various industries.

Keywords: Fracture mechanics; Mixed mode fracture; Brittle materials; Energy-based criteria.

1 INTRODUCTION

Structures often possess substantial pre-existing cracks that may or may not propagate, contingent on the level of load. If a material has a pre-existing crack, flaw, inclusion, or defect of unknown small size, the local stress concentration factor tends to approach infinity, making it practically futile for stress prediction. A head of the crack tip, the singularity stress field is completely defined for three modes of crack yip deformation [1], Fig. 1. (1) Mode I, opening mode, where the crack surfaces are displaced in opposite directions perpendicular to each other. (2) Mode II, in-plane sliding shear mode, where the crack surfaces move relative to each other, sliding perpendicularly to the crack's leading edge. (3) Mode III, tearing shear mode, where the surfaces of the crack undergo relative movement, parallel to the leading edge of the crack.

Brittle materials, e.g. rocks, glass, ceramics and certain polymers, show sudden and catastrophic fractures once crack exist. Brittle rocks are frequently utilized in various applications, such as rock cutting, tunneling, mining, and stability estimation of rock slop. The brittle collapse of rock occurs generally in mixed-mode I and II [2, 3]. Glasses, used in aerospace, are commonly exposed to both tensile and shear stress. This can cause pre-existing cracks to propagate more easily, leading to the failure of the material. Brittle materials may be prone to cracking during manufacturing or usage. When these materials are subjected to applied loads, cracks can propagate and lead to brittle failure and can result in serious damage to machines and equipment. The increasing demand for accurate predictions of component life and residual structure has led to a rising necessity for investigating crack growth in mechanical and structural elements. Conventional fracture mechanics primarily focused on

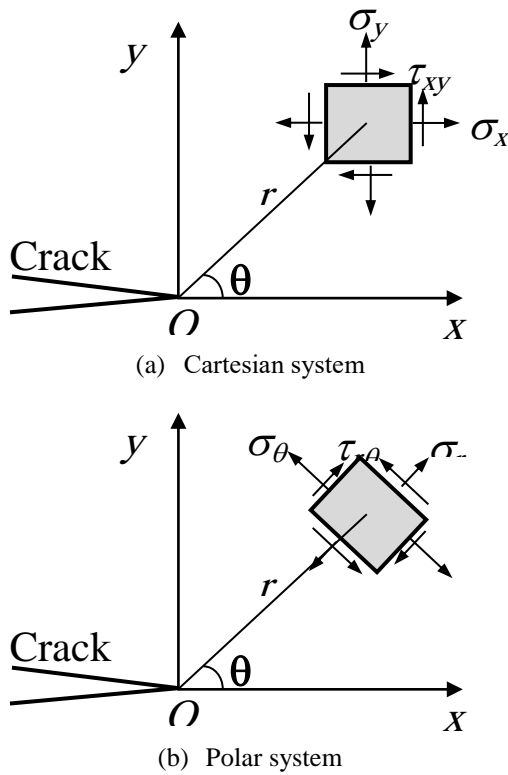


Fig. 1 The stress preceding the crack tip in various coordinate systems

cracks that grew in an opening mode pattern. Though, numerous service failures arise due to defects experiencing mixed-mode character. Many engineering applications provide examples of cracks loaded under mixed mode loadings.

Engineering components and structures loaded in a uniaxial manner frequently contain defects and cracks that are randomly oriented. Due to their direction to the loading axis, these cracks and defects often experience mixed mode conditions [4, 5]. A crack that starts from the surface of a tubing shaft in a transverse plane is exposed to combined loading when the shaft is under bending and torsion. An occurrence of mixed mode loading can be triggered during rolling contact with high-speed rotating bearings [6].

Cracks are a frequent issue in engineering materials and structures, posing a significant risk of damage and potential catastrophic

failure if not detected and addressed properly. Accurate prediction of crack initiation is essential to prevent structural failure, and researchers have recently developed various mixed-mode crack propagation criteria to predict crack extension under different loading conditions. This review article provides an inclusive analysis of the most applied mixed-mode crack initiation criteria. It briefly touches upon their limitations. The insights gathered here may provide an advance in the prediction of the crack behavior under mixed-mode loading.

Most of the serious problems of crack propagation is associated with rapid, catastrophic brittle failure of normally ductile materials at quite low elastic stresses. These stresses are only a small fraction of yield stress. A contemporary process for understanding the fracture resistance of materials that possess cracks is to investigate the displacement, stress and strain at the crack tip vicinity during its initial growth. Theoretical findings [1] indicates that at close proximity to the crack tip of an infinite two-dimensional plate under mode I and mode II loading, the elastic stress distribution is stated in Cartesian coordinates as:

$$\left\{ \begin{aligned} \sigma_x &= \frac{K_I}{\sqrt{2\pi r}} \cos \frac{\theta}{2} \left(1 - \sin \frac{\theta}{2} \sin \frac{3\theta}{2} \right) - \\ &\quad \frac{K_{II}}{\sqrt{2\pi r}} \sin \frac{\theta}{2} \left(2 + \cos \frac{\theta}{2} \cos \frac{3\theta}{2} \right) + O(\sqrt{r}) \\ \sigma_y &= \frac{K_I}{\sqrt{2\pi r}} \cos \frac{\theta}{2} \left(1 + \sin \frac{\theta}{2} \sin \frac{3\theta}{2} \right) + \\ &\quad \frac{K_{II}}{\sqrt{2\pi r}} \sin \frac{\theta}{2} \cos \frac{\theta}{2} \cos \frac{3\theta}{2} + O(\sqrt{r}) \\ \tau_{xy} &= \frac{K_I}{\sqrt{2\pi r}} \sin \frac{\theta}{2} \cos \frac{\theta}{2} \cos \frac{3\theta}{2} + \\ &\quad \frac{K_{II}}{\sqrt{2\pi r}} \cos \frac{\theta}{2} \left(1 - \sin \frac{\theta}{2} \sin \frac{3\theta}{2} \right) + O(\sqrt{r}) \\ \sigma_z &= \nu(\sigma_x + \sigma_y) \text{ plane strain} \\ &= 0 \text{ plane stress} \end{aligned} \right. \quad (1)$$

The distribution of elastic stress in polar coordinates can be defined as:

$$\left\{ \begin{array}{l} \sigma_{\theta} = \frac{K_I}{2\sqrt{2\pi r}} \cos \frac{\theta}{2} (1 + \cos \theta) - \\ \frac{3K_{II}}{2\sqrt{2\pi r}} \sin \frac{\theta}{2} (1 + \cos \theta) + O(\sqrt{r}) \\ \sigma_r = \frac{K_I}{2\sqrt{2\pi r}} \cos \frac{\theta}{2} (3 - \cos \theta) - \\ \frac{K_{II}}{2\sqrt{2\pi r}} \sin \frac{\theta}{2} (1 - 3\cos \theta) + O(\sqrt{r}) \\ \tau_{r\theta} = \frac{K_I}{2\sqrt{2\pi r}} \sin \frac{\theta}{2} (1 + \cos \theta) + \\ \frac{K_{II}}{2\sqrt{2\pi r}} \cos \frac{\theta}{2} (1 - 3\cos \theta) + O(\sqrt{r}) \end{array} \right. \quad (2)$$

Stress intensity factors (SIFs) K_I and K_{II} correspond to mode I and mode II, respectively. ν refers to Poisson's ratio. (x, y) and (r, θ) are defined Fig. 1. The crack tip experiences unique stress conditions due to the initial stresses from mode I and mode II. Higher-order non-singular stress terms of $O(\sqrt{r})$ are disregarded near the crack tip. These equations suggest that the distribution of the elastic stresses near the crack tip remains consistent across all components experiencing this manner of deformation. Consequently, the elastic stress field can be characterized by K_I and K_{II} .

2 CRACK INITIATION ANGLES UNDER MIXED-MODE LOADINGS

While crack propagation is commonly regarded as a significant driving mechanism to failure, additionally, it can function as a means of strengthening by facilitating crack kinking and generating unpredictable micro-cracks. Therefore, the exploration of crack propagation, stability, and interaction has been a central area of interest in the field of fracture mechanics. Since Griffith's pioneering research, there have been extensive studies in the field, specifically focusing on the behavior of crack kinking and branching in isotropic and anisotropic materials [8–13]. These studies concentrated on examining the state of the crack propagation path and its direction. By utilizing innovative computational methods

throughout each stage of propagation, it becomes possible to acquire related fracture parameters. Starting with a fundamental crack pattern, prediction of kink direction can be determined according to certain criterion. The choice of the most precise propagation criterion is material type dependent. Many studies suggested a comprehensive formulation for the examination of crack propagation based on displacement-boundary value problems [14]. These methods are currently in the developmental phase and may be used in situations involving multiple cracks. Numerous criteria were suggested to ascertain crack extension trajectory under mixed-mode fracture. Nevertheless, just a limited number of these criteria have been substantiated and demonstrated to yield results that align with certain experimental observations. Some of these criteria are reviewed here.

2.1 Minimum SED (MSED) Criterion

In 1974, Sih [15, 16] adopted local strain energy density (SED) and proposed the minimum SED (MSED) criterion. A comprehensive discourse is presented in [17]. The MSED criterion suggests that crack extends in a path that is aligned with the MSED direction along a fixed radius close to crack tip. The core region is defined by the area enclosed by this fixed radius. This theory presumes that the crack initiates in MSED path and extends as MSED has a critical value ($S_{cr} = S_{min}$). The variable S is defined in a manner that eliminates the singularity terms from the SED function and S is expressed as:

$$S = r_o \frac{dW}{dV} \quad (3)$$

In which, dW/dV refers to SED function per unit volume. r_o denotes a finite distance from the point where failure begins. When considering slit cracks, it is postulated that the crack tip acts as the point where failure initiates. Employing Eq. (1) of Cartesian

coordinates, the SED function per unit volume is expressed as:

$$\left\{ \begin{array}{l} S = a_{11}K_I^2 + 2a_{12}K_I K_{II} + 2a_{22}K_{II}^2 \\ a_{11} = \frac{(1 + \cos\theta)(k - \cos\theta)}{16G\pi} \\ a_{12} = \frac{\sin\theta [2\cos\theta - (k - 1)]}{16G\pi} \\ a_{22} = \frac{(k + 1)(1 - \cos\theta)}{16G\pi} + \frac{(1 + \cos\theta)(3\cos\theta - 1)}{16G\pi} \\ k = \frac{3 - \nu}{1 + \nu} \quad \text{plane stress} \\ k = 3 - 4\nu \quad \text{plane strain} \end{array} \right. \quad (4)$$

In which, G refers to modulus of rigidity. MSED criterion is mathematically indicated as:

$$\left\{ \begin{array}{l} \left. \frac{\partial S}{\partial \theta} \right|_{r=r_c, \theta=\theta_c} = 0, \quad \left. \frac{\partial^2 S}{\partial \theta^2} \right|_{r=r_c, \theta=\theta_c} > 0 \\ S|_{r=r_c, \theta=\theta_c} = S_{cr} \end{array} \right. \quad (5)$$

$$\left\{ \begin{array}{l} 2(1 + k)\lambda \tan^4 \frac{\theta}{2} + (2k(1 - \lambda^2) - 2\lambda^2 + 10)\tan^3 \frac{\theta}{2} - \\ 24\lambda \tan^2 \frac{\theta}{2} + (2k(1 - \lambda^2) + 6\lambda^2 - 14)\tan \frac{\theta}{2} + \\ 2(3 - k)\lambda = 0 \\ 2(k - 1)\lambda \sin\theta - 8\lambda \sin 2\theta + (k - 1)(1 - \lambda^2)\cos\theta + \\ 2(\lambda^2 - 3)\cos 2\theta > 0 \\ \text{in which, } \lambda = \frac{K_I}{K_{II}} \end{array} \right. \quad (6)$$

Once the equations for a crack in an infinite plane are derived, the SED function can be estimated using the stresses near the crack tip [18]. Utilizing the aforementioned formulation, the polar predicted angle (θ_c) that corresponds to the minimum MSED is determined in closed form. Once SIFs are acquired, you can utilize either (1) a closed form expression near the crack tip or (2) Employing a numerical approach, stresses at a particular distance from the crack tip can be determined. The analytical solution reveals that the result is contingent upon the type of material involved.

The MSED criterion stands as an indicator that unveils the interconnection between the angle at which cracks begin and the elastic

attributes of the material, as denoted by Poisson's ratio, alongside the prevailing stress conditions. The findings demonstrated a creditable concordance with empirical observations conducted on the Plexiglas material when considering $\nu = 1/3$ [16, 19, 20]. Kipp and Sih [21] employed the MSED to analyze elastic materials with notches. Their study focused on examining the fracture paths of plane elliptical cracks subjected to external tensile and compressive forces. They discovered a consistent

concurrency between the theoretical prediction and the empirical data. Gdoutos [22] authored a book encompassing a detailed exploration of the practical implementation of the MSED criterion in diverse crack configurations. Maiti and Smith [23] employed both MTS and MSED criterion to get the angle of crack extension, crack path, and critical load. They demonstrated that the MTS and SED are appropriate to estimate the threshold load for both elliptical and slit cracks that were subjected to uniaxial tensile loading. Carloni and Nobile [24] utilized the MSED to examine fracture characteristic of orthotropic materials. Their findings revealed that the extension of a crack was influenced by both the biaxiality parameter and the material's anisotropic properties. Alneasan and Behnia [25] utilized the MSED criterion to predict and describe the fracture envelope for low and high strain rates.

2.2 Maximum Energy Release Rate, ERR, (MERR) Criterion

In 1921, Griffith [26] proposed the initial criterion for fracture initiation. This criterion suggests that fracture transpires as the accumulated energy within the body surpasses the material's surface energy. This principle is only applicable to mode I load presuming a well-known crack extension beforehand. In 1974, Hussain et al. [27] formulated the maximum energy release rate, ERR, (MERR) criterion, which derives from the fundamental principles of Griffith energy. Their research illustrated that the onset of cracks transpires along the path aligned with the highest magnitude of energy release rate. In their work, Hussain et al. [24] developed the MERR criterion by assuming that, under combined loading, the crack advances along its original plane. Additionally, they considered the energy release rate (ERR), denoted as G , to be predetermined as follows:

$$\begin{cases} G = \frac{1}{E} (K_I^2 + K_{II}^2) \text{ for plane stress} \\ G = \frac{1 - \nu^2}{E} (K_I^2 + K_{II}^2) \text{ for plane strain} \end{cases} \quad (7)$$

Here, E represents the modulus of elasticity. In accordance with the MERR criterion, the following conditions must be met when the crack: (i) extends at MERR direction, and (ii) propagates when the MERR criterion is satisfied, indicating that the magnitude of MERR in that particular direction attains a critical threshold. That is,

$$\begin{cases} \left. \frac{\partial G}{\partial \theta} \right|_{r=r_c, \theta=\theta_c} = 0, & \left. \frac{\partial^2 G}{\partial \theta^2} \right|_{r=r_c, \theta=\theta_c} < 0, \\ G|_{r=r_c, \theta=\theta_c} = G_{cr} \end{cases} \quad (8)$$

In 1998, Awaji [20] introduced the notion of ERR pertaining to mixed mode loading. He expanded the applicability of Griffith's energy principle to encompass mode II fracture. To determine mode I and mode II SIFs ahead of a kink tip, denoted as k_1 and k_2 , respectively, at any given kink angle (θ), the coefficients K_{ij} can be computed through quadrature methods, as derived from the analysis conducted by Khrapkov [28]. Howard [29] performed calculations to determine these coefficients. In which, k_1 and k_2 are determined as follows:

$$\begin{cases} k_1 = K_I \left(\frac{3}{4} \cos \frac{\theta}{2} + \frac{1}{4} \cos \frac{3\theta}{2} \right) + \\ \quad K_{II} \left(-\frac{3}{4} \sin \frac{\theta}{2} - \frac{3}{4} \sin \frac{3\theta}{2} \right) \\ k_2 = K_I \left(\frac{1}{4} \sin \frac{\theta}{2} + \frac{1}{4} \sin \frac{3\theta}{2} \right) + \\ \quad K_{II} \left(\frac{1}{4} \cos \frac{\theta}{2} + \frac{3}{4} \cos \frac{3\theta}{2} \right) \end{cases} \quad (9)$$

The objective is to ascertain the angle (θ_c) of the actual crack extension. Therefore, any additional initial extension originating from the kink tip in that direction must align with the plane of the kink itself. Hence, when exploring the optimal onset angle that

maximizes the ERR, it is reasonable to restrict the search to extensions from the kink tip that align with the same path of the kink itself, i.e. co-planar extensions within the kink plane. For such kinks that lie within the same plane, the following equation is applicable.

$$\left\{ \begin{array}{l} g = g_1 + g_2 \\ \text{for plane stress;} \\ g_1 = \frac{k_1^2}{E}, g_2 = \frac{k_2^2}{E}, \\ g_c = \frac{K_{IC}^2}{E} \\ \text{for plane strain;} \\ g_1 = \frac{(1 - \nu^2)k_1^2}{E}, \\ g_2 = \frac{(1 - \nu^2)k_2^2}{E} \\ g_c = \frac{(1 - \nu^2)K_{IC}^2}{E} \\ \\ g_m = g_c \end{array} \right. \quad (10)$$

The MERR criterion can be expressed as $g_m = g_c$. In which g_m is the highest value of g . g_c is the material's ERR for fracture toughness. θ_c is calculated by maximizing g/g_c with respect to θ . K_{IC} is a material property that remains unaffected by the various loading modes present near to the crack tip [30].

2.3 T-Criterion

In 1982, Theocaris et al. [31–33] proposed the decomposition of the overall SED into two distinct components: dilatational and distortional. They asserted that: (i) the initiation of crack propagation occurs when the dilatational component, T_V , near the crack tip exceeds an essential threshold, $T_{V,cr}$, and (ii) the evaluation of T_V in the crack tip vicinity should be performed through the utilization of the elastic-plastic boundary determined by the von Mises yield condition. Therefore, the crack extends in the direction where the maximum dilatational strain energy is observed. The distortional component, T_D , keeps constant

within the elastic-plastic boundary. The quest for the maximum of T (entire strain energy described similarly to S in MSED criterion) is synonymous with the pursuit of peak values of T_V [31, 32]. Therefore, the disparity between the MSED and T criteria lies not in their distinct formats, but in their respective defined positions. In mathematical terms, the T-criterion can be represented as:

$$\left\{ \begin{array}{l} \frac{\partial T_V}{\partial \theta} \Big|_{r=r_c, \theta=\theta_c} = 0, \quad \frac{\partial^2 T_V}{\partial \theta^2} \Big|_{r=r_c, \theta=\theta_c} < 0, \end{array} \right. \quad (11)$$

$$\left\{ \begin{array}{l} T_V|_{r=r_c, \theta=\theta_c} = T_{V,cr} \\ T_V = \frac{1 - 2\nu}{6E} (\sigma_x + \sigma_y)^2 \\ T_D = \frac{1 + \nu}{3E} (\sigma_x^2 + \sigma_y^2 - \sigma_x \sigma_y + 3\tau_{xy}^2) \end{array} \right. \quad (12)$$

The equations for T_D and T_V are utilized under plane stress conditions; nevertheless, the outcomes remain consistent for plane strain conditions as well. Eq. (1) could be re-written as:

$$\left\{ \begin{array}{l} \sigma_x = \frac{1}{\sqrt{2\pi r}} f_x(\theta) \\ \sigma_y = \frac{1}{\sqrt{2\pi r}} f_y(\theta) \\ \sigma_{xy} = \frac{1}{\sqrt{2\pi r}} f_{xy}(\theta) \end{array} \right. \quad (13)$$

Using this notation, T_V and T_D can be written as:

$$\left\{ \begin{array}{l} T_V = \frac{1 - 2\nu}{12\pi E r} (f_x(\theta) + f_y(\theta))^2 \\ T_D = \frac{1 + \nu}{6\pi E r} (f_x^2(\theta) + f_y^2(\theta) - f_x(\theta)f_y(\theta) + 3f_{xy}^2(\theta)) \end{array} \right. \quad (14)$$

As the distortional strain energy remains constant within the elastic-plastic boundary specified by the von Mises approach, $T_{D,0}$ is a material constant.

$$\left\{ \begin{array}{l} r = \frac{1 + \nu}{6\pi ET_D} (f_x^2(\theta) + f_y^2(\theta) - \\ f_x(\theta)f_y(\theta) + 3f_{xy}^2(\theta)) \end{array} \right. \quad (15) \quad \left\{ \begin{array}{l} T_V = \left(\frac{(1 - 2\nu)T_{D,0}}{2(1 - \nu)} \right) \\ \left(\frac{(f_x(\theta) + f_y(\theta))^2}{(f_x^2(\theta) + f_y^2(\theta) - f_x(\theta)f_y(\theta) + 3f_{xy}^2(\theta))} \right) \end{array} \right. \quad (16)$$

Applying the T-criterion:

$$\left\{ \begin{array}{l} \tan^5 \frac{\theta}{2} - 4\lambda \tan^4 \frac{\theta}{2} + (5\lambda^2 - 1) \tan^3 \frac{\theta}{2} + \\ \frac{3 - 5\lambda^2}{2} \tan^2 \frac{\theta}{2} + \frac{\lambda^4 - 2\lambda^2 - 1}{2} \tan \frac{\theta}{2} + \\ \frac{(1 + \lambda^2)\lambda}{2} = 0 \\ (1 - 20\lambda^2 - 5\lambda^4)\cos\theta + 8(3 + 2\lambda^2 - \lambda^4)\cos 2\theta - \\ 3(3 - 12\lambda^2 + \lambda^4)\cos 3\theta + 2(13 + 5\lambda^2)\lambda\sin\theta + \\ 32(1 + \lambda^2)\lambda\sin 2\theta - 6(5 - 3\lambda^2)\lambda\sin 3\theta < 0 \end{array} \right. \quad (17)$$

In which, $\lambda = K_I/K_{II}$. Despite being derived from the modification of the MSED criterion, The T-criterion remains unaffected by Poisson's ratio or stress-state, displaying independence in both characteristics. Theocaris et al. [31–33] conducted experiments using polycarbonate material. Their predictions exhibited strong concordance with the experimental data regarding ductile failure [34]. As suggested by Theocaris and Andrianopoulos [31, 32], considering high brittle materials where the elastic-plastic border can be neglected, the boundary specified in the T-criterion may be approximated as a tiny circle, as proposed by the MSED criterion. In such conditions, the disparity between T-criterion and MSED criterion is minimal. Lam [35] identified another scenario where the discrepancy becomes insignificant, namely the presence of a long crack subjected to low levels of cyclic stress. In such cases, the reversed plastic zone boundary serves as the pertinent boundary between elastic and plastic behavior for the T-criterion and it is considerably smaller compared to the size of the monotonic zone of plasticity. Furthermore, the extent of the applied load during steady fatigue crack propagation is

generally significantly lower than the required load for fracture.

2.4 Y-Criterion

Although the T-criterion has gained widespread recognition in predicting material failure, many researchers have proposed that the distortional SED (DSED) might also have a notable influence on crack propagation. Thereafter, several based-SED fracture criteria were proposed [36–39]. In 1991, Yehia [39] presented a comprehensive formulation of the Y-criterion, a fracture criterion rooted in the distortional SEM component calculated at a fixed distance from the crack tip, representing an inherent material characteristic. The criterion incorporates a yield condition based on solid physical principles. It leverages the singular elastic stress within crack tip vicinity to determine the distortional SED component. The Y-criterion depends on a crucial threshold that can be determined through empirical methods using standardized tests. It can utilize yield conditions other than the Von-Mises yield state if their adequacy is ensured. Additionally, crack propagation

arises along the path of the minimum distortional SED, and propagation initiates when this minimum value exceeds or equals a critical threshold. An evaluation was conducted to assess the predictions of fracture loads and angle employing the Y-criterion with those of other mixed-mode fracture criteria within the framework of LEFM. The Y-criterion exhibited favorable predictions, especially when validated against existing experimental data. Its predictions demonstrated satisfactory and strong agreement with empirical findings and the MSED predictions across a wide range of ν values from 0.0 to 0.5.

2.5 Maximum Tangential SED (MTSED) Criterion

In 1991, Koo and Choy [40] suggested the maximum tangential SED (MTSED) criterion, demonstrating that the MTSED locus resides among the loci of the MTS and MTSN criteria. Subsequently, Ayatollahi et al. [41, 42] expanded the range of MTSED criterion to encompass analysis of mixed-mode I-II-III fracture behavior.

2.6 Average SED (ASED) Criterion

In 2001, Lazzarin and Zambardi [43] introduced the concept of the average SED (ASED) criterion in sharp V-notches. This criterion postulated that once the ASED surpassed a critical value within a designated control volume, the initial crack would initiate propagation. The ASED criterion garnered significant attention from many researchers and became widely adopted for analyzing failure in structures featuring cracks with V or U shapes [44–49]. Furthermore, a broad review was carried out to assess the usage of the ASED methodology in the context of welded structures and V-notches [46]. Their research findings indicated that a criterion based on volume demonstrated higher accuracy when compared to criteria based on points or lines. In 1985, Zhao [50] developed a thorough presentation for the MERR criterion,

applicable to various states involving mode I-II-III loading.

2.7 F-Criterion

In 1994, Shen et al. [51] proposed the F-criterion by introducing a modification to the MERR criterion. F-criterion takes into account the combined critical fracture energy of mode I and mode II, allowing for the evaluation of crack propagation under compression [52, 53]. In 2006, Chang et al. [54] introduced a general brittle fracture criterion for mode I-II fractures by the adoption of maximum potential ERR. They proposed a new expression for the energy release rate. They conducted fracture tests on aluminum alloy specimens subjected to mixed mode I-II loading conditions. Their objective was to validate the accuracy of MPERR criterion through experimental means. The results demonstrated excellent agreement between the theoretical predictions based on the MPERR criterion and the actual experimental findings.

3 CONCLUSIONS

A thorough analysis of the mixed mode I-II fracture criteria within the context of LEFM is presented. A comprehensive review of energy-based criteria is conducted, exploring their theoretical foundations, and investigating their practical applications. Furthermore, a concise discussion highlighting the advantages and limitations associated with these criteria is provided as well.

The onset of mixed mode cracks is a crucial parameter in determining the structural reliability and performance of a material. In evaluating mixed mode crack initiation, designers and engineers must consider the wide range of crack initiation criteria that exist and choose the one that is most accurate and suitable for their application. As a result, a general criterion for mixed-mode crack initiation is still a challenging topic in fracture mechanics, and researchers continue to explore new approaches to

developing a more reliable and practical criterion. These criteria are essential for predicting the performance of materials under complex loading and for designing structures that can endure such conditions.

The prediction of crack initiation and propagation varies significantly among different types of energy-based fracture criteria. None of these criteria can accurately predict experimental results for all cases. The choice of an appropriate fracture criterion is dependent on several factors, including the type of crack (open or closed), loading modes (tension-shear or compression-shear), and failure characteristics (tensile or shear failure).

REFERENCES

- Gdoutos, E.E.: Fracture mechanics. Springer Netherlands, Dordrecht (1993)
- Hammouda, M.M.I., Fayed, A.S.: Modes I/II SIF of a diametrically compressed Brazilian disc having a central inclined crack with frictional surfaces. *Fatigue Fract. Eng. Mater. Struct.* 41, 856–868 (2018). doi:10.1111/ffe.12733
- Fayed, A.S.: Numerical evaluation of mode I/II SIF of quasi-brittle materials using cracked semi-circular bend specimen. *Eng. Solid Mech.* 175–186 (2018). doi:10.5267/j.esm.2018.1.002
- Fayed, A.S., Sherbini, A.S., Abou El-Mal, H.S.S.: Mixed mode fracture behavior of fiber reinforced concrete; Experimental and numerical analysis adopting cracked Brazilian disc specimen. *Ain Shams Eng. J.* 14, 102132 (2023). doi:10.1016/J.ASEJ.2023.102132
- Fayed, A.S.: Numerical analysis of crack initiation direction in quasi-brittle materials. *Arab. J. Sci. Eng.* 44, 7667–7676 (2019). doi:10.1007/s13369-019-03860-4
- Ghosn, L.J.: Analysis of crack propagation in roller bearings using the boundary integral equation method—a mixed-mode loading problem. *J. Tribol.* 110, 408–413 (1988). doi:10.1115/1.3261643
- Williams, M.L.: On the Stress Distribution at the Base of a Stationary Crack. *J. Appl. Mech.* 24, 109–114 (1957). doi:10.1115/1.4011454
- Nemat-Nasser, S., Keer, L.M., Parihar, K.S.: Unstable growth of thermally induced interacting cracks in brittle solids. *Int. J. Solids Struct.* 14, 409–430 (1978). doi:10.1016/0020-7683(78)90007-0
- Cotterell, B., Rice, J.R.: Slightly curved or kinked cracks. *Int. J. Fract.* (1980). doi:10.1007/BF00012619
- Hayashi, K., Nemat-Nasser, S.: Energy release rate and crack kinking. *Int. J. Solids Struct.* 17, 107–114 (1981). doi:10.1016/0020-7683(81)90050-0
- Kfoury, A.P.: Crack extension under mixed-mode loading in an anisotropic mode–asymmetric material in respect of resistance to fracture. *Fatigue Fract. Eng. Mater. Struct.* 19, 27–38 (1996). doi:10.1111/J.1460-2695.1996.TB00929.X
- Qian, J., Fatemi, A.: Mixed mode fatigue crack growth: A literature survey. *Eng. Fract. Mech.* 55, 969–990 (1996). doi:10.1016/S0013-7944(96)00071-9
- Isaksson, P., Stahle, P.: Prediction of shear crack growth direction under compressive loading and plane strain conditions. *Int. J. Fract.* 113, 175–194 (2002). doi:10.1023/A:1015581922242/METRICS
- Hori, M., Vaikuntan, N.: Rigorous formulation of crack path in two-dimensional elastic body. *Mech. Mater.* 26, 1–14 (1997). doi:10.1016/S0167-6636(97)00008-2
- Sih, G.C.: Some basic problems in fracture mechanics and new concepts.

- Eng. Fract. Mech. 5, 365–377 (1973). doi:10.1016/0013-7944(73)90027-1
16. Sih, G.C.: Strain-energy-density factor applied to mixed mode crack problems. *Int. J. Fract.* (1974). doi:10.1007/BF00035493
 17. Sih, G.C.: *Mechanics of fracture initiation and propagation*. Springer Netherlands (1991)
 18. Sih, G.C.: *Methods of analysis and solutions of crack problems*. Springer Netherlands (1973)
 19. Erdogan, F., Sih, G.C.: On the crack extension in plane loading and transverse shear. *J. Basic Engr.* 85, 519–527 (1963). doi:10.1115/1.3656897
 20. Awaji, H.: The Griffith criterion for mode II fracture. *Int. J. Fract.* 89, L3–L7 (1998)
 21. Kipp, M.E., Sih, G.C.: The strain energy density failure criterion applied to notched elastic solids. *Int. J. Solids Struct.* 11, 153–173 (1975). doi:10.1016/0020-7683(75)90050-5
 22. Gdoutos, E.E.: *Problems of mixed mode crack propagation*. M. Nijhoff (1984)
 23. Maiti, S.K., Smith, R.A.: Comparison of the criteria for mixed mode brittle fracture based on the preinstability stress-strain field Part I: Slit and elliptical cracks under uniaxial tensile loading. *Int. J. Fract.* 23, 281–295 (1983). doi:10.1007/BF00020696/METRICS
 24. Carloni, C., Nobile, L.: Crack initiation behaviour of orthotropic solids as predicted by the strain energy density theory. *Theor. Appl. Fract. Mech.* 38, 109–119 (2002). doi:10.1016/S0167-8442(02)00089-7
 25. Alneasan, M., Behnia, M.: Analytical and experimental investigation on the effect of loading rate on the fracture toughness and fracture envelope in brittle rocks. *Theor. Appl. Fract. Mech.* 119, 103300 (2022). doi:10.1016/J.TAFMEC.2022.103300
 26. Griffith, A.A.: The phenomena of rupture and flow in solids. *Philos. Trans. R. Soc. London. Ser. A, Contain. Pap. a Math. or Phys. Character.* 4, 9–14 (1921). doi:10.1098/RSTA.1921.0006
 27. Hussain, M., Pu, S., Underwood, J.: Strain Energy Release Rate for a Crack Under Combined Mode I and Mode II. *Fract. Anal.* (1974). doi:10.1520/STP33130S
 28. Khrapkov, A.A.: The first basic problem for a notch at the apex of an infinite wedge. *Int. J. Fract. Mech.* 7, 373–382 (1971). doi:10.1007/BF00189109/METRICS
 29. Howard, I.C.: Simple approximate results for the stress intensity factors at the tip of a kinked crack. *Int. J. Fract.* 14, R307–R310 (1978). doi:10.1007/BF00116005/METRICS
 30. Kfoury, A.P., Brown, M.W.: A fracture criterion for cracks under mixed-mode loading. *Fatigue Fract. Eng. Mater. Struct.* 18, 959–969 (1995). doi:10.1111/J.1460-2695.1995.TB00920.X
 31. Theocaris, P.S., Andrianopoulos, N.P.: The T-criterion applied to ductile fracture. *Int. J. Fract.* (1982). doi:10.1007/BF01130617
 32. Theocaris, P.S., Andrianopoulos, N.P.: The mises elastic-plastic boundary as the core region in fracture criteria. *Eng. Fract. Mech.* 16, 425–432 (1982). doi:10.1016/0013-7944(82)90120-5
 33. Theocaris, P.S., Kardomateas, G.A., Andrianopoulos, N.P.: Experimental study of the T-criterion in ductile fractures. *Eng. Fract. Mech.* 17, 439–447 (1983). doi:10.1016/0013-7944(83)90040-1
 34. Khan, S.M.A. a, Khraisheh, M.K.: Analysis of mixed mode crack initiation angles under various loading conditions. *Eng. Fract. Mech.* 67, 397–419 (2000). doi:10.1016/S0013-7944(00)00068-0
 35. Lam, Y.C.: Fatigue crack growth under biaxial loading. *Fatigue Fract.*

- Eng. Mater. Struct. 16, 429–440 (1993). doi:10.1111/J.1460-2695.1993.TB00098.X
36. Du, Y., Aydin, A.: The maximum distortional strain energy density criterion for shear fracture propagation With applications to the growth paths of En Échelon faults. Geophys. Res. Lett. 20, 1091–1094 (1993). doi:10.1029/93GL01238
37. Yu-chuan, J., Qi-zhi, W.: A fracture criterion based on the deviator strain energy density factor. Eng. Mech. 22, 31–35 (2005)
38. Yishu, Z.: A strain energy criterion for mixed mode crack propagation. Eng. Fract. Mech. 26, 533–539 (1987). doi:10.1016/0013-7944(87)90096-8
39. Yehia, N.A.B.: Distortional strain energy density criterion: the Y-Criterion. Eng. Fract. Mech. 39, 477–485 (1991). doi:10.1016/0013-7944(91)90060-E
40. Koo, J.M., Choy, Y.S.: A new mixed mode fracture criterion: maximum tangential strain energy density criterion. Eng. Fract. Mech. (1991). doi:10.1016/0013-7944(91)90057-8
41. Ayatollahi, M.R., Saboori, B.: Maximum tangential strain energy density criterion for general mixed mode I/II/III brittle fracture. <http://dx.doi.org/10.1177/1056789514530745>. 24, 263–278 (2014). doi:10.1177/1056789514530745
42. Bahmani, A., Aliha, M.R.M., Berto, F.: Investigation of fracture toughness for a polycrystalline graphite under combined tensile-tear deformation. Theor. Appl. Fract. Mech. 90, 53–64 (2017). doi:10.1016/J.TAFMEC.2017.02.011
43. Lazzarin, P., Zambardi, R.: A finite-volume-energy based approach to predict the static and fatigue behavior of components with sharp V-shaped notches. Int. J. Fract. 112, 275–298 (2001). doi:10.1023/A:1013595930617/METRICS
44. Fan, H.B.O., Chung, P.W.K., Yuen, M.M.F., Chan, P.C.H.: An energy-based failure criterion for delamination initiation in electronic packaging. J. Adhes. Sci. Technol. 19, 1375–1386 (2005). doi:10.1163/156856105774784349
45. Lazzarin, P., Berto, F., Gomez, F.J., Zappalorto, M.: Some advantages derived from the use of the strain energy density over a control volume in fatigue strength assessments of welded joints. Int. J. Fatigue. 30, 1345–1357 (2008). doi:10.1016/J.IJFATIGUE.2007.10.012
46. Berto, F., Lazzarin, P.: A review of the volume-based strain energy density approach applied to V-notches and welded structures. Theor. Appl. Fract. Mech. 52, 183–194 (2009). doi:10.1016/J.TAFMEC.2009.10.001
47. Ayatollahi, M.R., Berto, F., Lazzarin, P.: Mixed mode brittle fracture of sharp and blunt V-notches in polycrystalline graphite. Carbon N. Y. 49, 2465–2474 (2011). doi:10.1016/J.CARBON.2011.02.015
48. Razavi, S.M.J., Aliha, M.R.M., Berto, F.: Application of an average strain energy density criterion to obtain the mixed mode fracture load of granite rock tested with the cracked asymmetric four-point bend specimens. Theor. Appl. Fract. Mech. 97, 419–425 (2018). doi:10.1016/J.TAFMEC.2017.07.004
49. Ayatollahi, M.R., Berto, F., Campagnolo, A., Gallo, P., Tang, K.: Review of local strain energy density theory for the fracture assessment of V-notches under mixed mode loading. Eng. Solid Mech. 5, 113–132 (2017). doi:10.5267/J.ESM.2017.3.001
50. Zhao, Y.: Generalized maximum energy release rate fracture criterion. J. Huazhong Univ. Sci. Technol. 1, 57–60 (1985)
51. Shen, B., Stephansson, O.:

- Modification of the G-criterion for crack propagation subjected to compression. *Eng. Fract. Mech.* 47, 177–189 (1994). doi:10.1016/0013-7944(94)90219-4
52. Shen, B.: Development and applications of rock fracture mechanics modelling with FRACOD: a general review. <http://dx.doi.org/10.1080/12269328.2014.969388>. 17, 235–252 (2014). doi:10.1080/12269328.2014.969388
53. Shen, B., Siren, T., Rinne, M.: Modelling Fracture Propagation in Anisotropic Rock Mass. *Rock Mech. Rock Eng.* 48, 1067–1081 (2015). doi:10.1007/S00603-014-0621-X/METRICS
54. Chang, J., Xu, J.Q., Mutoh, Y.: A general mixed-mode brittle fracture criterion for cracked materials. *Eng. Fract. Mech.* 73, 1249–1263 (2006). doi:10.1016/J.ENGFRACMECH.2005.12.011

مراجعة المعايير الرئيسية القائمة على الطاقة في إطار التحميل المختلط I-II للمواد الهشة

عمرو شحاته محمد فايد

قسم الهندسة الميكانيكية، كلية الهندسة، جامعة جازان، المملكة العربية السعودية

الملخص

يعد انتشار الشروخ عبر نمطي كسر مختلفين أو أكثر موضوع بحث مهم في مجال سلامة الهياكل وميكانيكا الكسر. حيث يوجد للشرخ تأثيرًا كبيرًا على أداء وسلامة أي هيكل، ولذلك من الضروري تحديد المعايير المناسبة لتوقع انتشار الشرخ نتيجة للتحميل بأنماط مختلطة. ولقد أجري العديد من الباحثين كثير من التجارب على نمط الكسر المختلط لإيجاد عدة متغيرات للمواد الهشة. تركزت هذه التجارب على إيجاد مقاومة الكسر ومعامل تركيز الإجهاد واتجاه تقدم الشرخ. تم التحقق نظريًا من النتائج المتحصلة من هذه التجارب باستخدام العديد من المعايير في حالة الكسر المختلط. وقام العديد من الباحثين بتطوير علاقات تجريبية لتقريب النتائج التي لم يكن ممكنًا الحصول عليها باستخدام المعايير المشهورة الحالية لميكانيكا الكسر. ستوفر هذه الورقة نظرة عامة على المعايير الحالية المستندة على الطاقة المستخدمة لتوقع انتشار الشرخ تحت تأثير الأنماط المختلطة، بما في ذلك الدراسات ذات الصلة. وهذه المعايير حيوية في تعزيز فهمنا لميكانيكا الكسر وستساعد في تطوير هياكل ومكونات أكثر أمانًا وموثوقية في مختلف الصناعات.

الكلمات المفتاحية: ميكانيكا الكسر، الوضع المختلط، مواد هشة، المعايير القائمة على الطاقة.

A hybrid ROA-KNN approach for botnet detection in IoT networks

Waleed Abdu Zogaan

Department of Computer Science, Faculty of Computer Science and Information Technology,
Jazan University, Saudi Arabia

Abstract

The Internet of Things (IoT) is integral part of various industries from healthcare to transportation and will continue to penetrate more industries in future. In this scenario, the satisfaction of security requirements plays a fundamental role. Botnet has become one of the most largest security threats to these networks. The Botnet detection has become more challenging due to its hidden and carrying capacity. Although machine learning (ML) models have enhanced Botnet detection, the curse of dimensionality significantly limits the performance of ML models. This paper uses a hybrid approach, Remora Optimization Algorithm (ROA) selects the most informative features, and then the selected features are fed to the ML model. Five different ML models comprising logistic regression, k-Nearest Neighbor (kNN), support vector machine, random forest, and AdaBoost are assessed and validated on two open-source IoT Botnet detection datasets. The developed ROA-kNN obtained the best results compared to the other comparative models.

Keywords: Botnet detection, IoT, machine learning, security

1. Introduction

In recent years, both academics and business have given the Internet of Things (IoT) a lot of attention. Internet-connected gadgets and IoT networks have gained enormous appeal in a variety of applications, including smart cities, smart healthcare, smart transportation, and smart farming, as a result of their incredibly rapid growth [1]. Also, IoT technology can participate in the applicability of efficient resourceful services for reaching a sustainable living standard as a target point in the presence of physical infrastructures.

Due to the widespread use of IoT systems and devices, a vast volume of data with specific characteristics can be collected [2]. The fact is that these collected data are only raw data with little valuable information. Therefore, data processing and analysis

techniques are required to extract valuable and meaningful information from the large data produced by IoT devices [3]. Making predictions with the help of these data can help to manage the potential future scenarios more effectively.

The smartness of IoT systems, or the transition from traditional IoT to intelligent IoT, is another critical topic in the IoT world [4]. ML models can be used to take this issue [5][6]. Recently, ML methods have shown great potential in detecting IoT Botnet [7,8,9,10]. In [11], the authors suggested a method for intelligently detecting harmful intrusions in IoT systems that makes use of efficient categorization of benign and malicious assaults. To find abnormalities and other harmful behaviour in the IoT, an ensemble approach combining several machine learning techniques and

deep learning is applied. In [12], a novel Feature Selection (FS) metric is developed that relies on the wrapper method to filter the features precisely. Then they utilized a random forest algorithm to identify harmful traffic detection in an IoT network.

In [13], a novel wrapper FS model that uses Emperor Penguin Colony method to select more informative features and k-Nearest Neighbor (kNN) classifier in IoT. Paper [14], explainable ML is explored for effective packet-based Botnet detection. The authors focused on feature selection to produce a realistic dataset to train an ML model to achieve very high accuracy. Paper [15], a Fuzzy Logic based feature engineering method is proposed to identify the fuzzy elements in the CTU-13 dataset. The features generated, using the proposed approach, are then used to feed an artificial neural network for Botnet detection.

ML techniques can be used to process, analyze, and extract useful information from a given data that, in most situations, is hard detectable by humans. However, IoT systems can become more intelligent and considerably more effective at making decisions by using ML models because they can find hidden patterns in data, identify semantic relationships between data points, and forecast the future based on the analysis of historical data. Meta-Heuristic (MH) methods are popular for FS purposes because of their strong self-learning capabilities, which can maintain a relatively high detection accuracy of Botnet features. In the current work, a hybrid approach employs ROA as FS-based MH method and then the selected informative features by the ROA are used as inputs to the ML model. This paper uses five different ML models

comprising Logistic Regression (LR), kNN, Support Vector Machine (SVM), Random Forest (RF), and AdaBoost (AB). The effectiveness of the hybrid approach is investigated using several quantitative evaluation measures on two publically available datasets for Botnet detection in an IoT environment. The ROA-kNN showed better performance than the other models for botnet detection.

The remaining parts of this paper are structured as follows: Section 2 describes the proposed method and a brief overview of ROA. In section 3, the description of the dataset is provided. In section 4, experimental results are presented. The paper is concluded with future research directions in section 5,

2. Methods and Materials

2.1. ROA

ROA [16] is a new MH method that mimics the concept of parasitism of Remora. Exploration and exploitation of ROA are briefly described in this section.

2.1.1. Exploration

▪ Swordfish Optimization Strategy

To explore new region the search space, the Remora's location is updated when it adheres to the swordfish using:

$$R_i^{t+1} = R_{ibest}^t - (rand(0,1)) \left(\frac{R_{ibest}^t - R_{rand}^t}{2} - R_{rand}^t \right) \quad (1)$$

where t is the number of current iterations; R_{ibest}^t refers to the best-obtained solution and R_{rand}^t indicates a random location, and $rand(0,1)$ is a random number in the range of 0–1.

- Attack experience

Remora takes small steps in the vicinity of the host end to identify whether or not to change the host based on fitness. This behavior mathematically can be presented as:

$$R_{att} = R_i^t + (R_i^t - R_{pre}) * randn \quad (2)$$

where is R_{att} the test step, R_{pre} is the Remora's position in prior iteration, and $randn$ is the small global random step of the Remora.

Then Remora randomly checks the change in the fitness values between the current response, $(f(R_i^t))$ and the tested response $(f(R_{att}))$. If $(f(R_i^t) > f(R_{att}))$, then, Remora employs local optimization using one of the feeding techniques, while if $(f(R_i^t) < f(R_{att}))$, Remora picks the host.

2.1.2. Exploitation (Thoughtful Nutrition)

- WOA Strategy

Remora's location when attached to the whale is updated as:

$$R_{i+1}^t = D * exp^\alpha * cos(2\pi x) + R_i^t \quad (3)$$

$$\alpha = rand(0,1) * (\alpha - 1) + 1 \quad (4)$$

$$x = -\left(1 + \frac{t}{T}\right) \quad (5)$$

$$D = [R_{best} - R_i] * R_i \quad (6)$$

where t is the number of iterations, α is a random number $[-1, 1]$, D presents the distance between the hunter and prey, α varies linearly from -2 to -1.

- Host nutrition

A minor step in the exploitation process called "host feeding" produces a solution space that gradually condenses around the host, improving the capabilities of local optimization. Mathematically this stage can be expressed as follows:

$$R_i^t = R_i^t + A \quad (7)$$

$$A = B * (R_i^t - C * R_{best}) \quad (8)$$

$$B = 2 * V * rand(0,1) - V \quad (9)$$

$$V = 2 \left(1 - \frac{t}{T}\right) \quad (10)$$

where A is a small step between the fish adhesive and host, C is the coefficient of stickiness in 0–0.3.

2.2. Developed approach

The investigations reported in the literature indicate that the use of ML models has significantly improved Botnet detection. The performance of commonly used ML models such as LR, kNN, and SVM depends on the size of the input dataset, the number of examples per class, and the feature dimensionality. Although network attacks are rare, care has been taken to represent attacks and regular network traffic in a balanced dataset. Hence, only feature dimensionality needs to be taken care of to improve the detection performance.

Although some ML models, such as random forest, and AdaBoost, have an inbuilt capacity to select essential features, the computational complexity of such models increases with redundant features. Hence, a hybrid approach with a unique feature selection algorithm and an ML model will improve Botnet detection performance. In recent years, MH algorithms have shown a good feature selection ability in various optimization problems. These algorithms are gradient-free and do not require large hyper-parameters. This work explores Remora Optimization Algorithm (ROA) to select the optimum feature set. Figure 1 shows a detailed architecture of the hybrid approach.

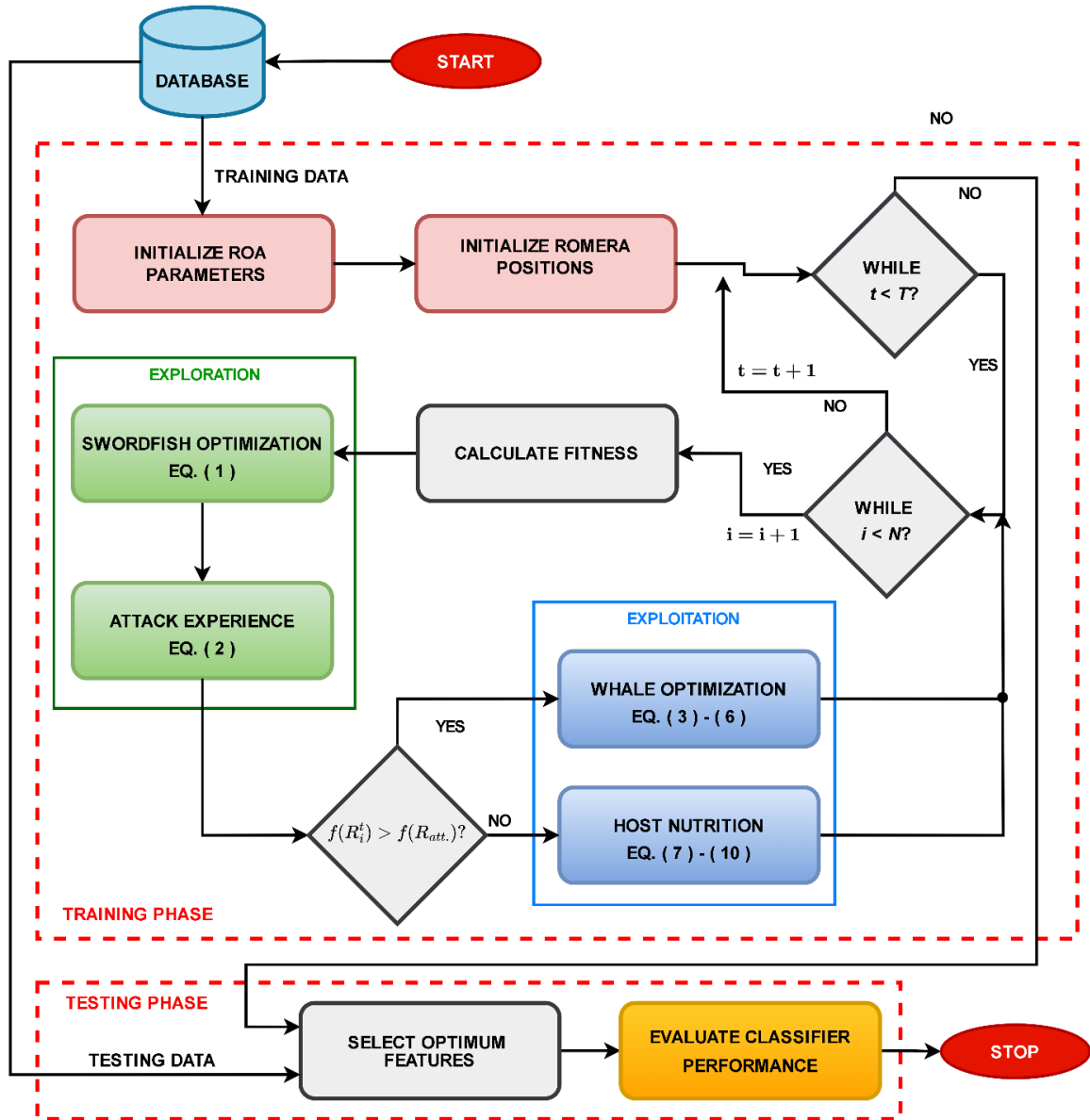


Figure 1. The ROA-based hybrid Botnet detection framework.

The dataset is divided into two mutually exhaustive subsets for training and testing. The training data is used to select the optimum feature subset by ROA with fitness function as an objective measure to optimize the process. The optimum feature set (OFS) obtained during the training is used to select the important features and then passed to the classifier for evaluation.

3. Datasets

3.1.1. Dataset 1

The N-BaIoT dataset is created in UNSW Canberra cyber center. The dataset is realistically created in an IoT network to simulate various botnet scenarios. It collaborates the regular and Botnet traffic

with the label using many virtual machines on the company's internal network to model various malicious attacks to capture legitimate and malicious traffic. The dataset comprises more than 72 million records with various malicious attacks, including DDoS, DoS, OS, Data exfiltration, and Keylogging assaults, as well as extra DDoS and DoS attacks [17]. The BoT-IoT dataset is grouped depending on attack categories and has a realistic testbed. This work uses 999,610 records with 994,828 botnet traffic and the remaining regular traffic. Each traffic record is represented by 115 real-valued features.

3.1.2. Dataset 2

Despite attempts to create datasets of assaults on IoT devices, several potential attacks in the IoT environment are not available in these datasets. The majority of datasets does not take into account a complex network architecture with actual IoT devices. CICIoT2023 is a real-time dataset for large-scale attacks in IoT environments [18]. It uses a brand-new, sizable IoT attack dataset to encourage the creation of security analytics tools for actual IoT operations. It comprises 33 attacks run over 105 IoT devices. Seven attacks, namely Web-based, Spoofing, Brute Force, DDoS, Recon, DoS, and Mirai, are used to categorise these attacks. Each traffic record is represented by 47 real-valued features.

Table 1. Dataset characteristics.

Dataset	Source	# features	No. of samples
N-BaIoT	[17]	115	999,610
CICIoT2023	[18]	47	10,340,161

Table 1 describes the basic characteristics of both datasets. The analysis of individual

datasets with class-specific distribution is provided in respective source articles and is not repeated here. Due to a huge number of traffic records, using an iterative FS such as MH methods will be computationally expensive. Hence, only 10% of the dataset is used for FS evaluation while maintaining the ratio of network activities.

4. Experimental results

4.1. Experimental setup

The standard parameters of ROA, such as population size and the maximum number of iterations, are empirically set as 30 and 100, and the optimization method is carried out by running 20 independent ROA executions. The hyper-parameters settings used for ROA and all classifiers are given in Table 2. All the experiments are conducted on a computer with 3.13 GHz PC with 32 GB RAM and Ubuntu 22.04.1 LTS operating system and implemented using Python sci-kit-learn.

4.2. Evaluation measures

Four quantitative measures are used to evaluate the hybrid model and are calculated as follows:

Table 2. Hyper-parameter settings for FS and classifiers.

Method	Parameters
ROA	$ld = 1$ and $\beta = 2$
LR	Penalty=L2, train_bias = True, solver='lbfgs', max_iter=200,
kNN	Neighbors = 15, algorithm = 'KDTree', leaf_size = 20, distance = 'minkowski'
SVM	Regularization = 10, kernel= 'rbf', gamma='scale', decision_function = one-vs-rest
RF	Estimators = 500, criterion='gini', max_depth = 8, min_samples_split = 5, max_features = 8
AB	Estimator = 'Decision Tree', estimators = 100, learning_rate = 0.9, algorithm='SAMME.R'

$$AC = \frac{TP + TN}{TP + TN + FN + FP} \quad (11)$$

$$\text{Precision} = \frac{TP}{TP + FP} \quad (12)$$

$$\text{Recall} = \frac{TP}{TP + FN} \quad (13)$$

$$\text{F1-score} = \frac{2PR}{P + R} \quad (14)$$

where, True Positive and (TP) and True Negative (TN) denote the samples of customers correctly detected as an attack or not, while False Negative (FN) and False Positive (FP) represent the number of misclassified positive and negative cases, respectively.

4.3. Experimental results and discussion

The five classifiers with optimum hyper-parameters, reported in Table 2, are used for Botnet detection using two datasets reported in Table 1. The performance of all classifiers

in terms of mean and standard deviation (SD) of detection accuracy is shown in Table 3. The AB and RF provide the highest mean detection accuracy for N-BaIoT and CICIoT2023 datasets. The primary reason for the slightly inferior performance of the remaining classifiers is the absence of an inbuilt feature selection.

Table 3. Botnet detection accuracy of five classifiers for N-BaIoT and CICIoT2023 datasets.

Model	N-BaIoT		CICIoT2023	
	Mean	SD	Mean	SD
LR	88.846	2.015	98.901	0.632
kNN	89.913	1.985	98.410	0.089
SVM	88.912	2.012	98.152	0.129
RF	90.486	1.616	99.672	0.083
AB	91.123	1.329	99.573	0.071

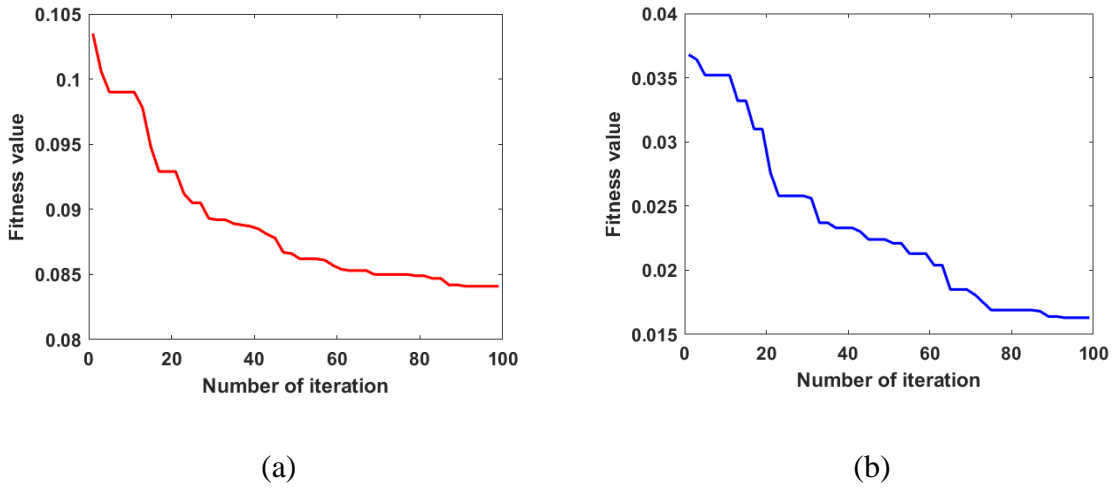


Figure. 2. Convergence behavior of ROA for Botnet detection using (a) N-BaIoT and (b) CICIoT2023 datasets.

To examine the efficiency of the hybrid approach, the real-world dataset provided in Table 1 is analysed using ROA. The convergence behavior of ROA-based feature selection for N-BaIoT and CICIoT2023 datasets is shown in Figure 2. It shows the variation of the fitness value, a combined measure of classification loss and fitness value, over different iterations [16]. The convergence behaviors shown in Figure 2 are the best among 20 independent runs for each dataset, ranked based on the final fitness value. As shown in the figure, the fitness value decreases rapidly at the start for both datasets. The fitness value converges to a minimal value of 0.0841 for the N-BaIoT dataset and 0.0163 for the CICIoT2023 dataset. This fitness value selects 64 optimum features out of 115 for the N-BaIoT dataset and 33 optimum features out of 47 for the CICIoT2023 dataset, i.e. approximately 44.34 % and 29.78 % compression in feature dimensionality for N-BaIoT and CICIoT2023 datasets, respectively.

The selected features are then passed as input to five classifiers. Table 4 shows the comparative analysis of the hybrid approach with ROA-based feature selection and five

classifiers for both datasets. The mean detection accuracy of all classifiers except LR and SVM for the N-BaIoT dataset has increased. The combination of ROA and kNN (ROA-kNN) shows the highest accuracy of 92.085 and 99.923 for the N-BaIoT and CICIoT2023 datasets. It can also be noted that the increase in the ROA-RF and ROA-AB mean accuracy values is smaller than classifiers without an inbuilt feature selection mechanism. The standard deviation of all classifiers for both datasets is reduced, indicating increased stability of the hybrid models.

Model	N-BaIoT		CICIoT2023	
	Mean	SD	Mean	SD
ROA-LR	88.235	1.011	97.621	0.411
ROA-kNN	92.085	1.016	99.923	0.009
ROA-SVM	89.231	1.184	98.414	0.606
ROA-RF	91.011	1.349	99.481	0.031
ROA-AB	90.562	1.105	99.689	0.029

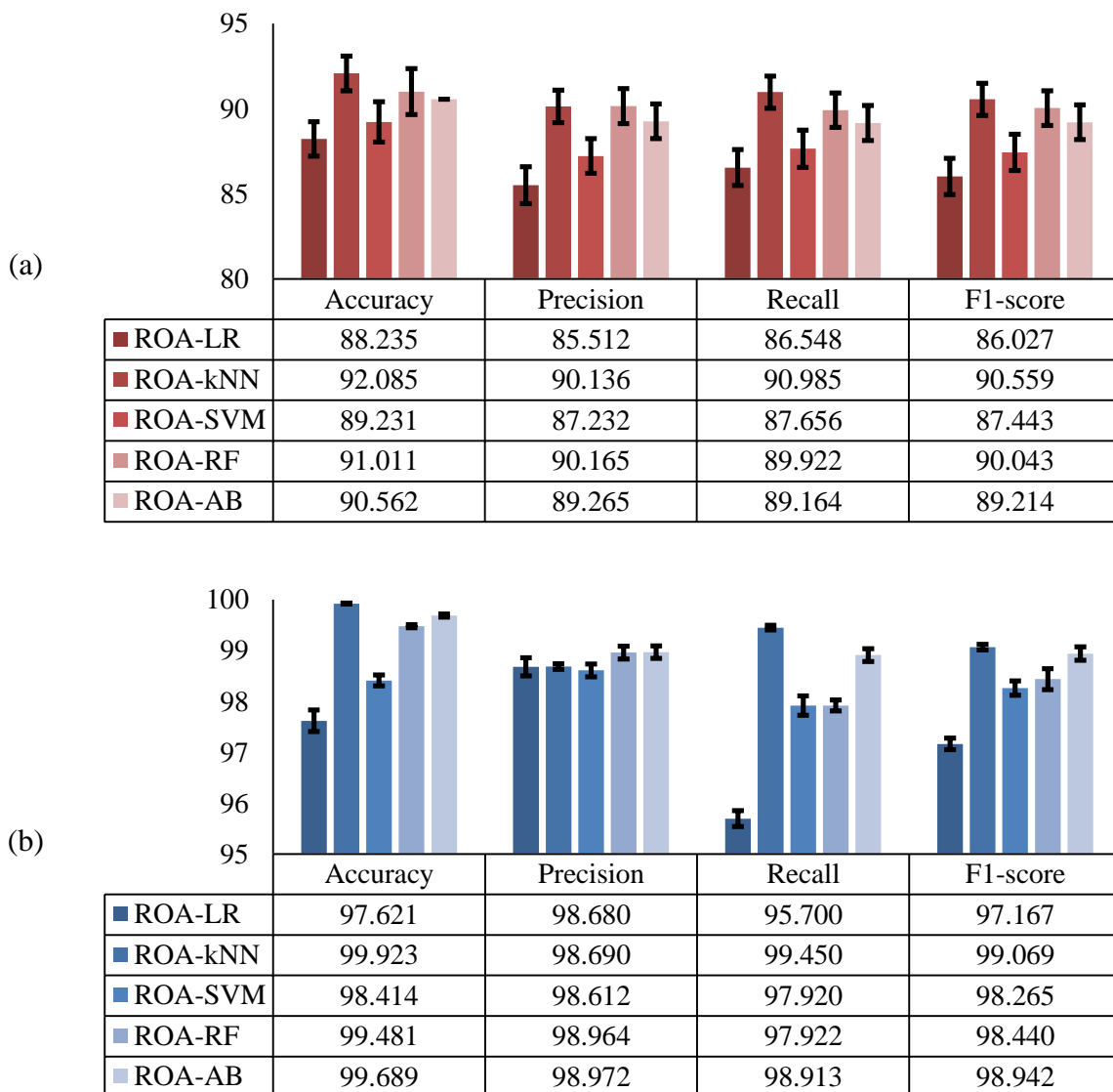


Figure 3. Comparative analysis of ROA-based hybrid models for Botnet detection using (a) N-BaIoT and (b) CICIoT2023 datasets.

The results of the hybrid classifiers in terms of accuracy, precision, recall, and F1-score for both N-BaIoT and CICIoT2023 datasets are illustrated in Figure 3. The mean of each measure is represented using a bar plot with a marker for SD. For the N-BaIoT dataset, ROA-RF has slightly higher precision than ROA-kNN but recall for the latter is significantly higher than the prior model. This can be seen by a higher F1-score for ROA-kNN than ROA-RF. Hence, ROA-kNN provides the best performance, followed by ROA-RF, ROA-AB, ROA-SVM, and ROA-LR. For the CICIoT2023 dataset, both ROA-RF and ROA-AB models have higher precision than ROA-kNN, but recall for the latter is highest amongst all the

hybrid models. The higher F1-score can confirm this for the ROA-kNN model. Hence, the performance-based ranking of the models for the CICIoT2023 dataset is: ROA-kNN, ROA-AB, ROA-RF, ROASVM, and ROA-LR.

5. Conclusion and future works

This paper presents a hybrid ML approach for Botnet detection in an IoT environment. It comprises the ROA as an FS and the selected informative features are used as inputs to the ML model for Botnet detection. Five different ML models are evaluated in this hybrid approach using two open-source datasets for Botnet detections. Results show that the ROA-kNN model gained better

results than ROA-LR, ROA-SVM, ROA-RF, and ROA-AB. In the future, the hybrid ROA-kNN models can be used for different applications such as intrusion detection, signal processing, and big data. Another possible lane is exploring other MH methods to be applied as an FS in Botnet detection. Lastly, the ROA-kNN model can be tested in real-time to measure its efficiency and handle different attacks accurately.

References

- [1] Khanna, A., & Kaur, S. (2020). Internet of things (IoT), applications and challenges: a comprehensive review. *Wireless Personal Communications*, 114, 1687-1762.
- [2] Lee, I., & Lee, K. (2015). The Internet of Things (IoT): Applications, investments, and challenges for enterprises. *Business horizons*, 58(4), 431-440.
- [3] Rashid, M. M., Kamruzzaman, J., Hassan, M. M., Imam, T., & Gordon, S. (2020). Cyberattacks detection in iot-based smart city applications using machine learning techniques. *International Journal of environmental research and public health*, 17(24), 9347.
- [4] Nguyen, T. N., Ngo, Q. D., Nguyen, H. T., & Nguyen, G. L. (2022). An advanced computing approach for IoT-botnet detection in industrial Internet of Things. *IEEE Transactions on Industrial Informatics*, 18(11), 8298-8306.
- [5] Popoola, S. I., Adebisi, B., Hammoudeh, M., Gui, G., & Gacanin, H. (2020). Hybrid deep learning for botnet attack detection in the internet-of-things networks. *IEEE Internet of Things Journal*, 8(6), 4944-4956.
- [6] Sarker, I. H., Khan, A. I., Abushark, Y. B., & Alsolami, F. (2022). Internet of things (iot) security intelligence: a comprehensive overview, machine learning solutions and research directions. *Mobile Networks and Applications*, 1-17.
- [7] Kumar, A., Shridhar, M., Swaminathan, S., & Lim, T. J. (2022). Machine learning-based early detection of IoT botnets using network-edge traffic. *Computers & Security*, 117, 102693.
- [8] Khan, S., & Mailewa, A. B. (2023). Discover Botnets in IoT Sensor Networks: A Lightweight Deep Learning Framework with Hybrid Self-Organizing Maps. *Microprocessors and Microsystems*, 104753.
- [9] Elsayed, N., ElSayed, Z., & Bayoumi, M. (2023). IoT Botnet Detection Using an Economic Deep Learning Model. *arXiv preprint arXiv:2302.02013*.
- [10] Pour, M. S., Mangino, A., Friday, K., Rathbun, M., Bou-Harb, E., Iqbal, F., ... & Erradi, A. (2019, August). Data-driven curation, learning and analysis for inferring evolving iot botnets in the wild. In *Proceedings of the 14th International Conference on Availability, Reliability and Security* (pp. 1-10).

- [11] Iftikhar, S., Khan, D., Al-Madani, D., Alheeti, K. M. A., & Fatima, K. (2022). An Intelligent Detection of Malicious Intrusions in IoT Based on Machine Learning and Deep Learning Techniques. *Computer Science*, 30(3), 90.
- [12] Pavaiyarkarasi, R., Manimegalai, T., Satheeshkumar, S., Dhivya, K., & Ramkumar, G. (2022, April). A Productive Feature Selection Criterion for Bot-IoT Recognition based on Random Forest Algorithm. In *2022 IEEE 11th International Conference on Communication Systems and Network Technologies (CSNT)* (pp. 539-545). IEEE.
- [13] Alweshah, M., Hammouri, A., Alkhalaleh, S., & Alzubi, O. (2022). Intrusion detection for the Internet of things (IoT) based on the emperor penguin colony optimization algorithm. *Journal of Ambient Intelligence and Humanized Computing*, 1-18.
- [14] Alani, M. M. (2022). BotStop: Packet-based efficient and explainable IoT botnet detection using machine learning. *Computer Communications*, 193, 53-62.
- [15] Joshi, C., Ranjan, R. K., & Bharti, V. (2022). A Fuzzy Logic based feature engineering approach for Botnet detection using ANN. *Journal of King Saud University-Computer and Information Sciences*, 34(9), 6872-6882.
- [16] Jia, H., Peng, X., & Lang, C. (2021). Remora optimization algorithm. *Expert Systems with Applications*, 185, 115665.
- [17] Koroniotis, N., Moustafa, N., Sitnikova, E., & Turnbull, B. (2019). Towards the development of realistic botnet dataset in the Internet of things for network forensic analytics: Bot-iot dataset. *Future Generation Computer Systems*, 100, 779-796.
- [18] Neto, E.C.P., Dadkhah, S., Ferreira, R., Zohourian, A., Lu, R., Ghorbani, A.A. (2023). CICIoT2023: A real-time dataset and benchmark for large-scale attacks in IoT environment. *Preprints.org*, 2023050443.

منهجية هجينه لاكتشاف هجمات Botnet على انترنت الأشياء باستخدام خوارزميات تعلم الآلة

وليد عبده زعقان

قسم علوم الحاسب الآلي، كلية علوم الحاسب وتقنية المعلومات، جامعة جازان

المملكة العربية السعودية

الملخص

يمثل انترنت الأشياء جزء أساسي وهام في العديد من الصناعات من القطاع الصحي الى النقل وسيستمر في اختراق الكثير من الصناعات في المستقبل. نظراً لهذي الأهمية، فإن استيفاء معايير الحماية يلعب دور هام للغاية في هذا المجال. هجمات Botnet أصبحت تمثل أحد أكبر التهديدات الأمنية لشبكات انترنت الأشياء. رصد هذه الهجمات أصبح يواجه تحدي كبير نظراً لسعته المخفية. رغم ان خوارزميات تعلم الآلة حسنت آليات رصد هجمات Botnet ولكن مشكلة الابعاد ما زالت تؤثر بشكل كبير على أداء خوارزميات تعلم الآلة. هذا البحث يستخدم منهجية هجينة تعتمد على خوارزمية ROA والتي تقوم باختيار الخصائص الأكثر مدلوليه وبعد ذلك يتم تغذية هذه الخصائص لخوارزميات تعلم الآلة. في هذا البحث تم اختبار خمس خوارزميات تعلم آلة مختلفة واختبارها وتقييمها باستخدام بيانات مفتوحة المصدر لرصد هجمات Botnet. الخوارزمية الهجينة التي تم تقديمها في هذا البحث أظهرت نتائج أفضل مقارنة بنتائج الخوارزميات الأخرى التي تم مقارنتها.

الكلمات المفتاحية: رصد Botnet، أنترنت الأشياء، اختيار الخصائص، تعلم الآلة، الحماية.

A review on Plackett-Burman Design

Ahlam Ali Alzharani

Department of Management Information System, Faculty of Collage of Business Administration,
Albaha University, Saudi Arabia.

Abstract

In the last decades, design of experiments (DOE) methodology has been statically valuable tool since it discovered the relationship between the response and factors. This feature increases the number of applications for DOE in many fields. Recently, Plackett-Burman design has been considered the most used design in industry and another field. Through the existing literature review across databases like Google Scholar, were searched for relevant papers for a time period between 2012 and 2022. Many industry cases using the Plackett-Burman design were identified and several papers show some problems related to the analysis for this design. The purpose of this literature review is to present the properties of this design and its applications, as well as, to show the most uncovered and unsolved problems related to the analysis for this design.

Keywords: Plackett-Burman Design, Projection, Two-factor interaction, Orthogonal.

1-Introduction

The investigator usually conducts an experiment to understand a particular process or system. In the experiment, any change in the input factors can be observe in the outcome (response). The design of the experiment is a powerful tool that could help determine which factor has a big impact on the response. Also, by designing an experiment methodology, the investigator could develop a model that related the response to the level of factors, and then use this model to improve the system, process or making decision. So, the design of an experiment is a statistical method used to plan, conduct and analyze the factors that control the response. This method involved a series of experiments that at the beginning looked broadly at many factors and then, focused on critical ones.

The first experiment in this series of experiments is called a screening experiment. The importance of this step is to finds the most important factors that have a significant impact on the response. This step is very important since it has an effect on the experiment's budget. Usually, the most common design used for screening experiment is a two-level factorial design. Two-level factorial design first introduced

by [7] which represented by 2^k , where k is the number of the main effects (MEs). Due to run size and time concerns, fractional factorial design is alternative to two-level factorial design.

Plackett-Burman design is one type of non-regular fractional factorial design, that was first produced by [15]. This design was developed for studying $k = N - 1$, MEs in N runs, where N is a multiple of 4. So, the run sizes for this design are 12, 20, 24, 28, and 36. Table 1 shows rows that contain signs (+ or -) which are usually used for generated Plackett-Burman designs. The usual way to generate Plackett-Burman designs is to use the cyclical pattern method. That means we must use one appropriate row, as shown in Table 1, as the first column, then develop the second column by moving the last element in the first column as the first element in second column, then place all elements in the first column. The third column is generated from the second column in the same way. Then, the process is to keep doing it until the last column k . In the end, a row of minus or plus signs should be added the last row. An example of the Plackett-Burman design for $N = 12$ and $k = 11$ is shown in Table 2.

Number of MEs	Number of runs	Signs
k=11	N=12	+ + - + + + - - - + -
k=19	N=20	+ + + + + - - + - + - - + + - - - + - - - -
k=23	N=24	+ + + + + - - + - + - - + + - - - + - - - -
k=35	N=36	- + - + + + - - - + + + + - + + + - + - - - - + - + - + + - - + -

Table 1: Starting rows for generating the Plackett-Burman designs

A	B	C	D	E	F	G	H	I	J	K
+	-	+	-	-	-	-	+	+	-	+
+	+	-	+	-	-	-	-	+	+	-
-	+	+	-	+	-	-	-	-	+	+
+	-	+	+	-	+	-	-	-	-	+
+	+	-	+	+	-	+	-	-	-	-
+	+	+	-	+	+	-	+	-	-	-
-	+	+	+	-	+	+	-	+	-	-
-	-	+	+	+	-	+	+	-	+	-
-	-	-	+	+	+	-	+	+	-	+
+	-	-	-	+	+	+	-	+	+	-
-	+	-	-	-	+	+	+	-	+	+
-	-	-	-	-	-	-	-	-	-	-

Table 2: Plackett-Burman design for N = 12 and k = 11

During the last two decades, Plackett-Burman designs have been widely used in screening design for their run size economy and detecting active effects, especially two-factor interactions (2FIs). [11] suggested a method for analyzing the Plackett- Burman design to estimate some 2FIs along with MEs, despite the complex aliasing structure of the design. However, the Plackett-Burman design in the literature is still rare especially for its properties and applications. In this paper, a review of the literature on the special properties and applications of Plackett-Burman design was conducted. The rest of this article is organized as follows: in Section 2, we provide a review of the special properties of the Plackett-Burman design. Next, in Section 3, we show some of the applications for Plackett-Burman design. Moreover, in Section 4, we conducted a simulation study to demonstrate the performance of the Plackett-Burman design in detecting the active effects. Finally, section 5 is the conclusion and future works.

2-Special Properties for Plackett-Burman Design

Plackett-Burman is an example of nonregular factorial designs that are constructed by Hadamard matrices [15]. The main feature of the Plackett-Burman design is that its run size is a multiple of four, which impacts the design chosen and has an effect on the sources for the experiment. So, by using the Plackett- Burman design, we could study 11 MEs with N=12 , while with the fractional factorial design, we need N=16 to do that. Also, the Plackett-Burman design has a special structure that helps to improve the analysis. It has partial aliasing between its effects. In fact, the aliasing structure shows the correlation between the columns for the effects. So, when partial aliasing appears, that means the correlation

between its effects could be equal to a fraction between 0, and 1. In this case, the chance of estimating 2FIs is higher. On the other hand, the simple aliasing structure usually appear in the regular design. With that, the correlation between the effects is either 0 or 1. When the correlation between the effects is 0, the two effects are orthogonal, which means each effect is estimated independently. While if the correlation between the effects is 1 or -1, that indicates a completely confounding effect between these effects. In this scene, it is hard to separate the impact of these effects on the response. An example of a partial aliasing structure for k = 5 of the Plackett-Burman design is shown below. [19].

$$A = \frac{1}{3} B C - \frac{1}{3} B E - \frac{1}{3} B E + \frac{1}{3} C D + \frac{1}{3} C E + \frac{1}{3} D E$$

$$B = \frac{1}{3} A C - \frac{1}{3} A D - \frac{1}{3} A E + \frac{1}{3} C D - \frac{1}{3} C E + \frac{1}{3} D E$$

$$C = \frac{1}{3} A B + \frac{1}{3} A D + \frac{1}{3} A E + \frac{1}{3} B D - \frac{1}{3} B E + \frac{1}{3} D E$$

$$D = -\frac{1}{3} A B + \frac{1}{3} A C + \frac{1}{3} A E + \frac{1}{3} B C + \frac{1}{3} B E + \frac{1}{3} C E$$

$$E = -\frac{1}{3} A B + \frac{1}{3} A C + \frac{1}{3} A D - \frac{1}{3} B C + \frac{1}{3} B D + \frac{1}{3} C D$$

From the partial aliasing chains, each ME is aliased with 2FIs that do not involve this ME. Also, obviously the MEs in this design are aliasing with the 2FIs with correlation $\frac{1}{3}$ or $-\frac{1}{3}$, which means the Plackett-Burman design has resolution $R = 3$. This indicates that the Plackett-Burman design is an orthogonal array for MEs, implying that the MEs in this design are independently estimated without being affected by other effects.

Traditionally, the partial aliasing structure of Plackett-Burman designs discouraged their use due to this feature. However, in the last decade, the attention paid these designs has increased due to their special properties for these designs in estimating the 2FIs. [11] showed that the partial aliasing can help detect active interaction effects. Also, [17] demonstrated how the structured alias pattern for Plackett-Burman design leads to a new interpretation of the half normal plot for a model. They used the amount of aliasing to explain the clustering of effects in the normal plots. Such that, the effects that are not biased will cluster in one group, while the other biased effects with the same amount of aliasing will cluster in another group, so the effects will be splitting into groups in the normal plots.

Moreover, the Plackett-Burman design has a hidden projection property. The projection property means a full factorial is produced for every subset of the k MEs. That means every pair of columns must contain pairs with the signs: $(- -)$, $(+ -)$, $(- +)$ and $(+ +)$ replicated m times. Which produces m

replicates of a full factorial design 2^2 . This especial structure could be used to improve the analysis. The hidden projection property makes advantage of the partial aliasing in Plackett-Burman design, where this aliasing allows some interactions to be estimated without any follow up runs. As the work for [19], they show the efficiency for the hidden projections of the 12, 20 run Plackett-Burman design on estimating MEs and up to 6 2FIs. Their main idea is to study the columns of m MEs for the Plackett-Burman designs based on their ability to estimate h 2FIs in addition to the MEs. In this way, they consider cases of the selected columns where $k = 4, 5, \text{ and } 6$, and up to 6 2FIs. Then, they used a criterion for measuring efficiency for estimating the MEs and 2FIs when comparing designs. Also, this property could be used for detecting active factors as in the work [17]. Moreover, [19] explored more about the hidden projection property of Plackett-Burman design. For more about this property see [12], [4], and [15].

Although the Plackett-Burman design is widely used, there are still some uncovered and unsolved problems related to its analysis, which include nonlinearity. The Plackett-Burman design assumes a linear relationship between the response variable and the independent variables. However, in some cases, this assumption may not hold, leading to inaccurate results. The work of [9] suggest a modification of the Plackett-Burman design which takes a consideration of nonlinear processes and they illustrate the effectiveness of their proposed method through an optimization case study. Also, they provide references to other studies that have observed nonlinear behavior in their experimental systems.

Another issue related to the analysis of Plackett-Burman design is the confounding. The design assumes no confounding between the main effects (MEs), such that each main effect has an independent effect on the response variable. However, in practice, some main effects may be confounded with two-factor interaction (2FIs) that does not involved this particular main effect, which can lead to incorrect conclusions. In the work for [21], the author discusses the confounding between the effects in the Plackett-Burman design and its potential impact on the analysis results. Moreover, the Plackett-Burman design may not be robust to outliers, missing data, and other violations of statistical assumptions. Therefore, researchers need to be careful in interpreting the results. [5] show the limitations of the Plackett-Burman design, including its lack of robustness to violations of statistical assumptions and they recommend conducting additional analyses to arrive at a conclusive result.

3-Application for the Used Plackett-Burman Design

In the last decades, the design of experiments methodology has been a valuable strategy since it has discovered the relationship between the response and factors. This feature increases the applications for the design of experiments in many fields. For instance, the design of experiments has application in the lithium-ion-battery filed, which considers the most promising technologies that help to improve portable electronic devices [16]. Also, design of experiments includes mathematical models such as response surface methodology which can be used for optimizing extracting processes which has many applications in industries as it shown in the work of [5].

Since the Plackett-Burman design provides a minimum number of experiments on a maximum number of effects, [16] mentioned that the Plackett-Burmen design is the most used design for chemical applications. Also, based on [1] Plackett-Burman design has 10 percent success rate among other designs that are used in industry. This indicates the suitability of the Plackett-Burman design for its application area in terms of efficiency.

Due to the special features of Plackett-Burman designs on estimating the MEs independently and potential estimating for 2FIs, many applications appeared for Plackett-Burman designs in many fields like industry, and health. The MEs orthogonal property for Plackett-Burmad design is a very useful property especially in cases where there is no interest in the interaction between the effects. For example, [14] used the experimental design method to find the main and influential factors that have impact on the surface of titanium. They found the active effects that have a large impact on the

surface of titanium by using the Plackett-Burman design. Moreover, [3] considered a first order without interaction model to find the key effects for biohydrogen production by using Plackett-Burman design. They discover that the ME on biohydrogen production was the factor formate. Also, by using the one factor strategy, they found the optimal level of formate concentration to get the critical value of biohydrogen production. Moreover, [15] used Plackett-Burman design to improve the industry's

environment and materials. [18] improved the methods traditionally used in industry to

$$\frac{\text{The number of correctly identify an active effects}}{\text{Total number of active effects}}$$

This method is a useful measurement for evaluating the effectiveness of a design. Researchers can assess the performance of different designs in detecting active effects by comparing this measurement for them. Typically, a simulation study is used to conduct this measurement.

The aim of the conducted simulation is comparing the performance of the two different designs.

assess the fuzzy process capability. Also, [8] used Plackett-Burman design to find the optimal setting for a wood chipper which could be used as a biomass solid fuel.

4- Simulation Study

Knowing the active effects is an important step in the analysis. The one popular method for detecting active effects involves computing the average proportion of correctly identified an active effect. This proportion equals to:

The first one is Plackett-Burman design with $k=6$ and $N=11$ which is column 1 through 6 in work [13]. The second one is a fractional factorial design with $k=6$ and $N=16$ denoted by 2^{6-2} . Table 3, and 4 show Plackett-Burman and fractional factorial designs respectively.

A	B	C	D	E	F
+1	+1	+1	+1	+1	+1
-1	-1	-1	+1	-1	+1
+1	-1	-1	-1	+1	+1
+1	+1	-1	-1	-1	-1
+1	+1	+1	-1	-1	+1
-1	+1	+1	+1	-1	-1
+1	-1	+1	+1	+1	-1
-1	+1	-1	+1	+1	+1
-1	-1	+1	-1	+1	-1
+1	-1	-1	+1	-1	-1
-1	+1	-1	-1	+1	-1
-1	-1	+1	-1	-1	+1

Table 3 : Plackett-Burman design for N=12 , and k=6

A	B	C	D	E	F
+1	+1	+1	-1	-1	-1
+1	-1	+1	+1	-1	+1
+1	-1	-1	+1	+1	-1
-1	+1	-1	-1	+1	-1
-1	+1	+1	+1	+1	-1
-1	-1	-1	-1	-1	-1
+1	+1	-1	-1	+1	+1
-1	+1	-1	+1	-1	+1
-1	-1	+1	-1	+1	+1
+1	+1	+1	+1	+1	+1
-1	-1	+1	+1	-1	-1
1	-1	-1	-1	-1	+1
1	+1	-1	+1	-1	-1
-1	+1	+1	-1	-1	+1
-1	-1	-1	+1	+1	+1
1	-1	+1	-1	+1	-1

Table 4: Fractional Factorial design for N=16, and k=6

The methodology for the simulation study is applied as follows. In each of 1000 iterations:

1. Consider a matrix M consisting of k columns representing MEs and g columns representing 2FIs.
2. Construct the matrix X by randomly selecting columns from M such that X corresponds to the matrix of active effects.
3. The number of selected active effects is starting from 2 until 6.
4. The response vector is generated as $y=X*\beta+e$, where $e \sim N(0, I)$.
5. The coefficients, β are generated by sampling values randomly from the set $\{-3, -2, -1, 1, 2, 3\}$ (with replacement).

6. The set of significant effects is chosen by using forward selection procedure.
7. At the end of 1000 iterations, (the average proportion of correctly identified active effects, that include both MEs and 2FIs), (the average proportion of correctly identified active MEs only), and (the average proportion of correctly identified active 2FIs only) are recorded.

Figure 1. We represent for the first Plackett-Burman design by PB6.1, and the second design by FF 16. In Figure 1, X-axes for the plots represent the number of active effects. The Y-axes represent the mean of proportion of identify active effects. Each line represents the performance of a design on detecting active effect which include both MEs and 2FIs. The results show that PB6.1 is better than FF 16 for two active effects. However, as the number of active effects increases, the performance of FF 16 improves.

The result of the simulation study for the percentage of active effects is displayed in

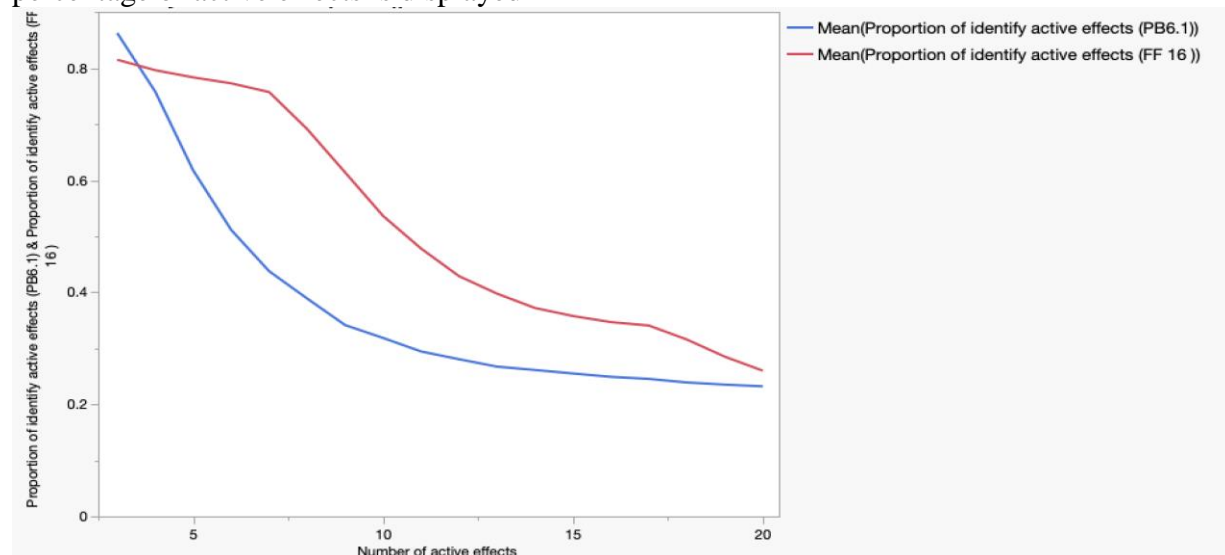


Figure 1: Mean of proportion of identify active effects for (PB6.1) and (FF 16)

As Figure 1, in Figure 2, X-axes for the plots represent the number of active MEs. The Y-axes represent the mean of proportion of identify MEs. Each line represents the performance of a design on detecting active MEs. Also, the result shows that the FF 16 is better than PB6.1 in detecting active MEs. The description for Figure 3 is similar to that of Figure 1 and 2. In Figure 3 the mean of proportion of identified active 2FIs for PB6.1 is better than that for FF 16 especially for 2 to 3 active 2FIs.

So, we can conclude from the simulation study the following. Although in most cases the fractional factorial design is better than Plackett-Burman design at identifying the active effects, the simulation study shows that there is a chance to obtain a better analysis of 2FIs, especially for a low number of active effects, by using Plackett-Burman design.

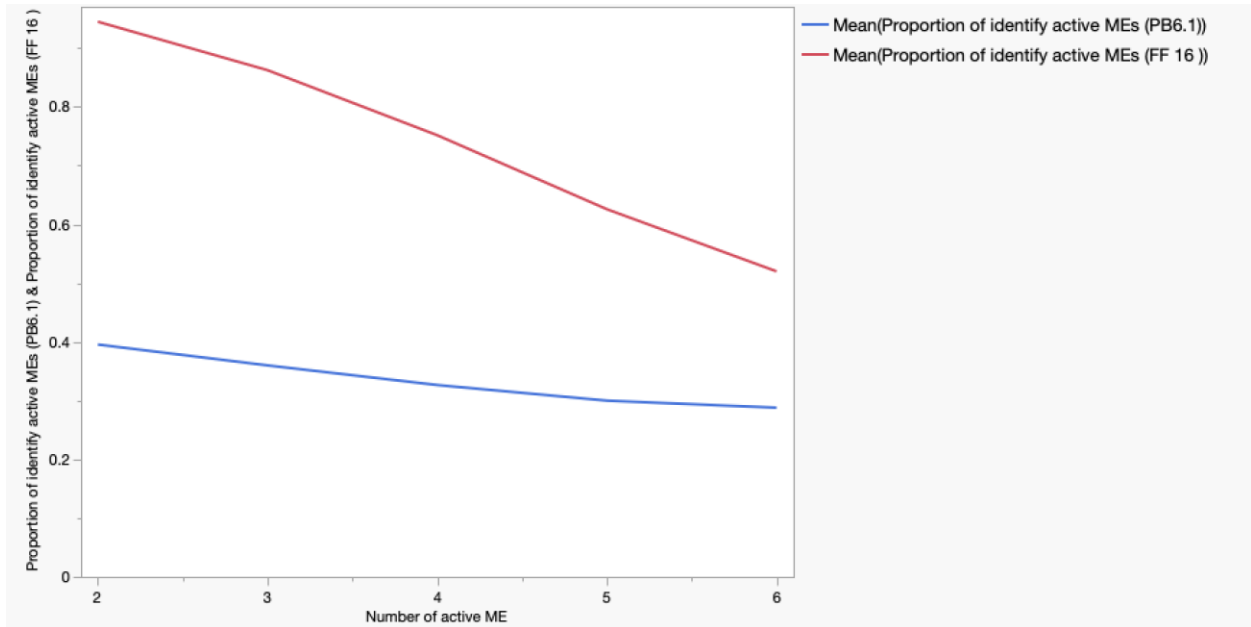


Figure 2: Mean of proportion of identify active MEs for PB6.1 and FF 16

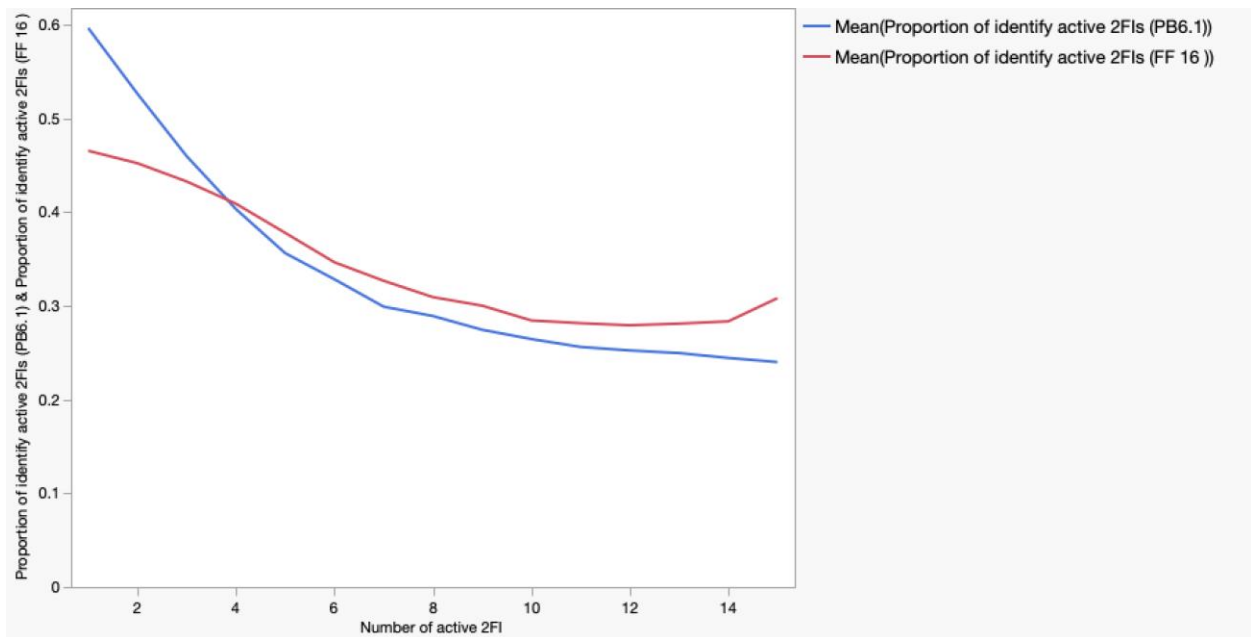


Figure 3: Mean of proportion of identify active 2FIs for PB6.1 and FF 16

5-Conclusion and Future Works

A better understanding of the structure of the Plackett-Burman design and knowledge of the available analysis and applications for these designs will result in a wider development in many scientific and applied fields. For this reason, gathering more detailed information about the Plackett-Burman design is needed. [17] find some explanation for the aliasing and projection properties to understand the attitude toward Plackett-Burman design. This is a motivation to search more for new explanations and understandings for the structure of Plackett-Burman design.

Also, there is a rich literature for application to Plackett-Burman design, which indicates the effectiveness of these designs for improving the analysis. However, there is a lack of literature on the ranking and classification of Plackett-Burman designs. [20] created a generalized resolution and generalization of the minimum aberration criterion for assessing nonregular factorials, which can be applied to the Plackett-Burman design. These ones are the only criteria that capture the projection properties of the Plackett-Burman design. This leads to think that it is possible to find another way to classify and rank Plackett-Burman designs based on the aliasing structure. Therefore, the aim of this literature is to encourage more research about ranking and classifying Plackett-Burman designs and to investigate the problems that remain unsolved.

References

[1] Antony, J., Viles, E., Torres, A.F., de Paula, T.I., Fernandes, M.M., Cudney, E.A.: Design of experiments in the service industry: a critical literature review and future research directions. *The TQM Journal* 32(6), 1159–1175 (2020)

[2] Box, G., Tyssedal, J.: Projective properties of certain orthogonal arrays. *Biometrika* 83(4), 950–955 (1996)

[3] Bakonyi, P., Nemestóthy, N., Lovitusz, E., B'elafi-Bakó, K.: Application of plackett-burman experimental design to optimize biohydrogen fermentation by *e. coli* (x11-blue). *international journal of hydrogen energy* 36(21), 13949–13954 (2011)

[4] Cheng, C.-S.: Some projection properties of orthogonal arrays. *The Annals of Statistics* 23(4), 1223–1233 (1995)

[5] Das, Anup K and Dewanjee, Saikat.: Optimization of extraction using mathematical models and computation: Elsevier: 75—106, (2018)

[6] Deng, L.-Y., Li, Y., Tang, B.: Catalogue of small runs nonregular designs from hadamard matrices with generalized minimum aberration. *Communications in Statistics-Theory and Methods* 29(5-6), 1379–1395 (2000)

[7] Fisher, R.A.: Design of experiments. *British Medical Journal* 1(3923), 554 (1936)

[8] Guerrini, L., Tirinnanzi, A., Guasconi, F., Fagarazzi, C., Baldi, F., Masella, P., Parenti, A.: A plackett-burman design to optimize wood chip- per settings. *Croatian Journal of Forest Engineering: Journal for Theory and Application of Forestry Engineering* 40(1), 81–87 (2019)

[9] Gao, Y., Zhang, R., & Zhang, C.: A modified Plackett-Burman design for non-linear processes: Application to optimization of a bioconversion process. *Biochemical Engineering Journal*: 143, 146-155 (2019)

- [10] Hibbert, D.B.: Experimental design in chromatography: a tutorial review. *Journal of chromatography B* 910, 2–13 (2012)
- [11] Hamada, M., Wu, C.J.: Analysis of designed experiments with complex aliasing. *Journal of quality technology* 24(3), 130–137 (1992)
- [12] Lin, D.K., Draper, N.R.: Projection properties of plackett and burman designs. *Technometrics* 34(4), 423–428 (1992)
- [13] Miller, A and Sitter, RR.: Choosing columns from the 12-run Plackett--Burman design: *Statistics & probability letters* 67(1), 193—201 (2004)
- [14] Ndaliman, M., Khan, A., Ali, M., Wahid, Z.: Determination of influential factors on edmed surface properties using plackett-burman design. *World Appl Sci J* 21, 88–93 (2013)
- [15] Plackett, R.L., Burman, J.P.: The design of optimum multifactorial experiments. *Biometrika* 33(4), 305–325 (1946)
- [16] Román-Ramírez, L., Marco, J.: Design of experiments applied to lithium-ion batteries: A literature review. *Applied Energy* 320, 119305 (2022)
- [17] Tyssedal, J., Samset, O.: Analysis of the 12 run plackett-burman design. *Preprint, Statistics* (8) (1997)
- [18] Villalón-Turrubiates, I.E., López-Herrera, R., García-Alcaraz, J.L., Díaz-Reza, J.R., Soto-Cabral, A., González-Lazalde, I., Grijalva-Avila, G., Rodríguez-Alvarez, J.L.: A non-invasive method to evaluate fuzzy process capability indices via coupled applications of artificial neural networks and the placket-burman doe. *Mathematics* 10(16), 3000 (2022)
- [19] Wang, J., Wu, C.J.: A hidden projection property of plackett-burman and related designs. *Statistica Sinica*, 235–250 (1995)
- [20] Wu, C.: Construction of supersaturated designs through partially aliased interactions. *Biometrika* 80(3), 661–669 (1993)
- [21] Wong, K. L., & Wong, L. L.: Screening for significant factors in Plackett-Burman designs: *Journal of Quality Technology*: 40(4), 342-355 (2008)

تصميم بلاكيت بورمان

أحلام علي الزهراني

قسم نظم المعلومات الإدارية، كلية إدارة الأعمال، جامعة الباحة

الملخص

في العقود الماضية، كان تصميم منهجية التجارب أداة إحصائية قيمة لأنه يكتشف العلاقة بين الاستجابة والعوامل. تعمل هذه الميزة على زيادة تطبيقات تصميم المنهجية التجريبية في العديد من المجالات. في الآونة الأخيرة، يعد تصميم بلاكيت بورمان هو التصميم الأكثر استخداماً في تطبيقات الصناعة والمجالات الأخرى. من خلال مراجعة الأدبيات الحالية عبر قاعدة بيانات الباحث العلمي من قوقل، تم البحث عن الأوراق ذات الصلة لفترة زمنية بين ٢٠١٢ إلى ٢٠٢٢. تم تحديد العديد من الحالات الصناعية باستخدام تصميم بلاكيت بورمان، وأظهرت العديد من الأوراق البحثية بعض المشكلات المتعلقة بتحليل لهذا التصميم. الغرض من هذه المراجعة الأدبية هو تقديم خصائص هذا التصميم وتطبيقاته، وأيضاً، لأظهار المشكلات التي لم يتم حلها و المتعلقة بتحليل هذا التصميم.

الكلمات المفتاحية: تصميم بلاكيت بورمان، تنبؤ، تفاعل عاملين، متعامد.

Studying of Solar radiation components over Jazan, the Kingdom of Saudi Arabia

A. M. Fathy

Faculty of Science, Physics Department, Jazan University

Abstract

This work was carried out in Jizan, ($17^{\circ} 30' N$, $42^{\circ} 30' E$, Elev: 7 m) which lie in the Southwest of the Kingdom of Saudi Arabia. The present work is done for monthly average values of solar radiation components (Global, Direct and diffuse) as well as the clearness index beside meteorological parameters data of the years (1983-2005). It's found that the highest monthly average values of most solar radiation components were in summer months, while the lowest values were in winter months except for the direct normal incident solar radiation value which has its highest values in winter and its lowest values in summer.

Keywords: Solar radiation components, clearness index, clear sky, air temperature, humidity and atmospheric pressure.

1. Introduction

The main permanent energy source is the solar energy, where it gave the earth about 170 trillion kW. Studying of solar radiation gives us an important information in assessment and designing of solar energy project. Interaction between solar radiation against atmospheric constituents done into two forms, absorption which is about 17 % of solar radiation and a part is reflected back to the atmosphere which is 30%, and the rest is 53% reaches to the earth surface into two parts of solar radiation. The first is the direct radiation (33%), while second is the diffuse radiation (22%). (Shaltout M. A.M et. al, 1998, Fathy A.M. 2008)

Solar radiation data helps us in agricultures, renewable and building energy studies. NASA

collects solar radiation components data in different sites as, global, direct and diffuse solar radiation beside its values in different spectral bands, as short wavelength (ultraviolet) and long wavelength (infrared). The atmospheric parameters and air pollution of the same sites. The data are, global solar radiation incident on a horizontal surface (H) for total a clear sky day (cloud amount < 10%) measured in (kWh/m²/day). Also, monthly averaged values of insolation clearness index (kt) of total and clear sky days. Finally, the monthly average values of direct normal radiation (I) has been collected in (kWh/m²/day), besides the monthly mean values of diffuse radiation measured on horizontal surface (D). Also, meteorological parameters have been collected in parallel with the radiation data such as the atmospheric pressure (P), relative humidity (RH%) and air temperature (T). All the previous

data has been collected by NASA for the years (1983-2005).

Solar radiation measured on the earth surface affected by its atmospheric constitutes via attenuation and absorption as the atmospheric gases and aerosols (Eladawy M.L., et. al, 2022).

Atlas of solar radiation for KSA has a measured collected data for the years (1971- 1980), by the Agriculture and water Ministry and the Meteorological and Environmental Protection Agency of KSA. This data used in CSR model where it gave us a resulting data grids and maps as a climatological monthly and annual averages (Solar radiation atlas for KSA, 1998) using a thirty years record data to deduce the climatological weather parameters. Future studies of solar energy in KSA are very important when we add a factor of health effect for using and for the indirect price of natural fuel such as coal or gas. Thus, using solar radiation via PV considered important process of generating kind of renewable energy, where we conclude from this study that, the price of solar energy as a clean energy becomes less than the price of the natural fuel such as coal or gas if environmental and health problems cost is taken into consideration (Jianyuan Zhang, et. al, 2017). Also, it studied the importance of generating electricity using renewable and solar energy specially by using the photovoltaic. Considering health effects and environmental protection, the economic studies of using renewable and solar energy, have to take in consideration the location of solar PV systems, and cloud

distribution in Saudi Arabia (WMO, 1967).

The pollutant materials in air give us an over view about health problem and its important role in reducing of solar radiation amount which the main source of generating a large scale of PV systems. Also, the dangerous of pollutant gases in the environment and in reducing the solar radiation by absorption and scattering (SANCST, 1983). Average monthly values of global solar radiation measured on horizontal surfaces was 5.62 (kWh/m²/day), while its direct solar radiation value was 4.39 (kWh/m²/day) (Almasoud A.H, et. al, 2015, Anon, Project 1977).

2. Data:

This study is devoted to study the solar radiation component distributions over Jazan, Saudi Arabia, (17° 30' N, 42° 30' E, Elev: 7 m) which lie in the Southwest of KSA for the years (1983-2005) to conclude if this site is good for solar energy applications or not. Through this work we study the distributions of Global, direct, diffuse radiation, clearness index beside some metrological parameters as monthly mean values.

3. Results and Discussion

3.1 Monthly averaged global solar radiation measured on horizontal surface:

Studying of distribution of monthly mean insolation values on a horizontal surface, where the highest values were in summer months with value 7.26 (kWh/m²/day) in May. The lowest values were in winter months with value 5.01 (kWh/m²/day) in

January. It has an annual mean value 6.24 (kWh/m²/day) as shown in figure 1.

The monthly mean clear sky insolation values on a horizontal surface has a highest value in

summer months with value 7.67 (kWh/m²/day) in April. The lowest values were in winter months with value 5.50 (kWh/m²/day) in December, with annual mean value 6.73 (kWh/m²/day) see figure 2

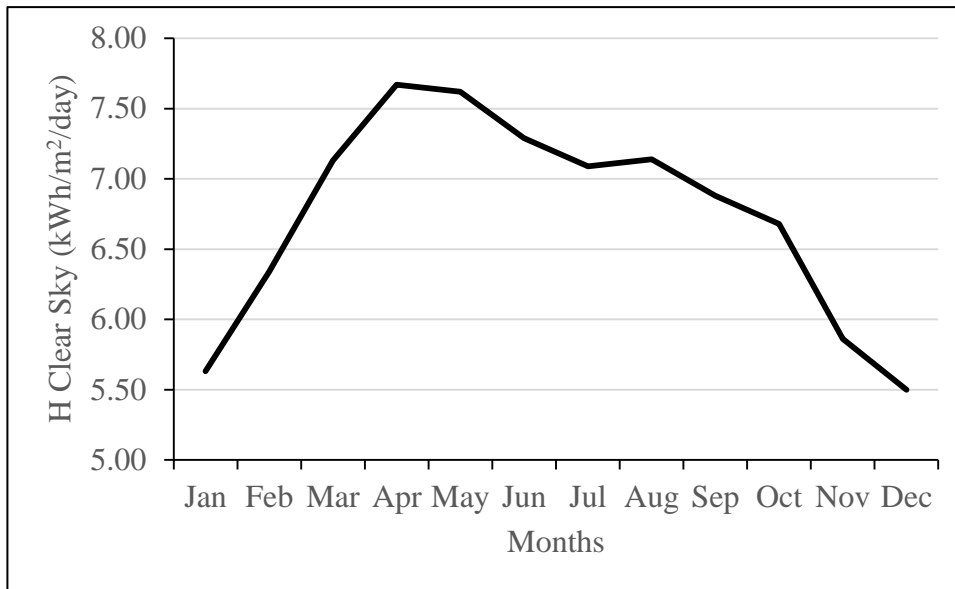


Fig. 1. Variations of monthly mean values of insolation on horizontal surface in (kWh/m²/day)

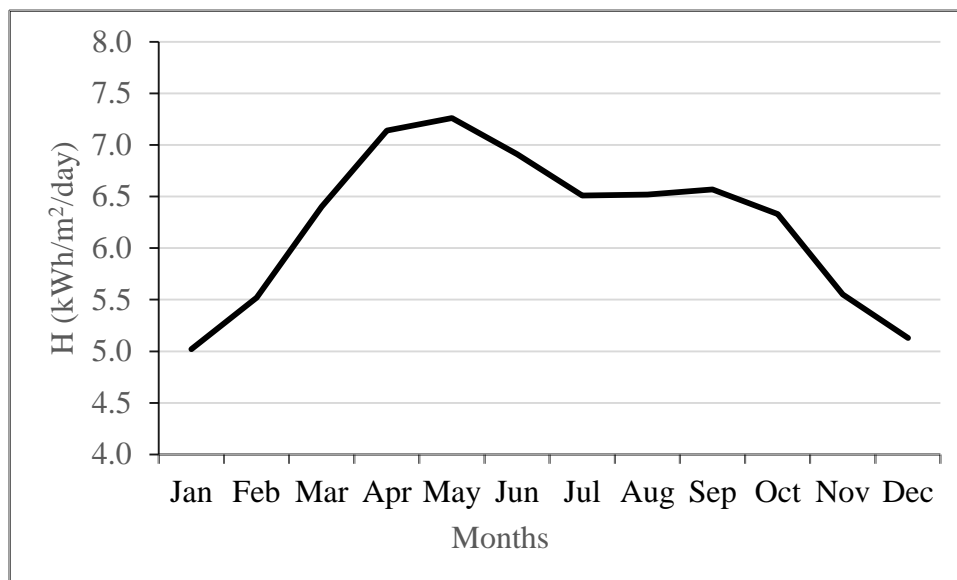


Fig. 2. Variations of the monthly variations values of clear sky insolation on a horizontal surface in (kWh/m²/day).

3.2 Monthly variations of diffuse solar radiation on horizontal surface:

Studying of the distribution of the monthly variations of diffuse radiation on a horizontal surface show that highest values were in

summer months with value 2.06 ($\text{kWh/m}^2/\text{day}$) in July. Lowest values were in winter months with a value of 1.08 ($\text{kWh/m}^2/\text{day}$) in December. It has an annual mean value of 1.60 ($\text{kWh/m}^2/\text{day}$) see figure 3.

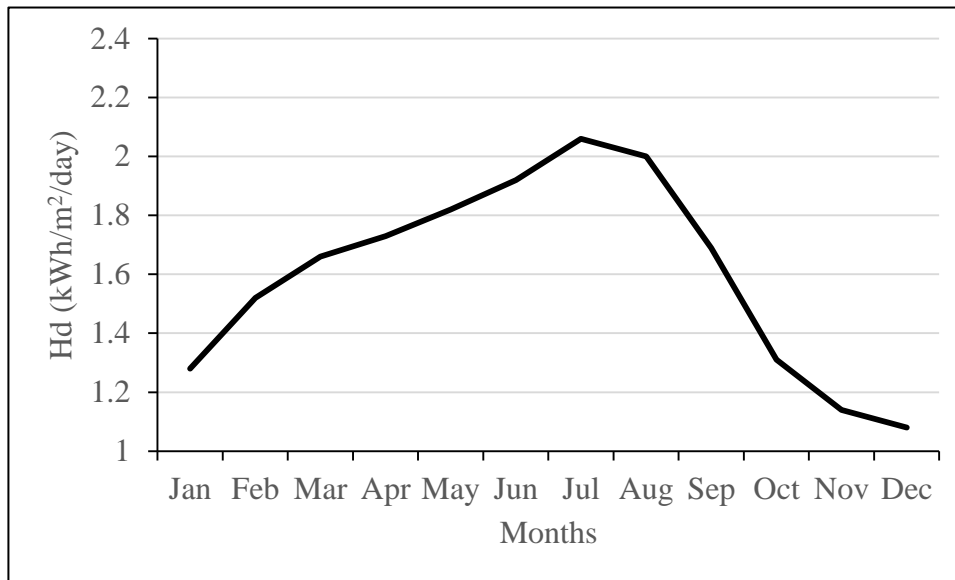


Fig. 3. Monthly mean diffuse radiation on a horizontal surface in ($\text{kWh/m}^2/\text{day}$).

3.3 Monthly mean values of direct incident solar radiation:

Studying of the distribution of the monthly mean direct incident solar radiation values shows that the highest value in October with a value of 7.86 ($\text{kWh/m}^2/\text{day}$). The lowest value was in

July with a value of 6.38 ($\text{kWh/m}^2/\text{day}$). It has an annual mean value of 7.14 ($\text{kWh/m}^2/\text{day}$) as shown in figure 4. The lowest direct solar radiation values in summer months were due to the dust storms blowing in Jazan in summer months.

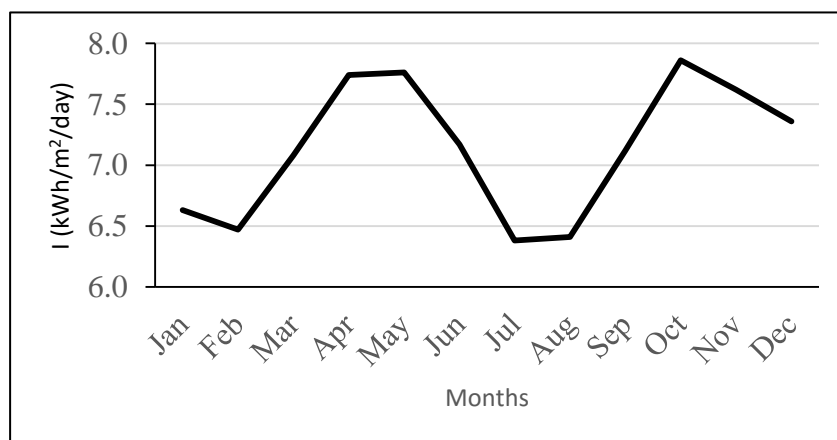


Fig. 4. Monthly mean direct incidence solar radiation in ($\text{kWh/m}^2/\text{day}$).

3.4 Monthly mean clearness index (0 to 1.0):

Clearness index K_t is defined as the ratio of the global solar radiation (H) reaches the earth surface to the corresponding values outside of the atmosphere (H_0), which named extraterrestrial solar radiation or the Solar constant with value (1367 W/m^2) which corrected by a yearly values of 3.3% due to the sinus function of amplitude getting from the earth's orbit ellipticity. Therefore, the Clearness Index K_t may be considered as an atmospheric attenuation factor for the atmosphere. It equal 1 for a clear atmosphere, and equal to 0 for pollute atmosphere. However, this measure due to the light scattering and absorption. it is not a percentage, and in our case it is a decimal value between (0-1) (Danny H.W, et. al, 2015, Hossein Khorasanizadeh a. n, et. al, 2016 and Victor H. et. al, 2017).

The highest K_t value was in winter and spring months with value 0.67 in November, April and May, while the lowest value was in summer months with value 0.61 in July. It has an annual mean value 0.65 as shown in figure 5.

The distribution of the monthly mean clear sky clearness index is shown in figure 6. The highest K_t value was in winter and spring months with value 0.72 in October, March and April, while the lowest value was in summer months with value 0.66 in July. It has an annual mean value of 0.70. From the values of K_t for the total and clear sky days, we consider Jazan atmosphere to be polluted in summer months, while it is clean atmosphere through the rest of the year months. The lowest K_t values in summer months were due to the dust storms blowing in Jazan in summer months.

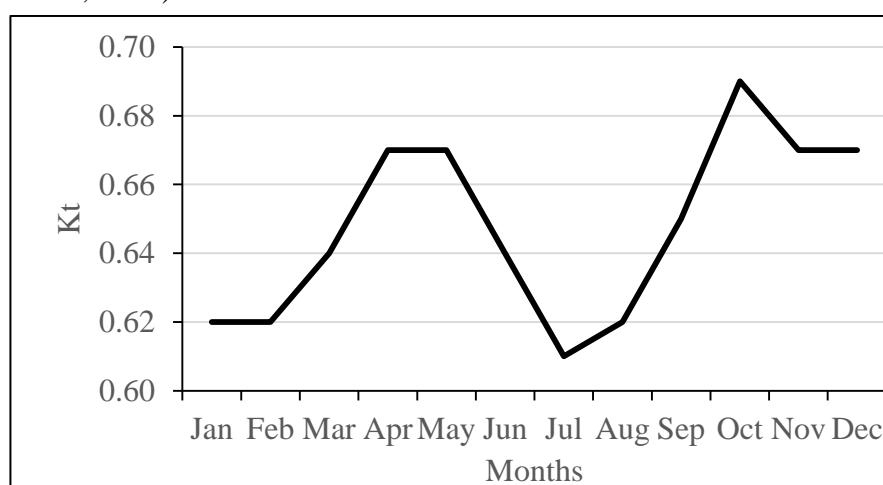


Fig. 5. Monthly averaged clearness index.

3.5 Monthly average values of metrological parameters:

Some metrological parameters which are important in solar radiation studies are air temperature, relative humidity and atmospheric pressure.

Studying of the monthly mean values of air temperature in ($^{\circ}\text{C}$) is shown in

figure 7, where the highest values were in summer months with value 31°C in June, while its lowest values were in winter months with value 24.2°C in January. The annual mean value of air temperature is 27.7°C .

The monthly mean values of relative humidity (%) is shown in figure 8,

where its highest values were in summer months with value 74.3% in August, while the lowest values were in winter months with value 48.3% in

December. The annual mean value 54.1%.

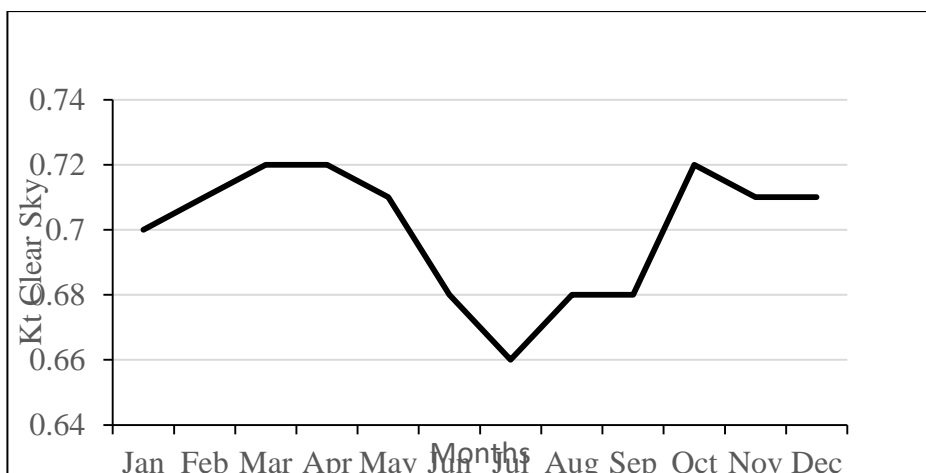


Fig. 6. Monthly averaged clear sky clearness index.

The monthly average values of the atmospheric pressure in kPa are shown in figure 9, where it's found that there are no differences between the values of atmospheric pressure from month to month. The values of atmospheric pressure are ranged from 96.6 kPa to 97.5 kPa.

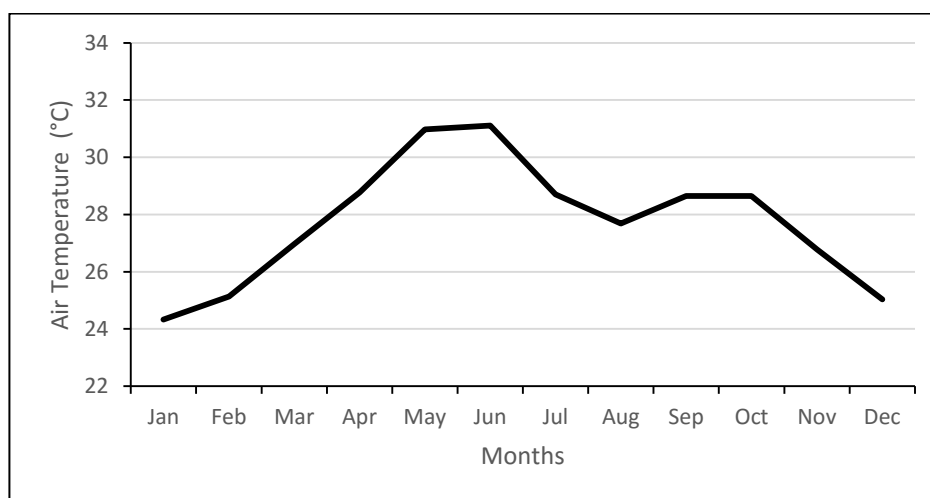


Fig. 7. Monthly averaged values of air temperature at 10m above the earth in °C.

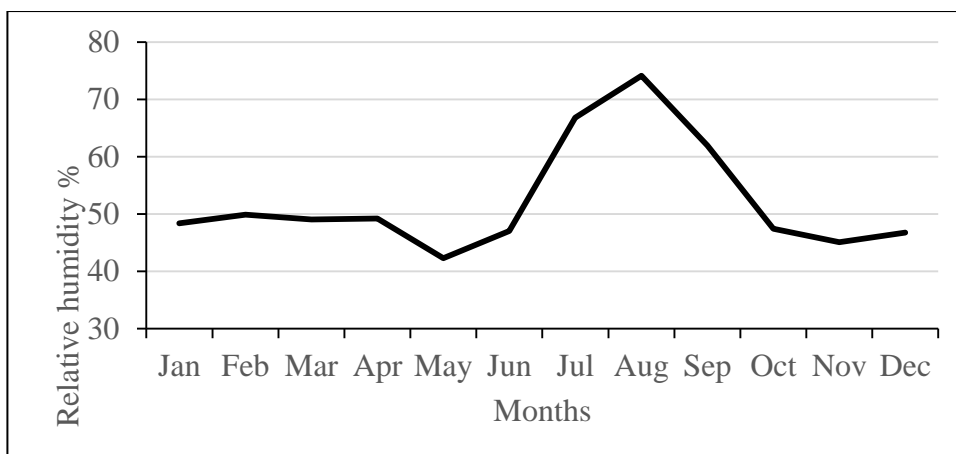


Fig. 8. Monthly averaged values of relative humidity %.

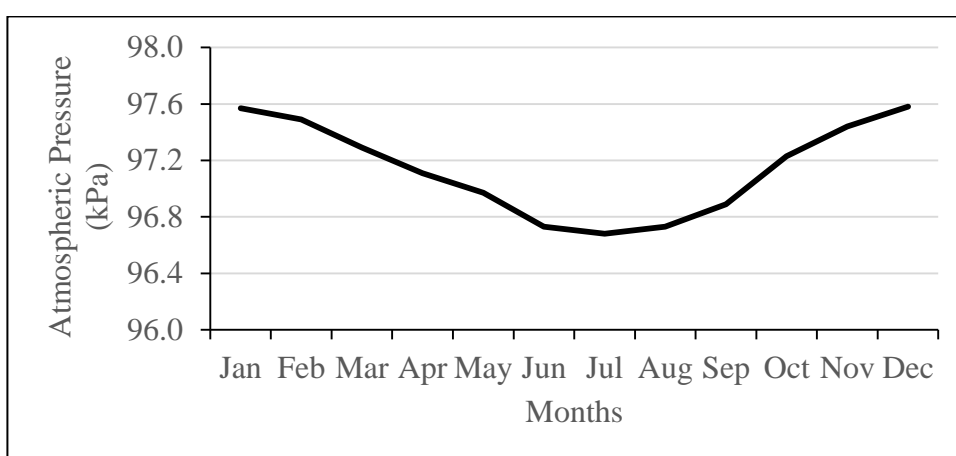


Fig. 9. Monthly averaged values of atmospheric pressure in kPa.

Conclusions:

In this study, monthly solar radiation and meteorological parameters average values over Jazan, Saudi Arabia has been discussed, where we got the following conclusions:

- The highest monthly mean values of insolation incident on a horizontal surface and diffuse solar radiation were in summer months, while its minimum value was in winter months.
- The highest monthly average value of direct normal incident solar radiation was in October, while its lowest value was in July due to the dust storms blowing in Jazan in summer months.
- The highest monthly average Kt values of both total and clear sky days was in winter and spring months, while the lowest value was in summer months due to the dust storms blowing in Jazan in summer months.
- The highest monthly average value of air temperature and relative humidity found to be summer and the lowest value was in winter.
- There are no differences between the average atmospheric pressure

monthly values from month to month.

Reference:

Shaltout M. A.M, Hassan A. H. and Fathy A. M. (1998), "Studying the ultraviolet and visible solar radiation over Cairo and Aswan and their correlation with climatological parameters", Proceedings of the Indian Academy of Sciences- Chemical Sciences volume 110, pages361–371

Fathy A.M. (2008), "Net Solar Radiation Over High Polluted Sites", First Middle East and Africa IAU-Regional Meeting Proceedings MEARIM No. 1.

Eladawy M.L, Mostafa Morsy, Korany M.H, Mohammed El-Adawy, Abdel Basset H., (2022), "Spatiotemporal variations of global solar radiation: Case Study" Alexandria Engineering Journal, Alexandria University, Egypt, January 2022, 20-29.

Solar radiation atlas for the Kingdom of Saudi Arabia (1998), National Renewable Energy Laboratory, Center for Renewable Energy Resources, Golden Colorado and Energy Research Institute, Renewable Energy Department and Kingdom of Saudi Arabia King Abdulaziz City for Science and Technology.

Jianyuan Zhang, Zhao Li , Shuai Deng, Weicong Xu, Ying Zhang (2017), "A critical review of the models used to estimate solar radiation", Renewable and Sustainable Energy Reviews, Volume 70, Pages 314-329.

WMO (1967). A Note on Climatological Normal, WMO No. 208, T.N. No. 84,

World Meteorological Organization, Geneva, Switzerland.

Saudi Arabian Solar Radiation Atlas SANCST (1983), Saudi Arabian National Center for Science and Technology (SANCST).

Almasoud A.H, and Hatim M Gandayah (2015), "Future of solar energy in Saudi Arabia, Journal of King Saud University - Engineering Sciences Volume 27, Issue 2, July, Pages 153-157.

Anon, Project Agreement Between the Saudi Arabian National Center for Science and Technology and the Saudi Arabian Ministry of Finance and the National Economy, Jointly, and the United States Department of Energy and United States Department of Treasury, Jointly, for Cooperation in the Field of Solar Energy. 1977, U.S. Department of Energy: Washington, D.C. and Riyadh, KSA.

Danny H.W. Li, Lou S.W., Joseph C. Lam (2015), "An Analysis of Global, Direct and Diffuse Solar Radiation", Energy Procedia 75, 388 – 393.

Hossein Khorasanizadeh a. n, Kasra Mohammadi (2016), "Diffuse solar radiation on a horizontal surface: Reviewing and categorizing the empirical models", Renewable and Sustainable, Volume 53, Pages 338-362.

Victor H. Quej, Javier Almorox a, Mirzakhayot Ibrakhimov b (2017), "Laurel Saito Estimating daily global solar radiation by day of the year in six cities located in the Yucatan Peninsula, Mexico Journal of Cleaner Production, Volume 141, Pages 75-82.

دراسة مركبات الأشعاع الشمسي فوق مدينة - جيزان بالمملكة العربية السعودية

أحمد محمد فتحي

قسم الفيزياء - كلية العلوم - جامعة جازان - المملكة العربية السعودية

ملخص

توضح الدراسة في هذا البحث توزيعات الاشعاع الشمسي الكلي والمشتت لكل الأيام والاشعاع الشمسي الكلي للأيام الصافية حيث وجد ان القيمة العظمي لتلك المركبات تقع في أشهر الصيف والقيم الصغرى تقع في أشهر الشتاء بينما توزيعات الاشعاع الشمسي المباشر وضحت وقوع القيم العظمي لهذا الاشعاع في شهر أكتوبر بينما القيم الصغرى كانت في شهر يوليه. بالنسبة لتوزيعات معامل نظافة الهواء فكانت القيم العظمي في أشهر الشتاء بينما القيم الصغرى كانت واقعة في أشهر الصيف لكل من الأيام الكلية والأيام الصافية ويرجع هذا الي هبوب الرياح المحملة بالأتربة والغبار خلال أشهر الصيف. بينت توزيعات العوامل المناخية الي وجود القيم العظمي لدرجات الحرارة نسبة الرطوبة النسبية خلال أشهر الصيف بينما القيم الصغرى فكانت خلال أشهر الشتاء ووجدت قيم الضغط الجوي متقاربة خلال كل اشهر السنة. وتكمن أهمية الدراسة في مساعدة المختصين في استخدامات تطبيقات الطاقة الشمسية كطاقة نظيفة في معرفة أفضل الشهور لاستخدامها وكمية الطاقة الشمسية وقيمها العظمي والصغرى على مدار شهور السنة.

الكلمات المفتاحية: مركبات الأشعاع الشمسي- معامل نظافة الهواء- سماء صافية- درجة حرارة الهواء- الرطوبة النسبية والضغط الجوي.

Effect of Soil Pollution with Lead and Cadmium on the Development of Heavy Metal-Tolerant Bacterial Isolates in Jazan Region, KSA

¹Azhar Y. Al-Nuaimi and ¹Mohamed N. Al-Leithy

¹Biology Department, College of Science, Jazan University, KSA

Abstract

Heavy metals are the major pollution sources in soil. The present work was carried out on soil samples from three locations in Jazan region; agricultural field in Al-adayah area (S1), soil irrigated by treated water from the Sewage Treatment Plant in Jazan (S2) and from Block factory in Al-maaboj area (S3). The soil total bacterial count of the three locations and the possible development of Pb²⁺ and Cd²⁺-tolerant bacteria were studied. The highly metal-tolerant bacteria were isolated and examined for their maximum metal tolerance. The amounts of total Pb²⁺ and Cd²⁺ were higher in sites S2, S3 than in S1, while the O.M % were lower in S2 and S3 than in S1 sites. Total bacterial counts in sites S3 and S2, being 0.32 and 5.3 x 10⁵ CFU.g⁻¹ soil, respectively, were markedly lower than those in site S1 of 78 x 10⁵ CFU.g⁻¹ soil. A range between 1.0 and 4.7 % of total bacterial count could tolerate 200 and 300 µg Pb²⁺.ml⁻¹, respectively, while lower numbers tolerated 400 and 500 µg Pb²⁺.ml⁻¹. 13.40 and 14.7 % of the total bacterial counts tolerated 5 µg Cd²⁺.ml⁻¹ in site S2 and S3, respectively. Two bacterial cultures Gram-positive spore-former rods, named SS/1 and SS/2 were isolated from Pb²⁺ and Cd²⁺-provided plates, respectively and exposed to three concentrations (500, 2000 and 6000 µgPb²⁺.ml⁻¹ and 25, 250 and 500 µg Cd²⁺.ml⁻¹) for SS/1 and SS/2 cultures, respectively. These concentrations were found to cause a reduction in the counts by <25, Ca.50 and >90 %.

Key words: Pollution, Heavy metals, Microorganisms, Heavy metal Tolerance, Soil

Introduction

Pollution is the most serious of all environmental problems and poses a major threat to the health and well-being of millions of people and global ecosystems. Heavy metal pollution is accounted as the most polluting aspects of the environment and has dramatically increased in recent years due to various human activities, such as agriculture, mining and other industrial processes. It can be argued that soil irrigated by municipal treated water and that exposed to industrial pollution, has been contaminated with many trace elements including Pb^{2+} and Cd^{2+} (Rajaganapathy, 2011 and Briffa *et al.*, 2020). The higher concentrations of these elements above threshold levels have very detrimental effects on the microbial communities and their vital activities, and some of them, once enter the soil they become irreversible immobilized components.

Microorganisms, particularly those that inhabit in metal polluted soils, have developed several mechanisms to tolerate/resist such higher concentrations of heavy metals. Thus, microbial populations exposed to heavy metals present in the environment contain bacteria which have acquired a variety of mechanism for adaptation and resistance to these toxic elements (Johncy *et al.*, 2010, Tarekegan *et al.*, 2020 and Demnerova *et al.*, 2005).

The present work was designed to study some aspects concerning microbial-metal interaction. Soil samples, exposed to heavy metals contamination, will be collected and the effect of this pollution on the total microbial population will be examined. The Pb^{2+} - and Cd^{2+} -tolerant bacterial

isolates will be selected, and the efficiency of these isolates should be tested for bioaccumulation of the metals under study at different levels.

In addition to an agricultural field in El-Adya area, away from any source of pollution, the Sewage Treatment Plant in Jazan and the Block Factory in El-maaboij area were considered as a source of pollution with heavy metals.

The objectives of this study are: (1) determining the total bacterial counts from different heavy metal-contaminated soils in Jazan region, (2) studying the tolerance of indigenous soil bacteria to different concentrations of Lead (Pb^{2+}) and Cadmium (Cd^{2+}), and (3) isolating the most lead (Pb^{2+}) and cadmium (Cd^{2+})- tolerant bacteria from these soils according to their morphologically characterize, and studying their maximum tolerance to each metal will.

Materials and methods

1. Soil sampling

In November 2020, a fertile sandy loam soil, presumably uncontaminated with heavy metals, was obtained from an agricultural field in El-Adya area located in (17°09'52.3"N 42°35'32.1"E) and named (S1). This location is away from any source of pollution. Additionally, two soil samples were collected; first one from soil irrigated by the treated water drained from the Sewage Treatment Plant in Jazan which located in (16°47'06.1"N 42°40'29.1"E) and named (S2), and the second was that adjacent to the Block Factory in El-maaboij area which located in (16°53'45.1"N 42°36'14.9"E) and named (S3).

From each location, one composite sample consisting of five sub-samples,

at layer of 0-10cm, from five locations within area of 1m^2 was obtained. Soils were air-dried, crushed to pass a 2mm sieve, thoroughly mixed and kept for investigations.

2. Heavy metals

Two heavy metals; Pb^{2+} and Cd^{2+} , were used throughout the work as $\text{Pb}(\text{CHCOOH})_2 \cdot 3\text{H}_2\text{O}$ and $\text{CdCl}_2 \cdot \text{H}_2\text{O}$, respectively. Standard stock solutions of each metal salt were prepared and used to supplement the culture medium to attain the desired metal-ion concentrations.

3. Microbiological determinations

For the enumeration of soil bacteria, a 10.0 g representative soil sample was taken after thoroughly mixing three equal portions of each soil sample. Total plate counts, presumably bacterial counts, were determined on nutrient agar medium (Karki, 2020). Colony counts of intrinsically resistant-microorganisms to lead and cadmium ions were determined on the aforementioned media supplemented with known volume of sterile lead acetate and cadmium chloride monohydrate solutions to reach 100, 200, 300, 400 and $500 \mu\text{g Pb}^{2+} \cdot \text{ml}^{-1}$ and 5, 10, 15, 20 and $25 \mu\text{g Cd}^{2+} \cdot \text{ml}^{-1}$.

Colonies developing on suitable agar plates of various Pb^{2+} and Cd^{2+} concentrations were chosen according to variation in cultural characteristics and colony formation. A number of tolerant isolates were selected, purified, and arranged in groups according to Gram-reaction and Malachite green staining.

Pure bacterial isolates cultures were tested for their maximum tolerable concentration of lead and cadmium ions by inoculation on nutrient agar plates

provided with 100, 200, 300, 400 and $500 \mu\text{g Pb}^{2+} \cdot \text{ml}^{-1}$ and 5, 10, 15, 20 and $25 \mu\text{g Cd}^{2+} \cdot \text{ml}^{-1}$. Cultures that, only, able to grow at concentration of $500 \mu\text{g Pb}^{2+} \cdot \text{ml}^{-1}$ and $25 \mu\text{g Cd}^{2+} \cdot \text{ml}^{-1}$ were subjected to further metal stress till reach their maximum metal-tolerance. These selected isolates were counted on nutrient agar medium supplemented with three increased concentrations of each metal, which resulted in a reduction of the bacterial counts by $< 25\%$, *ca.*50% and $> 90\%$. These concentrations were 500, 2000 and $6000 \mu\text{g Pb}^{2+} \cdot \text{ml}^{-1}$ medium and 25, 250 and $500 \mu\text{g Cd}^{2+} \cdot \text{ml}^{-1}$ medium. The pure cultures were sub-cultured on nutrient agar and preserved at *ca.* 4°C for further investigations.

4. Mechanical and chemical analysis of soils

The three soil samples were subjected to mechanical and chemical examinations. Soils were analyzed for the determination of total soluble salts (T.S.S) and organic matter content (O.M) according to Richards (1954). The total lead and cadmium ions were determined by using ICP-OES according to the methodology of EPA 200.7 the Central Laboratory for Analysis of Pesticides Residues and Heavy Metals in Food (QCAP), the official laboratory of the Egyptian Ministry of Agriculture (Agricultural Research Center, Egypt).

Results

1. Effect of soil pollution with Pb^{2+} and Cd^{2+} on the total bacterial counts and the development of metal-tolerant bacteria

It can be argued that soil that was exposed to industrial pollution (S3) and

irrigated by municipal treated water (S2) have been contaminated with amount of Pb^{2+} and Cd^{2+} higher than that away from any source of pollution (S1). Concentrations of total Pb^{2+} and Cd^{2+} in the three sites under investigation are given in Table (1) and illustrated in Figure (1b). Amounts of Pb^{2+} in S3, S2 and S1 soil samples recorded 2.04, 0.86 and 0.64 $\mu g Pb^{2+}.g^{-1}$ air-dried soil, respectively. The same trend was observed for the concentration of Cd^{2+} , where 0.34, 0.11 and 0.04 $\mu g Cd^{2+}.g^{-1}$ air-dried soil were

found in the locations S3, S2 and S1, respectively.

Regarding total soluble salts, it is clear from Table (1) that salt accumulation was similarly higher in location S2 and S3 than S1. On the other hand, the percentage of the organic matter (O.M) content showed an opposite approach, where 0.42, 0.65 and 1.70 O.M % were recorded for the soils of S3, S2 and S1, respectively (Figure 1a).

Table (1): Mechanical and chemical properties of the soil samples from Agricultural Field in Aladya Area (S1), Agricultural Field Irrigated with Treated Water from the Sewage Treatment Plant in Jazan (S2) and Field of Block Factory in Al-Maabouj Area (S3)

Locations:	(S1)	(S2)	(S3)
Mechanical Analysis			
Type of soil:	Sandy loam	Sandy loam	Loamy
Sand (%)	50.00	56.00	46.00
Silt (%)	44.50	39.00	45.00
Clay (%)	5.50	4.50	8.50
Chemical Analysis			
1- Total Soluble Salts (T.S.S %)	0.09	0.82	0.98
2- Organic Matter (O.M %)	1.70	0.65	0.42
3- Metal determination:			
a- Total Pb^{2+} ($\mu g.g^{-1}$ soil)	0.64	0.86	2.04
b- Total Cd^{2+} ($\mu g.g^{-1}$ soil)	0.04	0.11	0.34

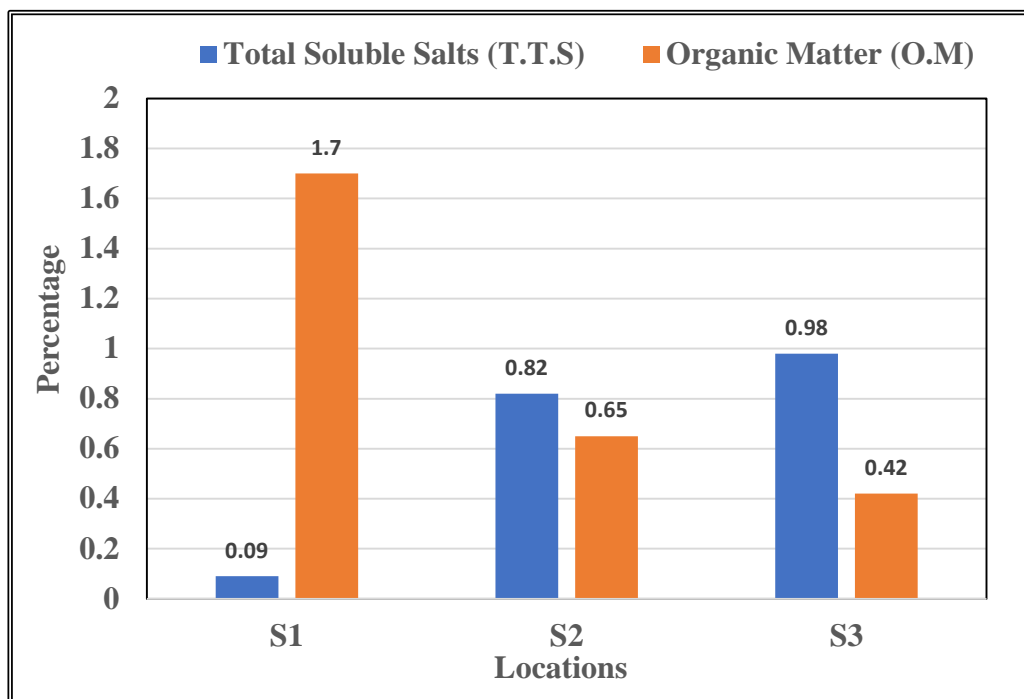


Figure (1a): Percentages of the Total Soluble Salts (T.S.S) and organic matter content (O.M) in the locations under investigation.

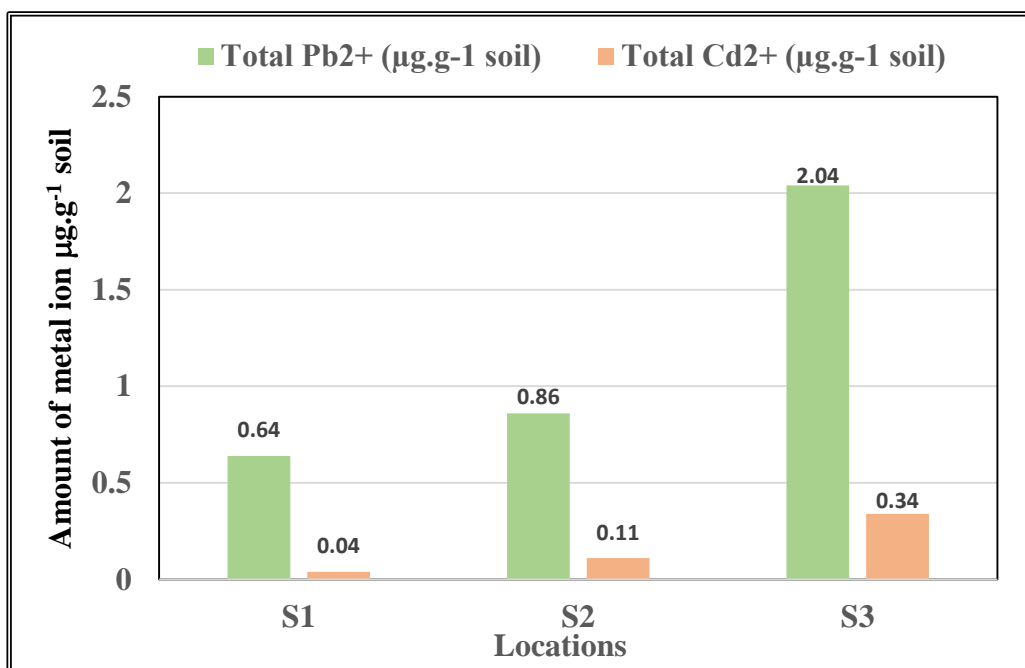


Figure (1b): Amount of the total Pb²⁺ and Cd²⁺ in the locations under investigation.

Total colony counts were determined on metal-free nutrient agar medium, as well as, on the same medium provided with known concentrations of Pb^{2+} and Cd^{2+} . Counts obtained on medium supplemented with a specific concentration of Pb^{2+} or Cd^{2+} indicate bacteria that can tolerate this metal concentration. Relating these numbers to the corresponding counts on Pb^{2+} and Cd^{2+} -free medium will indicate the percentage of metal-tolerant bacteria in total count prevailing in the soil samples.

As shown in Table (2), total bacterial counts in the examined soil samples were widely varied from one site to another. Results showed a drastic decrease in microbial counts with metal concentration increase. Counts in the heavily Pb^{2+} - and Cd^{2+} - polluted sites (S2) and (S3), being 5.3×10^5 and 0.32×10^5 CFU.g⁻¹ air-dried soil, respectively, were markedly lower than those in site (S1) of 78.0×10^5 CFU.g⁻¹ air-dried soil characterized by its low Pb^{2+} and Cd^{2+} content.

It was found of interest to investigate if soil pollution with the heavy metals could result in the development of bacterial groups able to tolerate/resist the toxic effect of Pb^{2+} and Cd^{2+} . Field samples from the three locations were analyzed to determine the number of bacteria able to tolerate different concentrations of Pb^{2+} from 100 to 500 $\mu\text{g Pb}^{2+}.\text{ml}^{-1}$ medium and Cd^{2+} from 5 to 25 $\mu\text{g Cd}^{2+}.\text{ml}^{-1}$ medium.

Data given in Table (2) and illustrated in Figure (2a), showed that 11.7 and 24.4 % of the total bacterial count in the highly Pb^{2+} polluted sites (S2) and (S3), respectively, could tolerate the presence of 100 $\mu\text{g Pb}^{2+}.\text{ml}^{-1}$

medium. The other site (S1) owing less amount of Pb^{2+} contamination, harbored lower percentage of 6.66 of total count which could tolerate the same concentration of Pb^{2+} .

Regarding bacterial tolerance to higher Pb^{2+} concentrations in the three sites, a range from 1.0 to 4.7 % of total bacterial count could tolerate 200 and 300 $\mu\text{g Pb}^{2+}.\text{ml}^{-1}$ medium. Lower numbers of bacteria in soil samples (S1) and (S2) tolerate 400 and 500 $\mu\text{g Pb}^{2+}.\text{ml}^{-1}$ medium where they represented 0.005 & 0.07 % and 0.0008 % & 0.016 of the corresponding total counts, respectively. It is worth mentioning that in S3 site, although less numbers of bacteria tolerated the concentrations of 400 and 500 $\mu\text{g Pb}^{2+}.\text{ml}^{-1}$ medium (0.27 and 0.04 %, respectively), it is still having higher percentage of tolerated bacteria than those in sites (S1) and (S2) at the same two concentrations.

Taking into consideration the soils content of cadmium, results recorded in Table (2) and illustrated in Figure (2b) showed that 13.40 and 14.7 % of the total bacterial counts were having the ability to tolerate a concentration of 5 $\mu\text{g Cd}^{2+}.\text{ml}^{-1}$ medium in soil samples of sites (S2) and (S3), respectively. On the other hand, the site (S1), which owing less contamination of Cd^{2+} , recorded a percentage of 7.95 of total bacterial count were tolerated the same aforementioned concentration. Less numbers of bacterial counts were able to tolerate a concentration of 10 and 15 $\mu\text{g Cd}^{2+}.\text{ml}^{-1}$ medium in the soil samples of site (S1). The percentage of tolerated bacterial counts for these two concentrations was 0.07 and 0.01, respectively. Meanwhile, increased

percentages of the tolerated bacteria were recorded for the same two concentrations (0.89, 0.12 % and 2.03, 1.22 %) in the other two sites S2 and S3, respectively. Almost the same trend was observed at concentrations of 20 and 25 $\mu\text{g Cd}^{2+} \cdot \text{ml}^{-1}$ medium for the three investigated sites. Concerning (S1) site, only 0.005 and 0.0001 % were able to tolerate 20 and 25 $\mu\text{g Cd}^{2+} \cdot \text{ml}^{-1}$ medium, respectively. A slightly higher

percentage was recorded for the tolerated bacteria at the same aforementioned two concentrations in S2 and S3 sites (0.015, 0.001 % and 0.18, 0.015 %, respectively).

More investigations were carried out on some selected isolates from the plates supplemented with different concentrations of Pb^{2+} and Cd^{2+} .

Table (2): Effect of soil pollution with different concentrations of Pb^{+2} and Cd^{+2} on the total bacterial counts and the percentages of the tolerant bacteria in the studied areas of Agricultural Field in Aladya Area (S1), Agricultural Field Irrigated with Treated Water from the Sewage Treatment Plant in Jazan (S2) and Field of Block Factory in Al-Maabouj Area (S3)

Locations:	(S1)		(S2)		(S3)	
Microbiological Analysis						
Metal Concentrations in medium ($\mu\text{g} \cdot \text{ml}^{-1}$)	1- Total Bacterial Counts (CFU x 10⁵) determined on agar medium provided with different concentration of Pb^{+2} and the percentage of tolerant bacteria					
	T.C	%	T.C	%	T.C	%
0	78.0	100.0	5.3	100	0.32	100
100	5.2	6.66	0.62	11.7	0.078	24.40
200	2.3	2.95	0.21	3.96	0.015	4.70
300	0.78	1.00	0.067	1.26	0.0052	1.63
400	0.004	0.005	0.0038	0.07	0.00086	0.27
500	0.0006	0.0008	0.00057	0.016	0.00012	0.04
Metal Concentrations in medium ($\mu\text{g} \cdot \text{ml}^{-1}$)	2- Total Bacterial Counts (CFU x 10⁵) determined on agar medium provided with different concentration of Cd^{+2} and the percentage of tolerant bacteria					
	T.C	%	T.C	%	T.C	%
0	78.0	100.0	5.3	100	0.32	100
5	6.20	7.95	0.71	13.40	0.047	14.70
10	0.054	0.07	0.047	0.89	0.0065	2.03
15	0.0087	0.01	0.0062	0.12	0.0039	1.22
20	0.0041	0.005	0.00078	0.015	0.00056	0.18
25	0.000083	0.0001	0.000049	0.001	0.000047	0.015

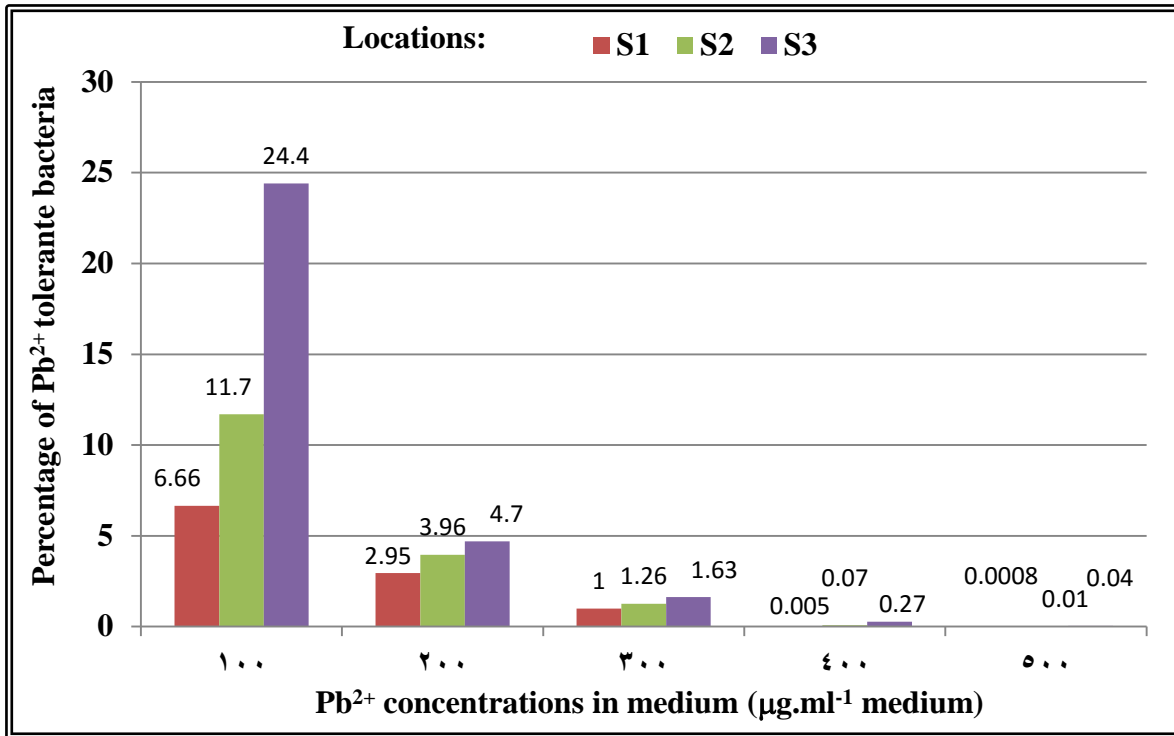


Figure (2.a): Percentages of Pb^{2+} -tolerant bacteria in soils taken from locations S1, S2 and S3.

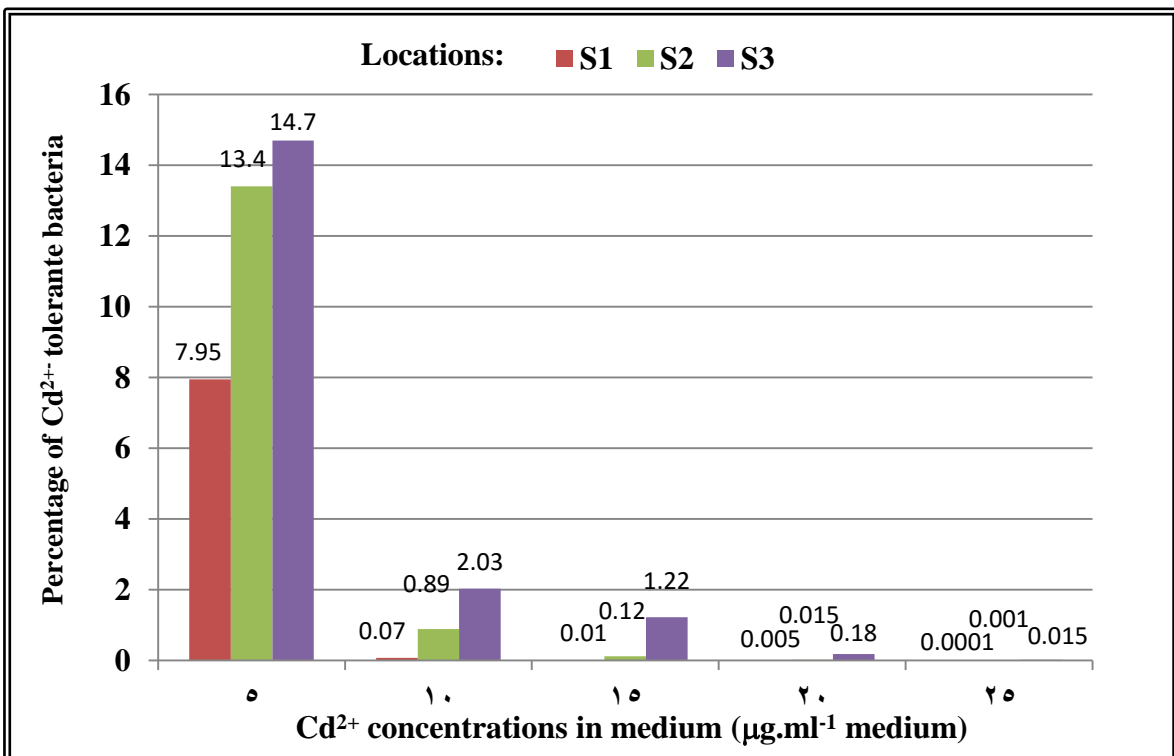


Figure (2.b): Percentages of Cd^{2+} -tolerant bacteria in soils taken from locations S1, S2 and S3.

2. Screening and isolation of developed metal-tolerant bacteria

A total of 18 bacterial purified cultures were isolated from agar plates used for counting Pb^{2+} - and Cd^{2+} -tolerant bacteria. For more selection of the higher metal-tolerant isolate(s), an inoculum of each culture was spreaded on nutrient agar plate supplemented with 100 to 500 $\mu g Pb^{2+} .ml^{-1}$ medium and 5 to 25 $\mu g Cd^{2+} .ml^{-1}$.

Morphological examination of pure isolates from plates supplemented with Pb^{2+} concentrations revealed that among the ten isolates, 6 (60.0 %) were Gram-positive spore-formers, 3 (30.0 %) were Gram-positive non-sporing rods and 1 (10.0 %) were Gram-negative non-sporing short rods. Concerning the isolates from Cd^{2+} -supplemented plates, they were 4 (50.0 %) Gram-positive spore-forming rods, 1 (12.5%) Gram-positive non-sporing rods and 3 (37.5%) Gram-negative non-sporing short rods (Table 3).

As might be expected, most of the eighteen isolates could grow properly in presence of 100 $\mu g Pb^{2+}$ and 5 $\mu g Cd^{2+}$, where colony formation, as an indicator for bacterial growth, was almost quite comparable to that in the corresponding control medium devoid of Pb^{2+} and Cd^{2+} . It is clear that 50 % of the isolates were able to tolerate up to 100 $\mu g Pb^{2+} .ml^{-1}$ medium, and 62.5 % of the eight isolates tolerated up to 5 $\mu g Cd^{2+} .ml^{-1}$ medium. Concerning the bacterial group of Gram-positive spore-forming rods, one isolate, for each, was able to tolerate the concentrations 200, 300 400 and 500 $\mu g Pb^{2+} .ml^{-1}$ medium. On the other hand, only one Gram-positive non-sporing rod isolate tolerated up to

200 $\mu g Pb^{2+} .ml^{-1}$ medium and one Gram-negative non-sporing short rod isolate was able to tolerate up to 100 $\mu g Pb^{2+} .ml^{-1}$ medium.

Concerning isolates from plates provided with different concentrations of Cd^{2+} , results showed that five isolates (62.5%) of the eight ones were able to tolerate up to only 10 $\mu g Cd^{2+} .ml^{-1}$ medium, while only one Gram-positive spore-forming rod isolate, one Gram-positive non-sporing rod isolate, and one Gram-negative non-sporing short rods isolate, were able to tolerate concentrations of Cd^{2+} up to 25, 10 and 10 $\mu g Cd^{2+} .ml^{-1}$ medium, respectively.

From the results obtained in the present experiment, it was found that one Gram-positive spore-forming bacterial isolate was able to tolerate Pb^{2+} concentration up to 500 $\mu g .ml^{-1}$, named (SS/1) and another Gram-positive spore-forming one was able to tolerate concentration of 25 $\mu g .ml^{-1} Cd^{2+}$, named (SS/2). The SS/1 isolate was rods characterized by central spore, while the SS/2 isolate was slightly thin long rods with spore of lateral position (photo 1a and b and photo 2a and b).

Table (3): Arrangement of Pb²⁺- and Cd²⁺-tolerant bacterial isolates into groups according to their morphological characteristics, and their maximum Pb²⁺- and Cd²⁺-tolerable concentration.

Bacterial Group	No. of Isolates (percentage to total isolates)	Tolerable metal concentration (µg.ml ⁻¹)	Isolates tolerating different concentrations of metal	
			No. of Isolates ⁽¹⁾	% ⁽²⁾
1- Nutrient agar medium supplemented with Pb²⁺ concentrations				
Gram-positive spore-forming	6 (60 %)	100	2	20
		200	1	10
		300	1	10
		400	1	10
		500	1	10
Gram-positive non-sporing	3 (30 %)	100	2	20
		200	1	10
		300	0	0
		400	0	0
		500	0	0
Gram- negative non-sporing	1 (10 %)	100	1	10
		200	0	0
		300	0	0
		400	0	0
		500	0	0
2- Nutrient agar medium supplemented with Cd²⁺ concentrations				
Gram-positive spore-forming	4 (50 %)	5	3	37.5
		10	0	0
		15	0	0
		20	0	0
		25	1	12.5
Gram-positive non-sporing	1 (12.5 %)	5	0	0
		10	1	12.5
		15	0	0
		20	0	0
		25	0	0
Gram-negative non-sporing	3 (37.5 %)	5	2	25.0
		10	1	12.5
		15	0	0
		20	0	0
		25	0	0

(1): Number of isolates tolerating the specified Pb²⁺- and Cd²⁺- concentration indicated in the adjacent column.

(2): Percentage of the tolerating bacterial number in corresponding to the total number of its bacterial group.

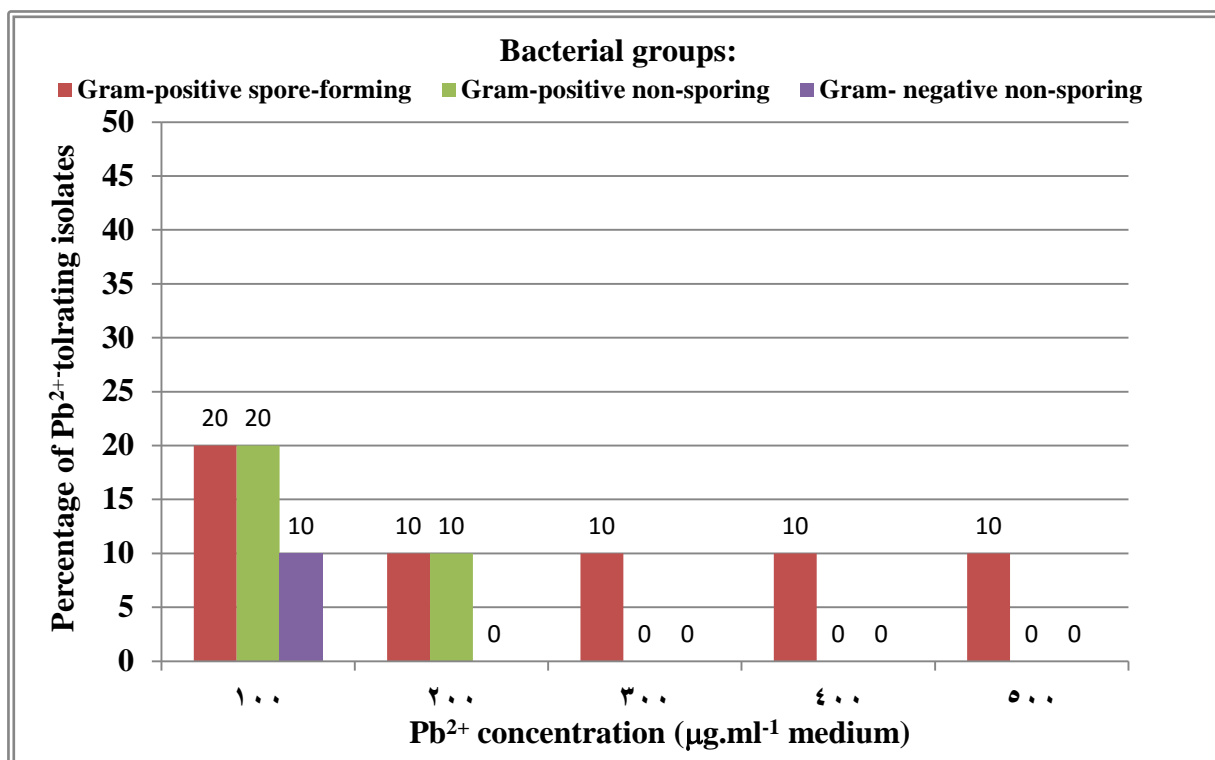


Figure (3.a): Percentages of the bacterial groups tolerating different concentrations of Pb²⁺

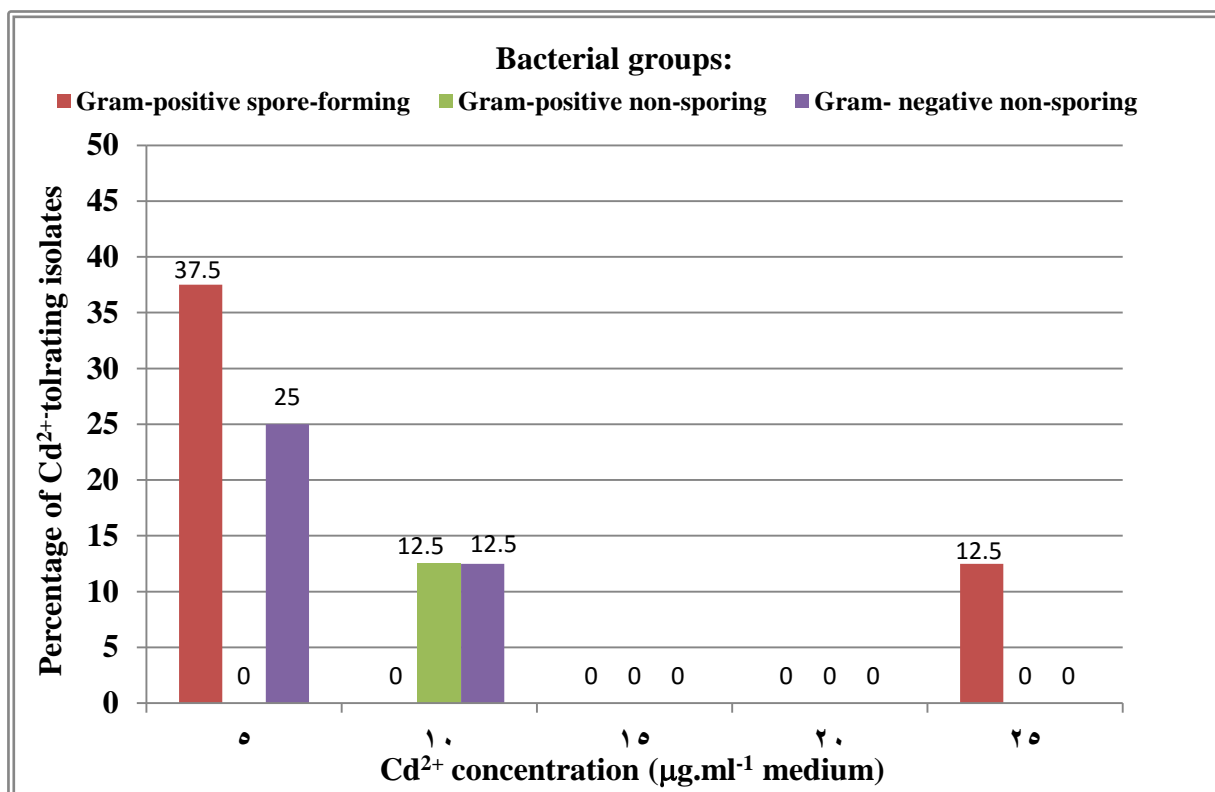
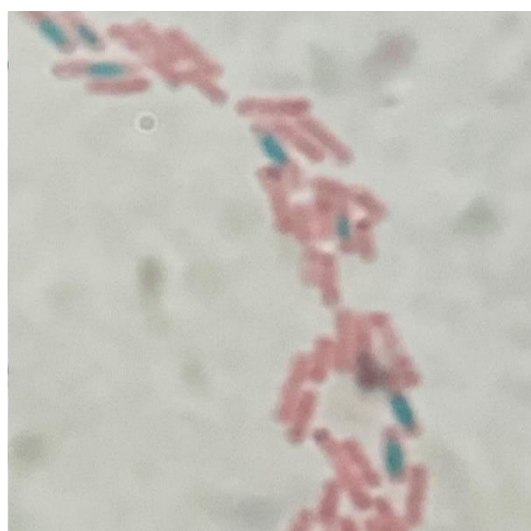


Figure (3.b): Percentages of the bacterial groups tolerating different concentrations of Cd²⁺



(a)



(b)

Photo (1): Gram-positive spore-forming SS/1 bacterial isolate film stained by Gram-stain (a) and malachite green stain (b).



(a)



(b)

Photo (2): Gram-positive spore-forming SS/2 bacterial isolate film stained by (a) Gram-stain and (b) malachite green stain.

Pure cultures of SS/1 and SS/2 isolates that were able to grow at 500 $\mu\text{g Pb}^{2+}.\text{ml}^{-1}$ and 25 $\mu\text{g Cd}^{2+}.\text{ml}^{-1}$, respectively were subjected for further metal stress till reach their maximum metal-tolerance. Three concentrations for each metal, which resulted in a reduction of the bacterial counts by

< 25%, *ca.*50% and > 90% were chosen. These concentrations were 500, 2000 and 6000 $\mu\text{g Pb}^{2+} \text{ml}^{-1}$ medium for isolate SS/1 and 25, 250 and 500 $\mu\text{g Cd}^{2+} \text{ml}^{-1}$ medium for isolate SS/2. The decrease in their count and percentage of metal inhibition was recorded in table (4) and illustrated in figure (4).

Table (4): Effect of three Pb^{+2} and Cd^{+2} concentrations on the counts of two highly metal-tolerant bacterial isolates.

Metal concentrations in medium ($\mu\text{g}.\text{ml}^{-1}$)	Total bacterial counts ($\text{CFU} \times 10^7$)	Decrease in bacterial counts ($\text{CFU} \times 10^7$) ⁽¹⁾	Inhibition percentage ⁽²⁾
1- Pb^{2+}-Tolerable Isolate (14/100)			
Control (0-metal)	23.80	0.00	0.00
500	18.19	5.61	23.57
2000	11.61	12.19	51.20
6000	2.03	21.77	91.47
2- Cd^{2+}-Tolerable Isolate (D/25)			
Control (0-metal)	26.93	0.00	0.00
25	20.22	6.71	24.91
250	12.32	14.63	54.32
500	2.57	24.43	90.71

(1): Decrease in bacterial count relative to the control medium ($\text{CFU} \times 10^7$).

(2): Percentage of decrease in bacterial count relative to the control medium.

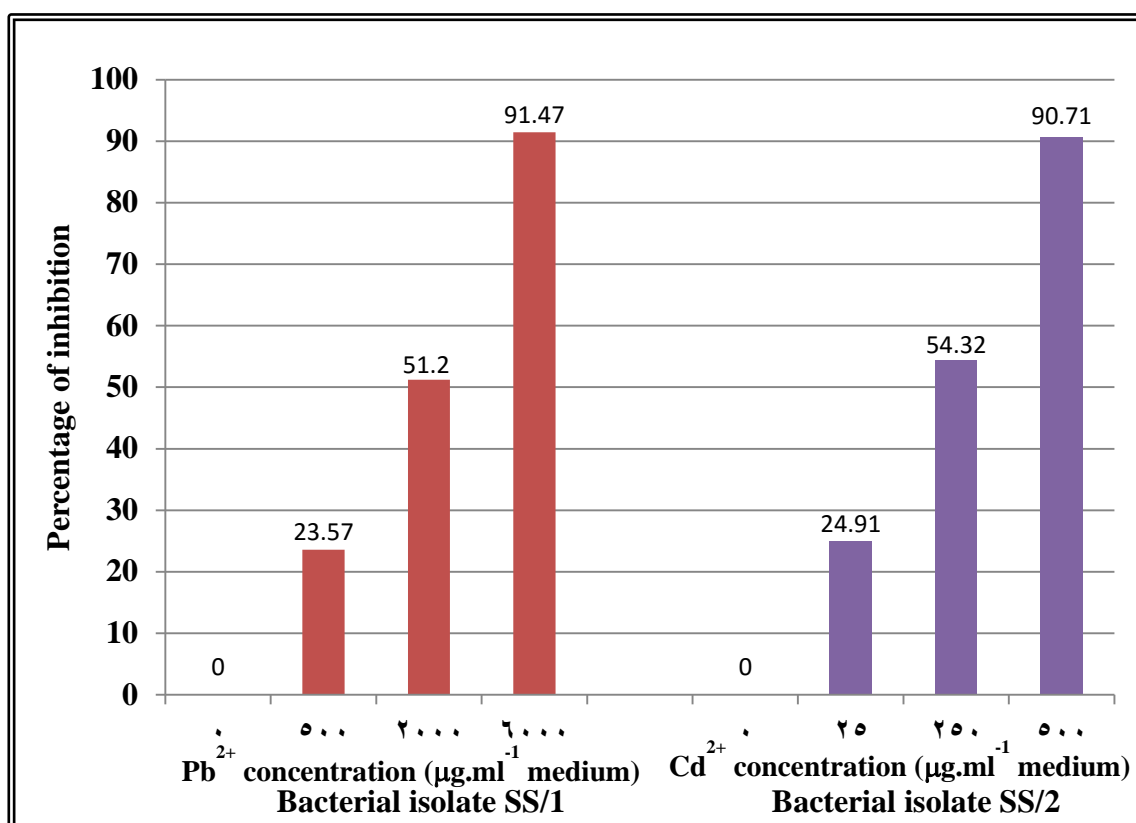


Figure (4): Inhibition percentage in microbial counts of (SS/1) and (SS/2) bacterial isolates as affected by three levels of Pb²⁺ and Cd²⁺.

Discussion

1. Effect of soil pollution with Pb²⁺ and Cd²⁺ on the total bacterial counts and the development of metal-tolerant bacteria

Heavy metal pollution has emerged due to anthropogenic activities, which is the prime cause of pollution. Industrial processes such as metal and coal mining, fossil fuel combustion, dust from chimneys of factories and disposal of wastes and effluents has greatly increased the burden of heavy metal pollution in soil.

Results clearly point out that soil adjacent to Block Factory (S3) is subjected to heavy metal pollution of Pb²⁺ and Cd²⁺ higher than that recorded in soil (S2) that was irrigated by treated water from the Sewage Treatment Plant. On the other hand, less pollution by

Pb²⁺ and Cd²⁺ was observed in the soil of agriculture field in Al-Adaya area (S1) which lies away from any source of pollution. In connection with this point, it is noteworthy that examination of soils located near sources of pollution with heavy metals example Pb²⁺, Cd²⁺, As²⁺.... etc. have been found to harbor higher amount of metals than those in locations far from the pollution sources (Briffa *et al.*, 2020). In addition, they found that presence of metals in the soils alter its properties and impact its quality.

As might be expected, total bacterial counts in the soil that exposed to industrial pollution (S3) and that was irrigated by treated water from the Sewage Treatment Plant (S2) were harbored lower microbial counts compared to that away from any source

of pollution (S1). It was clearly noticed that there is a close opposite relation between the three soil content of Pb^{2+} and Cd^{2+} , and their bacterial population. Results obviously showed drastic reduction in bacterial counts in soils of high Pb^{2+} and Cd^{2+} content, in which metal causes toxicity to microorganisms by deactivation or inhibition of enzymatic activities (Ayele *et al.*, 2021), destruction of nucleic acids and proteins, inhibition of microbial respiration and disruption of their cell wall (Hamsa *et al.*, 2017; Igiri *et al.*, 2018 and Tarekegan *et al.*, 2020). However, it should be realized that such high concentration of heavy metals could not be the only reason for reduced bacterial numbers in the areas under investigation but may be considered as one of the most important suppressive factors for microbial proliferation. It is well known that microbial population densities are affected by a combination of several physical and chemical factors. Actually, total soluble salts in soil may have a part in reducing the bacterial numbers in the S2 and S3 sites. The high salt content in addition to the heavy metal pollution with lead and cadmium may be the reason for the low bacterial counts recorded. It was found of interest to investigate if soil pollution with heavy metals could result in the development of bacterial groups able to tolerate / resist the toxic effect of Pb^{2+} and Cd^{2+} .

The general trend of the results obtained indicated that presence of high Pb^{2+} and/ or Cd^{2+} concentrations in soil resulted in the development of a number of microorganisms which adapt themselves for the toxic effect of the metal. This result was in harmony with

the findings of Neis (1999) who stated that to survive under metal-stressed conditions, bacteria have evolved several types of mechanisms to tolerate the high concentrations of heavy metals. These mechanisms include the efflux of metal ions inside the cell and reduction of heavy metal to a less toxic state. Another explanation for the development of Pb^{2+} and Cd^{2+} tolerant bacteria, may be given, where any possible decrease in Pb^{2+} and / or Cd^{2+} -sensitive bacteria could be compensated by an increase in Pb^{2+} and / or Cd^{2+} -tolerant ones. More investigations were carried out on some selected isolates from the plates supplemented with different concentrations of Pb^{2+} and Cd^{2+} .

2. Screening and isolation of metal-tolerant bacteria

Results obtained from this experiment point out to a marked variation between selected soil bacterial isolates, differing in their morphological and physiological characteristics to resist the toxic effect of different concentrations of Pb^{2+} and Cd^{2+} in culture medium. From another point of view, bacteria can play an important role in removing heavy metals from solution; a phenomenon of great importance included under the so called "microbial-metal interaction".

Results of the previous experiment indicated that within the different soil bacterial groups, there is a number of isolates which can resist the harmful effects of the two heavy metals (Pb^{2+} and Cd^{2+}). Accordingly, it is of importance to screen and isolate the bacteria that are capable of tolerating the highest metals concentration for further investigation.

It was found that 10 % of the total six Gram-positive spore-forming bacteria were able to tolerate the highest concentration of Pb^{2+} (500 $\mu g.ml^{-1}$ medium), and 12.5 % of the total four Gram-positive spore-forming bacteria tolerated Cd^{2+} concentration of 25 $\mu g.Cd^{2+}.ml^{-1}$ medium. The least Pb^{2+} and Cd^{2+} -tolerable isolates were recorded for the groups of Gram-positive non-sporing and Gram-negative non-sporing bacteria.

Results agreed with that observed by **Gadd (1990)** who stated that the walls of Gram-positive bacteria are efficient metal chelators. This type of bacteria has the carboxylic group of glutamic acid of peptidoglycan which is the major site of metal deposition. Moreover, **Ray et al. (2006)** confirmed this finding by saying that *Bacillus cereus* M996 has similar cell wall properties as Gram-positive bacteria. In a different study, **Mounaouer et al. (2013)** reported that isolates of Gram-negative bacteria were more resistant to the mixture of metals than those of Gram-positive ones. An explanation for Gram-positive spore forming tolerance of heavy metals, was introduced by **Selenska-Pobell et al. (1999)** who described that, the spore passes the capability to irreversibly bind large amounts of metals such as Al, Cd and U.

It is clear that the metal-tolerant bacteria owing different mechanisms to resist the harmful effects of heavy metals. From another point of view, these metal-tolerant isolates employ one or several of these mechanisms to remove / remediate Pb^{2+} and Cd^{2+} from the contaminated soil. It is of importance and seriously recommended

to study the efficiency of the most two metal-tolerable isolates to adsorb Pb^{2+} and Cd^{2+} from a nutritive medium, as well as, from a soil microcosm system.

Further experimental work was recommended to study the efficiency of the two selected isolates (SS/1) and (SS/2), which differ in their properties, to adsorb Pb^{2+} and Cd^{2+} , respectively, from a nutritive solution, as well as from a soil microcosm system.

Conclusion

Pollution of agricultural soil with heavy metals is one of the most harmful kinds of pollution, which adversely affects soil fertility and its productivity. Summing up the results obtained in the present study, it can be concluded:

1. Both Pb^{2+} and Cd^{2+} exhibited an adverse effect on total microbial population, and this effect was increased with the increase of heavy metals pollution rate.
2. The general trend points out that Cd^{2+} may have a higher toxicity level on soil bacteria compared to Pb^{2+} .
3. Although there are bacteria that are naturally resistant to heavy metals, the study suggested that exposure to accumulative and increasing pollution from these metals can result in species that can resist and adapt themselves to the toxic effect of heavy metals.
4. It is highly recommended to subject the highly metal-tolerant bacterial species found in this study to further studies that examine their capability to absorb different heavy metals from contaminated environments. This will be of importance to use them in the biological disposal (bioremediation) of heavy metals.

References

- Ayele, A., Haile, S., Digafe, A., and Kamaraj, M. (2021). Comparative Utilization of Dead and Live Fungal Biomass for the Removal of Heavy Metal: A Concise Review. *Science World Journal*. 2021: 5588111.
- Briffa, J., Sinagra, E. and Blundell, R. (2020). Heavy metal pollution in the environment and their toxicological effects on humans. *Heliyon*. 6(9): e04691.
- Demnerová, K., Mackova, M., Speváková, V., Beranova, K., Kochánková, L., Lovecká, P., Ryslavá, E., and Macek, T. (2005). Two approaches to biological decontamination of groundwater and soil polluted by aromatics characterization of microbial populations. *International Microbiology*. 8: 205-211.
- Gadd, G. M. (1990). Heavy metal accumulation by bacteria and other microorganisms. *Experientia*. 46: 834-840.
- Hamsa, N., Yogesh, G., Koushik, U. and Patil, L. (2017). Nitrogen Transformation in Soil: Effect of Heavy Metals. *International Journal of Current Microbiological Application Science*. 6(5): 816-832.
- Igiri, B., Okoduwa, S., Idoko, G., Akabuogu, E., Adeyi, A. and Ejiogu, I. (2018). Toxicity and Bioremediation of Heavy Metals Contaminated Ecosystem from Tannery Wastewater: A Review. *Journal of Toxicology*. 2018: 2568038.
- Johny Rani, M., Hemambika, B., Hemapriya, J., and Rajeshkannan, V. (2010). Comparative assessment of heavy metal removal by immobilized and dead bacterial cells: A biosorption approach. *Global Journal of Environmental Research*. 4 (1): 23-30.
- Karki, G. (2020). Enumeration of bacteria by plate count technique. In: "Karki, G." (Ed.). *Biology Practical, Microbiology practical*.
- Mounaouer, B., Nesrine, A., and Abdennaceur, H. (2013). Identification and characterization of heavy metal-resistant bacteria selected from different polluted sources. *Desalination and Water Treatment*. 52: 37-39.
- Nies, D. H. (1999). Microbial heavy-metal resistance. *Applied Microbiology and Biotechnology*. 51: 730 - 750.
- Rajaganapathy, V., Xavier, F., Sreekumar, D., and Mandal, P. K. (2011). Heavy Metal Contamination from Soil, Water and Fodder and Their Presence in Livestocks and Products: A Review. *Journal of Environmental Science and Technology*. 4: 234-249.
- Ray, L., Paul, S., Bera, D., and Chattopadhyay, P. (2006). Bioaccumulation of Pb (II) from aqueous solutions by *Bacillus cereus* M1 16. *Journal of Hazardous Substance Research*. 5: 1-22.
- Richards, L. A. (1954). U. S. Salinity laboratory Staff. Diagnosis and Improvement of Saline and Alkaline Soils. Agricultural Handbook N° 60.
- Selenska-Pobell, S., Panak, P.; Miteva, V., Boudakov, I., Bernhard, G., and Nitsche, H. (1999). Selective accumulation of heavy metals by three indigenous *Bacillus* strains, *B. cereus*, *B. megaterium* and *B. sphaericus*, from drain waters of a

uranium waste pile. *FEMS Microbiology Ecology*. 29 (1): 59–67.

Tarekegan, M., Salilih, F., and Ishetu, A. (2020). Microbes used as a tool for bioremediation of heavy metal from the environment. *Cogent Food and Agriculture*. 6: 1783174.

تأثير تلوث التربة بالرصاص والكاديوم على نشأة عزلات بكتيرية مقاومة للعناصر الثقيلة

في منطقة جازان، المملكة العربية السعودية

أزهار يحيى النعمي^١، محمد نصر الليثي^١^١ قسم الأحياء، كلية العلوم، جامعة جازان، المملكة العربية السعودية

المخلص

العناصر الثقيلة من أهم مصادر التلوث في بيئة التربة. أُجرى البحث على عينات تربة بمنطقة جازان. تم العمل على ثلاثة مواقع: حقل زراعي بمنطقة العداية (S1)، تربة تروى بمياه معالجة بمحطة معالجة مياه الصرف الصحي في جازان (S2)، وتربة من مصنع بلوك في منطقة المعبوج (S3). تمت دراسة تأثير تلوث التربة بعنصري الرصاص والكاديوم على الكثافة الميكروبية، والتطور المحتمل للبكتيريا المقاومة للعناصر الثقيلة. تم عزل البكتيريا شديدة التحمل للعنصرين ودراسة مدى تحملها لأقصى تركيز من العنصرين. كانت كميات الرصاص والكاديوم الكلية كانت أعلى في المواقع S2 و S3 عنها في S1، بينما كانت نسبة المادة العضوية أقل في S2 و S3 عنها في S1. كان العدد الكلي البكتيري في الموقعين S2 و S3 (٥,٣، ٠,٣٢ x ١٠⁵ مستعمرة ميكروبية. جم⁻¹ تربة، على التوالي) أقل بشكل ملحوظ من تلك الموجودة في الموقع S1 (٧٨ x ١٠⁵ مستعمرة ميكروبية. جم⁻¹ تربة). كانت نسبة التحمل للتركيزين ٢٠٠ و ٣٠٠ ميكروجرام رصاص. مل⁻¹ ما بين ١,٠ - ٤,٧٪ من العدد الإجمالي للبكتيريا، على التوالي، بينما أعداد قليلة تحملت التركيزين ٤٠٠ و ٥٠٠ ميكروجرام رصاص. مل⁻¹. تحمل ١٣,٤٠ و ١٤,٧٪ من العدد الإجمالي للبكتيريا تركيز ٥ ميكروجرام كاديوم. مل⁻¹ في الموقعين S2 و S3 على التوالي. تم عزل مزرعتين بكتيريتين من النوع العصوي المتجرثم وموجبة الصبغ لجرام، من الأطباق المعاملة بتركيزات من الرصاص والكاديوم وسميت SS/1 و SS/2، على التوالي. تم تعريض العزلة البكتيرية SS/1 للتركيزات ٥٠٠، ٢٠٠٠، ٦٠٠٠ ميكروجرام رصاص. مل⁻¹ والعزلة البكتيرية SS/2 للتركيزات ٢٥، ٢٥٠، ٥٠٠ ميكروجرام كاديوم. مل⁻¹. أختيرت هذه التركيزات لكونها تسبب انخفاض في العدد بنسبة $Ca.50, 25$، 90٪، على التوالي.

الكلمات المفتاحية: التلوث، العناصر الثقيلة، الميكروبات، التحمل للعناصر الثقيلة، التربة.

Real-Time Identification of System Users in Complex Settings using Machine Learning

Yahya Muhammed Alqahtani
Jazan University

Abstract

In today's technological era, user experience (UX) design is the primary focus of all software product developments. Rather than developing a system with a specific user group in mind, software systems are now offered to all types of users, from novice to expert. The system employs various methods to aid users during their interactions. These methods are tailored to suit users' needs, especially if they are new to the systems. It is critical to identify users who require assistance based on their interactions with the system. This paper proposes a method for identifying system users in a complex interaction environment using Support Vector Machine (SVM) classification and k-means clustering. Several factors are taken into account to identify vulnerable users, including interface complexity, user response time, and user thinking time. The user dataset is obtained from a complex interface setting. After clustering, the model is trained to identify users who require assistance in moving forward using a classifier. The classifier's performance is evaluated with k-fold validation using a test dataset. The proposed model is a state-of-the-art method for improving user experience in complex system environments, and it will pave the way for future research in this area.

Keywords: User Experience (UX), Human-Computer Interaction (HCI), Machine Learning (ML), K-Means, Support Vector Machine (SVM)

1. INTRODUCTION

Ergonomics, or human factors, is a field that utilizes various methods, principles, and knowledge to improve the design of systems, ultimately leading to improved performance and well-being for humans. It is a subfield of the study of human-system interactions. Basic research from key supporting disciplines, design science that is unique to the area, and application of the resultant data and concepts to specific design challenges are all vital to the discipline of human factors. As a result, human factors

professionals are involved in research as well as the application of study findings

to all stages of system development and evaluation. The importance of basic human capacities, such as perceptual abilities, cognitive abilities, and physical constraints, is embodied in the notion of human factors [1]. The human factors professional must understand the limitations of these talents and apply this knowledge to system design.

There is now a vast amount of scientific evidence regarding human capacities' limits. This field has a century old

history and is at the heart of the larger study of human competence. Human factor research includes examining the processes that support the acquisition, maintenance, transfer, and execution of skillful performance [2] [3]. The study looks for characteristics that limit various parts of a person's performance, evaluates difficult activities by breaking them down into simpler components, and calculates basic human capabilities. We can anticipate how well users will be able to accomplish both easy and complex activities using this data.

Codasyl reported [4] on the initial efforts to understand and describe the occurrence of end-user computing on computing systems. In this study, end users were divided into three groups: direct end users, who use terminals directly; intermediate end users, who specify information needs for reports they finally receive; and indirect end users, who use systems through intermediaries. People who use computer-based systems are included in all three types. Those who only used computer-based systems for business purposes were included in the first type. Participation in report creation, a development activity, fell under the second type, and direct terminal use, or the capacity to take part in system operation, fell under the third. The end-users' primary operations include the operation, development, and control of computer-based systems [5].

Normally, the business provides end-user support to assist with problems and interruptions. End-user support

professionals serve as the initial point of contact when a user has a problem with programs or applications or a fault in a computer program. They are in charge of many different things. They may also provide in-person assistance sessions. The rapid assistance of customers is the main objective of end-user support. End-user support services encompass all concerns related to hardware, software, and networks. End-user support specialists first evaluate the customers' demands and make an effort to provide a prompt and correct response. Users typically start off this process by having someone guide them through issues, teach them how to install software, and answer their queries about network infrastructure. Agents that provide end-user assistance also help users with hardware problems, printing problems, and the reporting of software program flaws. With the rise of remote work, virtual support systems are becoming more important. Virtual assistance allows virtual clients to help users from any location.

While considering universal usability motives, there are three primary classes of system users: novice, intermittent, and expert. Novice users typically have a low grasp of interface ideas and are most often found participating in online activities. Novice users have the most difficulty navigating complicated interfaces. Many attempts are made to reach the users in need using a number of strategies. The work presented here is a highly innovative approach using machine learning techniques to identify system

end users in complex environments who are struggling to move forward. The prime objectives of this research include:

- Review of related literature on system user activity identification or evaluation frameworks
- Study ML-based frameworks for UX and human factors.
- Propose an ML-based classification of system users in real-time to identify vulnerable users.

The structure of this document is as follows: section 2 provides a comprehensive review of related work, section 3 details the methodology of the proposed model, section 4 provides the results of the ML framework, followed by discussions, and section 5 summarizes the outcome of the proposed research.

2. RELATED WORK

Despite the fact that a large number of research papers have been published to address usability issues with various interfaces, the challenges based on user capabilities are quite limited. This section examines and reports on a number of studies on usability, user identification, and classification in a variety of contexts.

Examining user online activities with machine learning is one of the most cutting-edge methods for uncovering insights, including user interaction patterns. Using semi-supervised learning, Labayen et al. [6] devised a technique for categorizing user activities from network traffic. The system

identifies the user's online activity based on the behavior displayed over the network, taking into account all of the data generated by the user within a particular timeframe. The information retrieved from the network is used to characterize user activity at such intervals. A model consisting of three layers is suggested for the classification task. A k-means algorithm is used in the first two layers of the model, while a Random Forest is used in the last layer to obtain the activity labels. According to the authors, the optimal combination of ML algorithms in this work is k-means and a Random Forest.

Suchacka et al. [7] proposed an e-commerce platform-based prediction model using ML-based classification. In each session, user activity in the e-store is represented as a 23-element feature vector. An SVM classification model is introduced based on historical data from an online bookshop, splitting user sessions into two classes: browsing sessions and purchase sessions. According to the authors, the SVM classifier with a linear kernel was found to be quite effective both in terms of overall predictive accuracy and the capacity to forecast purchase sessions.

Revathi et al. [8] designed and implemented an approach to measuring the speed at which a user can process information. The authors used a test to assess this, which included a set of nine comprehension questions. They employed a timekeeper for each question to determine how much time the user spends on each problem, as well as the

time it took to comprehend and gain an exact formula and the accuracy of the individual's calculations. The k-means classification technique was then used to classify users into their appropriate groups. This support is said to improve students' outcomes and future prospects, and the k-means cluster method is useful for clustering students with comparable performance characteristics.

Cui et al. [9] devised a user clustering technique based on the k-means ML algorithm. Furthermore, they suggested a k-means based online user categorization technique in order to increase the computational efficiency in a practical setting where new users arrive in a continuous manner. In an attempt to enhance the suggested mmWave-NOMA (Millimeter-wave non-orthogonal multiple access) system even more, the authors used the successive decoding feature to determine the optimal power allocation strategy. The proposed mmWave-NOMA system effect was improved by the proposed framework when compared to traditional user clustering methods, and the proposed on-line user clustering algorithm, which is based on k-means, performed as well as the traditional k-means method while trying to hit a good equilibrium between effectiveness and efficiency.

Roberto et al. [10] introduced a deep neural network based clustering approach that uses the Hierarchical Rate Splitting mechanism to maximize the rate achieved and learns and groups users based on an instant chaotic channel. The suggested technique is

based on a shallow NN architecture, which allows it to learn and cluster users based on the simultaneous noisy channel in a very short amount of time. The suggested technique relies on a shallow NN architecture, which enables it to learn and group users based on the noisy parallel channel in a very short amount of time. It is claimed that the scheme put forth was capable of reaching a proportion equivalent to existing research and was less difficult than previous methods. This also aided in the investigation of more complex NN structures, such as Graph NN, that can learn covariance among multiple users in order to create clustering.

Pennacchiotti et al. [11] proposed the problem of user categorization on social media networks, using Twitter as an example. They used observable information like user behavior, network structure, and the linguistic content of the user's Twitter feed to automatically deduce the values of user traits like political leaning and ethnicity. They adopted a machine learning technique that relies on a large number of features collected from such user data. It was reported that promising experimental findings were obtained on three tasks with diverse features: detecting political affiliation, identifying ethnicity, and detecting affinity for a specific firm. Ultimately, the results show that rich language variables consistently contributed to success in each of the three tasks and held great potential for future user segmentation needs.

Sassirekha et al. [12] proposed a methodology for tracking and predicting progress in higher education via online learning. The goal of this strategy was to get the greatest prediction results so that we might construct a user-dependent learning system in the future. Logistic regression, linear discriminant analysis (LDA), k-Nearest Neighbor (kNN), classification and regression trees, support vector machine, random forest, and naive bayes were all used on the dataset. Similarly, Dhilipan et al. [13] developed a machine learning-based student academic growth analysis. The analysis makes use of KNN classifiers, entropy, decision trees, and binomial logical regression. It was anticipated that the approach would help the teacher make more informed decisions about the students' progress and plan more efficient strategies for improving their academic achievement.

Alam Sher Khan et al. [14] proposed a user personality classification framework grounded on the Myers-Briggs Type Indicator (MBTI) model, in which the XGBoost classifier is used to predict four personality traits from input text, namely Introversion-Extroversion, intuition-Sensing, Feeling-Thinking, and Judging-Perceiving. To further investigate the personality from expressed text, pre-processing techniques such as tokenization, word stemming, stop words elimination, and feature selection were used. According to the authors, the work provided the foundation for evolving a personality identification system that could assist

organizations in recruiting and selecting appropriate personnel as well as improving their enterprise by knowing the personality and interests of their clients.

Zou et al. [15] proposed a sentiment analysis framework based on machine learning. The features are generated using basic words-bag methods, which do not take into account the syntactic properties of words, which could be important in judging sentiment meanings. They added several sentiment features to the basic words-bag features. Naive Bayes and support vector machines were used to train such features. The results showed that word dependencies and POS tags improved the accuracy of the bigram method. There wasn't much optimization in the clause features.

Rashid et al. [16] explored the potential of controlling assistive devices with an individual's wink using a highly scientific method. The brain signals of the five subjects were recorded in order to identify the left wink, right wink, and no wink. Emotive insight, which has five channels, was used to capture the brain signals. To extract the features, the Fast Fourier transform and the sample range were computed. The obtained features were classified using support vector machine, linear discriminant analysis, and k-Nearest Neighbor. The classifier's performance was assessed. According to the results obtained, a person's wink can be used to control assistive devices.

Saleema et al. [17] presented a data-driven user modeling framework that builds student models for online learning environments using ML. They used the framework to create student models for two different learning environments. Considering the limitations of our dataset's size, they provided an early indication that the system can identify influential interaction behaviors that may be utilized to create new ML models for the online categorization of brand-new student behaviors. It was also demonstrated that the framework can be transferred between applications and data types.

Kim et al. [18] formed TRUE, a framework for tracking real-time user experience, by combining the behavioral aspects of data gathering and analysis with existing HCI approaches. They discussed how they have refined instrumentation methods and analysis to vastly facilitate the development of video games, with two case studies as examples. The authors claim TRUE will be adopted by the larger HCI research community and will become a powerful tool for gathering deep insights into user behavior and improving design for other complex computing systems.

Li et al. [19] introduced a supervised machine learning strategy for classifying host roles that uses On-Line Support Vector Machine and Decision Tree. They collected sFlow data from a major campus network's principal gateways. The authors claimed that their classification accuracy was particularly high when it came to different user

groups. To figure out what a user is doing on his or her computer, Zhang et al. [20] used a tiered classification system using machine learning methods. They also tested the categorization system's performance in a variety of network contexts, including at home, at work, and in public locations, using various application scenarios. According to the researchers, the results demonstrated that the system can accurately discriminate across users of distinct web apps.

Despite the fact that the preceding research papers displayed a variety of methodologies and contexts, they were all focused on user behavior in different application scenarios. The summary of the frameworks chosen for review is listed in Table 1.

Table 1 Summary of the frameworks chosen for review

Ref.	Reported Work	ML Algorithm Used	User Role
Labayen et al. [6]	User classification	K-Means, Random Forest	Network user
Suchacka et al. [7]	User Prediction framework in E-commerce platform	SVM	User in Online bookstore
Revathi et al. [8]	Clustering of e-learning users based on performance	K-Means	e-learning student
Cui et al. [9]	User Clustering in Millimeter-Wave-NOMA Systems	K-Means	Online users
Roberto et al. [10]	User Clustering for Rate Splitting	Neural Network	Multiple role
Pennacchiotti et al. [11]	User classification in social media, using Twitter	LDA	Twitter User
Sassirekha et al. [12]	Predicting students' academic progression	LDA, kNN, SVM, RF	E-learning student
Dhilipan et al. [13]	Predicting students' performance	LR, DT, kNN	E-learning student
Khan et al. [14]	User personality classification	XGBoost	Multiple role
Zou et al. [15]	Sentiment classification	Naive Bayes, SVM	Social Media
Mamunur et al. [16]	Wink based facial expression classification	SVM, LDA, kNN	Multiple role
Saleema et al. [17]	Data-driven user modeling framework in online learning	K-Means	E-Learning student
Kim et al. [18]	Tracking Real-Time User Experience	HCI approaches	Video game user
Li et al. [19]	classify host roles on line using sFlow	SVM, DT	Multiple role
Zhang et al. [20]	Inferring users' online activities through traffic analysis.	SVM, NN	Network users

3. MATERIALS AND METHODS

The following is the methodology for the proposed work: The k-means and SVM algorithms that are used in the proposed work are described in Sections 3.1 and 3.2, respectively. The dataset is described in Section 3.3, and the proposed user identification framework is presented in Section 3.4.

3.1 K-Means Clustering

K-means clustering is one of the unsupervised machine learning methods that works well for large datasets. Unsupervised algorithms infer from datasets solely on the basis of input

vectors, rather than referring to known or labeled outcomes. K-means is a technique for finding underlying patterns by combining similar data points. To do this, K-means scans a dataset for a predetermined number (k) of clusters. A cluster is a group of data items that have been put together because of similar qualities. The desired number of centroids in the dataset, k, is set as the target. A centroid is a place, either real or imaginary, that symbolizes the cluster's center. Each data point is sorted into a cluster by reducing the in-cluster squared sum. In other words, while keeping the centroids as small as feasible, the k-means method determines

k centroids and then allocates each data item to the nearest cluster.

The k-means algorithm can be viewed as a descent of gradients, starting at the initial centroids and altering these euclidean distances iteratively to minimize the objective function [21]. It halts cluster formation and optimization if any of the following conditions are met: (i) the centroids are settled, meaning their values haven't changed as a result of clustering being successful; or (ii) the required number of iterations have been run. Loops are iterated repeatedly until the k-median method converges and the euclidean distance is calculated, with the positive number 1 signifying the iterations of the k-median algorithm. Even within the same dataset, the value of l varies depending on where the cluster centroids initialize. The approach has an $O(nkl)$ time complexity, where n is the total number of items in the dataset, k is the number of identified clusters, and l is the number of iterations.

Let $X = \{x_i\}, i \in U$, the collection of U M-dimensional elements which will make K clusters; $C = \{C_k, k \in K\}$. In particular, the potential function of clustering refers to J's objective function. It is worth noting that the greedy algorithm k-means can reach a plateau [22]. Despite this, latest research has established that, especially when clusters are well-separated, k-means can settle to the optimal solution with a strong possibility [19]. In a bid to lower the squared error of the points in various clusters, k-means begins by creating a starting division of K clusters and awards points to clusters. Because the mean square error continuously drops as the cluster counts increases ($J(C) = 0$ while $K = U$), minimization of mean square error is only useful for a predetermined number

of clusters. The key steps of the k-means algorithm are shown in Algorithm 1, where the distance measurement is the potential function., i.e., $J = f[dist(.,.)]$.

Algorithm 1 K-Means User Clustering

- 1 Select K users arbitrarily as the user epicenters of cluster C_1, \dots, C_k , respectively.
- 2 Measure the distance $dist(x_i, \mu_k), k = 1 \dots K$, then add user i into the cluster with the least distance.
- 3 Up till all users have been identified, repeat step 2.
- 4 Using the following equation, recalculate the center of each cluster:

$$\mu_k = \frac{1}{|C_k|} \sum_{i \in C_k} x_i$$

- 5 Repeat steps 2–4 until the cluster members are no longer changing or the objective function J(C) is no longer changing significantly.
-

3.2 Support Vector Machine (SVM) Classifier

The Support Vector Machine (SVM) classifier is used to classify between vulnerable and typical users. The working principle of a two-class SVM is detailed in [23]. The supervised learning method used by SVM is based on finite sample theory [24].

The user dataset acquired after k-means clustering must be divided into two different classes in the proposed

$$S = \{ (x_i, y_i), i = 1 \dots l \}$$

So that if each sample $x_i \in \mathbb{R}^d$ corresponds to a group $y_i \in \{+1, -1\}$. Here, the boundary is defined as in [25]:

$$\omega \cdot x + a = 0 \quad (1)$$

where ω is a weight vector and a is a bias. The data is then split into two groups using the decision function:

$$g(x) = \text{sign}(\omega \cdot x + a) \quad (2)$$

To get the optimal plane, we need to minimize

$$\frac{1}{2} \|\omega\|^2 \quad (3)$$

subject to: $y_i [(\omega \cdot x_i) + a] - 1 \geq 0, i = 1 \dots l$

The optimization problem is rewritten by using Lagrange multipliers $\beta_i \geq 0$ as follows [26]: Minimize

$$M(\omega, \alpha, \beta) = \sum_{i=1}^l \beta_i \frac{-1}{2} \sum_{i,j=1}^l \beta_i \beta_j y_i y_j (x_i \cdot x_j) \quad (4)$$

Subject to $\beta_i \geq 0$, and

$$\sum_{i=1}^n \beta_i y_i = 0$$

The resulting decision function is then provided as follows:

$$g(x) = \text{sign} \left(\sum_{i=1}^l \beta_i y_i (x_i \cdot x) + a \right) \quad (5)$$

classification framework. SVM creates a border between two classes with the goal of increasing the margin. In all classes, it refers to the maximum distance between the boundary and the nearest data points. Support vectors are the data points that are closest to the boundary. Given a training data segment, perform the following:

If the two classes cannot be separated using a linear boundary, a higher-dimensional hyper plane must be developed to allow for linear separation. This will be accomplished by utilizing the proper kernel function. The SVM classifier is depicted in Figure 1, where the kernel is optional.

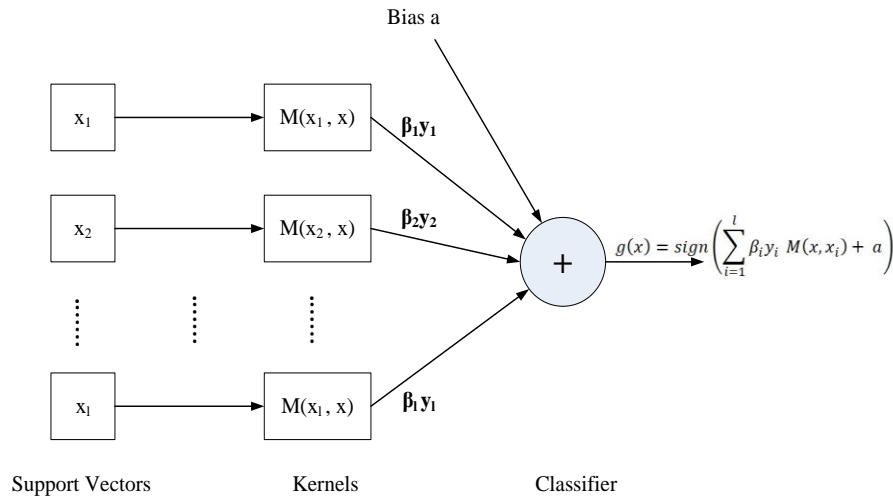


Figure 1 Two-class SVM classifier

3.3 User Dataset

A user dataset is obtained by placing a desktop agent on 150 online student users who were using a particular programming environment. The data were collected over a 30-minute timeframe with multiple tasks assigned. The agent measured system response time, user thinking time, the number of errors obtained, and the number of errors resolved. To eliminate outliers, the data are standardized using Z-score normalization, followed by Principal

Component Analysis (PCA). Despite the fact that there are fewer features, the feature strength will be populated with two principal components thanks to PCA. This will aid in the clustering process being optimized in less time. To facilitate the training of the ML classification model, the entire dataset is clustered into three categories, namely novice, intermittent, and expert, using k-means clustering as detailed in Section 3.1. Figure 2 shows the scatter plots of the user data after preprocessing.

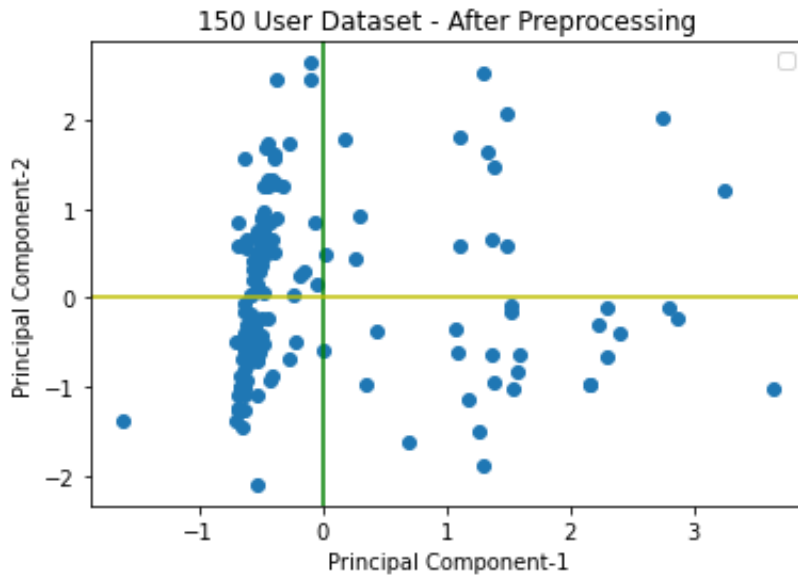


Figure 2 Scatter plot of user dataset after PCA

3.4 The Proposed User Identification Framework

The proposed clustering framework for identifying vulnerable users for extending assistance is given in Figure 3.

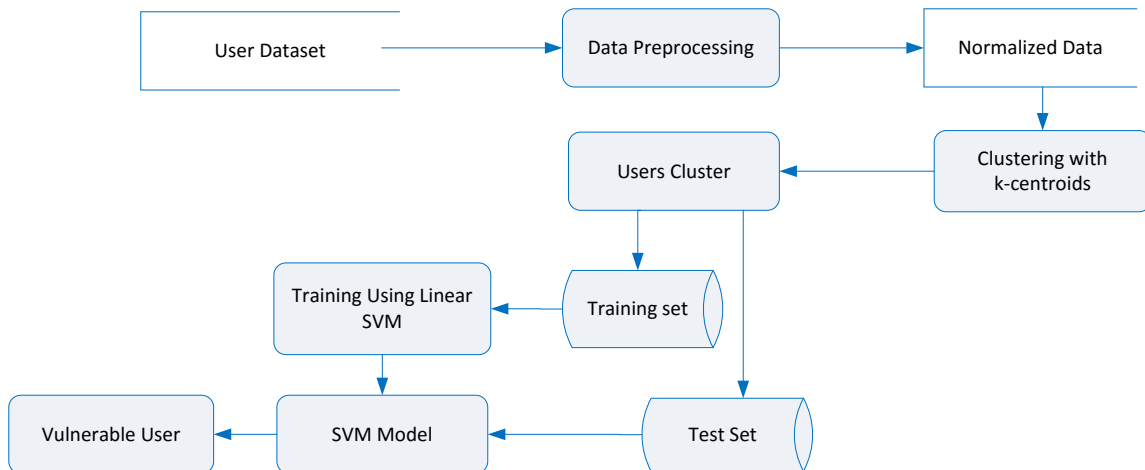


Figure 3 Proposed Framework for user identification

Phase-1: Clustering User Data:

In the first phase of the framework, user data after normalization is presented to the k-means clustering model to form three user groups. In order to do that, three centroids as reference points have been chosen to categorize novice users, intermittent users, and expert users. The

k-means technique is vulnerable to outliers because an object with an extremely large value can drastically distort the data distribution. Due to the adoption of the square-error function, this impact is amplified much further. Instead of utilizing the mean value of the objects in a cluster as a reference point,

it can be used as one representative item per cluster to represent the clusters. The remaining objects are paired with the symbolic one that most closely resembles them. After that, the partitioning strategy is used with the intention of minimizing the total difference between each entity and its corresponding reference point.

Phase 2: User Classification and Identification

The prime objective of the framework is to identify vulnerable users who are in need of assistance. Hence, the novice, intermittent, and expert user clusters are used for further classification to locate the vulnerable users. Binomial classification is carried out between two categories: (i) Novice vs. intermittent; (ii) Novice vs. Expert. In our framework, the SVM linear classifier (described in Section 3.2) is utilized for this purpose. The SVM classifier is used here for the reason that SVM is relatively best when data points are presented with a clear margin of separation of classes; in our case, this is true.

Training and test datasets are prepared for the classifier model. To provide a fair estimation of classification performance, K-fold cross-validation is employed as the training-test strategy. In particular, input datasets are separated into K equal portions, with K-1 used for classifier training and the remaining one used to test classification performance. This technique is done K times, with each iteration testing a new portion. Finally, the classifier performance assessment is determined as the average of the total testing parts.

Clusters have a significant impact on classifier performance. As a result, determining which pair of clusters the classifier performs best is important for evaluating its performance. On these two classification experiments, the performance of the classifier is determined by computing the ratio of precision and recall, which is represented by the f-score. The f-score is stated as,

$$f - score = \frac{2 \times Precision \times Recall}{Precision + Recall} \quad (6)$$

$$\text{where: } Precision = \frac{TP}{TP+FP}, \text{ and } Recall = \frac{TP}{TP+FN}$$

4. RESULTS AND DISCUSSIONS

The novice and intermittent user clusters are presented for training and then validation testing in the first classification scenario. The dataset is randomly partitioned into K equal-sized units in K-fold cross-validation, X_i , $i = 1, \dots, K$. We retain one of the K units as the validation set and merge the

remaining K-1 parts to make up the training set to generate each pair. It produces K combinations by repeating this process K times, every time taking out one of the K units. In our experiments, 5-fold cross-validation was adopted during training.

Training scores were recorded at each stage of the 5-fold cross validation,

which is presented in Table 2. The F-score gradually increased at each stage of the 5-fold validation and eventually reached 93.8 percent, which is a very good result in the binary classification of novice and intermittent users, as these clusters share sharp margins.

Similarly, in the second scenario, the classifier is trained using novice and

expert user data clusters. During 5-fold cross validation, it was shown that the classifier improves its performance with each cycle until it converges with an f-score of 95.1 percent at the fifth fold. This is due to the wide margin between the two clusters.

Table 2 Classifier Performance (in percentage)

5-Fold	Precision	Recall	F-score	Precision	Recall	F-score
	Novice vs. Intermittent			Novice vs. Expert		
1	94.7	83.7	88.9	97.4	84.8	90.7
2	93.9	86.2	89.9	97.6	86.6	91.8
3	97.7	87.5	92.3	96.1	86.5	91.0
4	98.1	88.6	93.1	98.5	87.8	92.8
5	98.7	89.4	93.8	99.3	91.2	95.1

There is an indication that the k-means clustering greatly contributed to the classifier by defining a clear margin for the separation of classes. There are very few similar works presented by researchers in the domain of usability analysis using ML. Because different and conventional approaches to performance evaluations were used, this work is considered unique and incomparable.

5. CONCLUSION

User Experience (UX) design is one of the major objectives of all interface designers. It is impractical to consider universal users while designing interfaces. Users at large are presented with different skill levels, especially users with disabilities, children, and the elderly. In an effort to provide a pleasant user experience with the interfaces, this framework was designed and proposed. The proposed work will be landmark research in that it will track the users who are in need of assistance in a real-time environment. Here, the potential

users are being identified using ML algorithms. In this way, the proposed

method locates the users who are in need of technical assistance. This concept could be implemented in e-learning environments, traditional educational settings, and even data centers. This work could be extended to vulnerability analysis, user performance analysis, and many more areas by using appropriate features for the extended work.

REFERENCES:

- [1] Robert, W. Proctor., & Trisha, Van Zandt. (2018). Human Factors in Simple and Complex Systems. CRC Press.
- [2] Johnson, A., & Proctor, R. W. (2016). *Skill Acquisition and Training: Achieving Expertise in Simple and Complex Tasks* (1st ed.). Routledge.
- [3] Matthews, G. , Davies, D.R. , Westerman, S.J. & Stammers, R.B. (2000). Human Performance: Cognition, Stress and Individual Differences. Hove: Psychology Press.
- [4] Codasyl. (1979). end-user facilities committee status report. Info. Manag. TUIO. North Holland. 137-163.
- [5] Cotterman, W. W., & Kumar, K. (1989). User cube: a taxonomy of end users. *Communications of the ACM*, 32(11), 1313–1320. <https://doi.org/10.1145/68814.68816>.
- [6] Labayen, V., Magaña, E., Morató, D., & Izal, M. (2020). Online classification of user activities using machine learning on network traffic. *Computer Networks*, 181, 107557. <https://doi.org/10.1016/j.comnet.2020.107557>
- [7] Suchacka, Grażyna., Skolimowska, Magdalena., & Potempa, Aneta. (2015). Classification of E-Customer Sessions Based on Support Vector Machine. Proceedings - 29th European Conference on Modelling and Simulation, ECMS 2015. 594-600. <https://doi.org/10.7148/2015-0594>
- [8] Vankayalapati, R., Ghutugade, K. B., Vannapuram, R., & Prasanna, B. P. S. (2021). K-Means Algorithm for Clustering of Learners Performance Levels Using Machine Learning Techniques. *Revue d'Intelligence Artificielle*, 35(1), 99–104. <https://doi.org/10.18280/ria.350112>
- [9] Cui, J., Ding, Z., Fan, P., & Al-Dhahir, N. (2018). Unsupervised Machine Learning-Based User Clustering in Millimeter-Wave-NOMA Systems. *IEEE Transactions on Wireless Communications*, 17(11), 7425–7440. <https://doi.org/10.1109/twc.2018.2867180>
- [10] Pereira, Roberto & Deshpande, Anay & Vaca Rubio, Cristian Jesús & Mestre, Xavier & Zanella, Andrea & Gregoratti, David & de Carvalho, E. & Popovski, Petar. (2022). User Clustering for Rate Splitting using Machine Learning. <https://doi.org/10.48550/arXiv.2205.11373>
- [11] Pennacchiotti, M., & Popescu, A.-M. (2021). A Machine Learning Approach to Twitter User Classification. *Proceedings of the International AAAI Conference on Web and Social Media*, 5(1), 281-288.

- [12] Sassirekha, M. S., & Vijayalakshmi, S. (2022). Predicting the academic progression in student's standpoint using machine learning. *Automatika*, 63(4), 605–617. <https://doi.org/10.1080/00051144.2022.2060652>
- [13] J. Dhilipan, N., Vijayalakshmi., S, Suriya., and Arockiya, Christopher. (2020) Prediction of Students Performance using Machine learning. International Virtual Conference on Robotics, Automation, Intelligent Systems and Energy (IVC RAISE 2020) 15th December 2020.. *IOP Conf. Ser.: Mater. Sci. Eng.* 2021. 1055 012122. <https://doi.org/10.1088/1757-899X/1055/1/012122>
- [14] Khan, A. S., Ahmad, H., Zubair, M., Khan, F., Arif, A., & Ali, H. (2020). Personality Classification from Online Text using Machine Learning Approach. *International Journal of Advanced Computer Science and Applications*, 11(3). <https://doi.org/10.14569/ijacsa.2020.0110358>
- [15] H. Zou., X. Tang., B. Xie., & B. Liu. (2015). Sentiment Classification Using Machine Learning Techniques with Syntax Features. 2015 *International Conference on Computational Science and Computational Intelligence (CSCI)*. 175-179, <https://doi.org/10.1109/CSCI.2015.44>
- [16] Rashid, Mamunur & Sulaiman, Norizam & Mustafa, Mahfuzah & Bari, Bifta & Sadeque, Md. Golam & Hasan, Md Jahid. (2020). Wink based facial expression classification using machine learning approach. *SN Applied Sciences*. 2. <https://doi.org/10.1007/s42452-020-1963-5>
- [17] Amershi, Saleema. (2009). Combining Unsupervised and Supervised Classification to Build User Models for Exploratory Learning Environments. *Journal of Educational Data Mining*. 2.
- [18] Kim, Jun., Gunn, Daniel., Schuh, Eric., Phillips, Bruce., Pagulayan, Randy., & Wixon, Dennis. (2008). Tracking Real-Time User Experience (TRUE): A comprehensive instrumentation solution for complex systems. *Conference on Human Factors in Computing Systems - Proceedings*.443-452. <https://doi.org/10.1145/1357054.1357126>
- [19] Li, Bingdong., Gunes, Mehmet., Bebis, George., & Springer, Jeff. (2013). A supervised machine learning approach to classify host roles on line using sFlow. *HPPN 2013 - Proceedings of the 2013 ACM Workshop on High Performance and Programmable Networking*. 53-60. <https://doi.org/10.1145/2465839.2465847>

- [20] Zhang, Fan., He, Wenbo., Liu, Xue & Bridges, Patrick. (2011). Inferring users' online activities through traffic analysis. *WiSec'11 - Proceedings of the 4th ACM Conference on Wireless Network Security*. 59-70. <https://doi.org/10.1145/1998412.1998425>
- [21] Jain, A. K. (2010). Data clustering: 50 years beyond K-means. *Pattern Recognition Letters*, 31(8), 651–666. <https://doi.org/10.1016/j.patrec.2009.09.011>
- [22] M, Inaba., N, Katoh., & H, Imai. (1994). Applications of weighted voronoi diagrams and randomization to variance-based K-clustering: (extended abstract). in *Proceedings of the Tenth Annual Symposium on Computational Geometry*. NY, USA. ACM.
- [23] V N, Vapnik. (1998). *Statistical Learning Theory*. John Wiley & Sons, New York. USA.
- [24] Han, K. J. (2022). *Data Mining Concepts and Techniques* (3rd ed.). ELSEVIER INDIA.
- [25] Cheng, J., Yu, D., & Yang, Y. (2008). A Fault Diagnosis Approach for Gears Based on IMF AR Model and SVM. *EURASIP Journal on Advances in Signal Processing*, 2008(1). <https://doi.org/10.1155/2008/647135>
- [26] Khandoker, A. H., Lai, D. T. H., Begg, R. K., & Palaniswami, M. (2007). Wavelet-Based Feature Extraction for Support Vector Machines for Screening Balance Impairments in the Elderly. *IEEE Transactions on Neural Systems and Rehabilitation Engineering*, 15(4), 587–597. <https://doi.org/10.1109/tnsre.2007.906961>

التعرف في الوقت الفعلي على مستخدم النظام في البيئات المعقدة باستخدام التعلم الآلي

يحيى محمد القحطاني
جامعة جازان

الملخص

في العصر التقني اليوم ، يعد تصميم تجربة المستخدم هو المحور الأساسي لجميع عمليات تطوير منتجات البرامج. بدلاً من تطوير نظام مع وضع مجموعة محددة من المستخدمين في الاعتبار ، يتم الآن تقديم أنظمة البرامج لجميع أنواع المستخدمين ، من المبتدئين إلى الخبراء. يستخدم النظام طرقاً مختلفة لمساعدة المستخدمين أثناء تفاعلهم. تم تصميم هذه الأساليب لتناسب احتياجات المستخدمين ، خاصة إذا كانوا جددًا على النظام. من الأهمية تحديد المستخدمين الذين يحتاجون إلى المساعدة بناءً على تفاعلاتهم مع النظام. تقترح هذه الورقة العلمية طريقة لتحديد مستخدمي النظام في بيئة تفاعل معقدة باستخدام تصنيف دعم آلة المتجهات (SVM) وكذلك تجميع العناصر (k-means). يتم أخذ العديد من العوامل في الاعتبار لإبراز المستخدمين المعرضين للخطر ، بما في ذلك تعقيد الواجهة ووقت استجابة المستخدم ووقت تفكير المستخدم. تم الحصول على مجموعة بيانات المستخدم من إعداد واجهة معقدة. بعد التجميع ، يتم تدريب النموذج على تحديد المستخدمين الذين يحتاجون إلى المساعدة في الماضي قدمًا باستخدام المصنف. يتم تقييم أداء المصنف من خلال التحقق من صحة k-fold باستخدام مجموعة بيانات الاختبار. النموذج المقترح هو طريقة حديثة لتحسين تجربة المستخدم في بيئات النظام المعقدة ، وسوف يمهد الطريق للبحث المستقبلي في هذا المجال.

الكلمات المفتاحية : خبرة الاستخدام ، تفاعل الانسان مع الحاسب ، تعلم الآله ، تجميع العناصر K-Means ، دعم آلة المتجهات SVM .

MRI Diagnosis of Endometriosis Fungating Out of a Caesarean Scar: A Case Report

Sara Ali¹

¹ Diagnostic Radiography Technology Department, College of Applied Medical Sciences, Jazan University, Saudi Arabia

ABSTRACT

This case report presents a 43-year-old female with a history of previous C-sections who presented to the hospital with pelvic pain and inconclusive US results. After being assessed clinically and radiologically using several modalities, MRI images shows a 4x6 cm grape-like vesicular mass is seen fungating out of the assumed Caesarean scar with some high vesicular intensities suggestive of endometriosis. Endometriosis is a challenging diagnosis to make, as its symptoms are often nonspecific and can mimic other conditions. In this case, the diagnosis of endometriosis was made with MRI, which is considered the gold standard for imaging the pelvis in endometriosis cases. The patient's treatment consisted of hormonal therapy and pain management to manage the symptoms. This case report highlights the importance of considering endometriosis as a differential diagnosis in patients with a history of previous C-sections presenting with pelvic pain. Early diagnosis and management of endometriosis are crucial to improve the quality of life for affected individuals. Healthcare providers should be aware of the typical symptoms, risk factors, and diagnostic modalities for endometriosis to provide optimal care for their patients.

Keywords: endometriosis, MRI, cesarian section, ultrasound.

INTRODUCTION

Endometriosis is a common gynecological condition that occurs in women of reproductive age and is characterized by the growth of endometrial-like tissue outside the uterus [1,2]. The condition can cause debilitating pelvic pain, infertility, and other severe symptoms [3]. Endometriosis is a chronic condition that requires long-term management and can negatively impact the quality of life for those affected [4].

The underlying mechanisms of endometriosis remain unclear, and there is no definitive cure [5]. Several hypotheses attempt to explain the origin of endometriosis, including genetic predisposition, altered immune function, and environmental factors [6-8]. Recent studies suggest that endometriosis is a multifactorial disease that may result from a combination of genetic, environmental, and immunological factors. Firstly, genetic factors play a crucial role in the development of endometriosis. Family studies have shown that first-degree relatives of women with endometriosis have a higher risk of developing the disease [9]. Moreover, genome-wide association studies (GWAS) have identified several genetic loci

associated with the development of endometriosis, including the WNT4 and GREB1 genes [10,11]. Secondly, exposure to certain chemicals has been linked to an increased risk of developing endometriosis. For example, dioxins, which are environmental pollutants, have been found to accumulate in fatty tissues, and animal studies have shown that exposure to dioxins can lead to the development of endometriosis-like lesions [12]. Finally, immune system dysfunction may also contribute to the development of endometriosis. Women with endometriosis have been found to have altered immune function, including impaired natural killer cell activity and increased levels of pro-inflammatory cytokines [13]. Further research is required to fully elucidate the pathogenesis of endometriosis and develop effective treatment options [4,14].

The ectopic endometrial-like tissue that grows in endometriosis is hormonally responsive and undergoes cyclic menstrual-like changes [3]. This can lead to the formation of adhesions and scarring, as well as the development of endometriomas, which are ovarian cysts filled with endometrial-like fluid [15]. The most common symptom of endometriosis is chronic pelvic pain, which may be cyclical

or non-cyclical and can be severe enough to interfere with daily activities. Other common symptoms include dyspareunia (painful sexual intercourse), dysmenorrhea (painful periods), and infertility [7,16]. Women with endometriosis may also experience gastrointestinal symptoms, such as bloating, constipation, or diarrhea. The severity of the symptoms can vary widely among individuals with endometriosis, and some individuals may be asymptomatic despite having the condition [7]. Accurate diagnosis of endometriosis requires a thorough medical history, physical examination, and diagnostic imaging, such as transvaginal ultrasound or magnetic resonance imaging (MRI) [2,17,18]. MRI is considered the gold standard for imaging the pelvis in endometriosis cases, as it can detect various types of endometriosis lesions, such as superficial, cystic ovarian, and deep endometriosis. MRI can also show characteristic features of endometriosis, such as high T1 signal with T2 shading, T2 dark spot sign, and thin hypointense walls. MRI can help to differentiate endometriosis from other pelvic disorders, such as hemorrhagic ovarian cysts, peritoneal inclusion cysts, and adenomyosis.

Endometriosis is a common condition that affects an estimated 10% of

women of reproductive age worldwide [5,8,19]. It is more prevalent among women with a family history of the condition and those with a longer duration of menstrual cycles [20]. Additionally, endometriosis is more commonly diagnosed in women who have not given birth, suggesting a potential protective effect of pregnancy. Although endometriosis can occur in individuals of any ethnicity, it is more frequently diagnosed in women of European descent [21].

However, endometriosis in a caesarean scar (CS) is a rare entity, with an estimated incidence of 0.03% to 0.4% among women who have undergone caesarean delivery [22]. It can present as a painful mass or nodule in the lower abdomen or as cyclic bleeding from the scar. The diagnosis of endometriosis in a CS can be challenging, as it can mimic other conditions such as hematoma, abscess, suture granuloma, or malignancy [16,23].

In this case report, we present a rare case of endometriosis fungating out of a caesarean scar in Jazan city, Saudi Arabia that was diagnosed with magnetic resonance imaging (MRI) and treated with hormonal therapy and pain management. This case is important because it can provide valuable

insights into the diagnosis and management of this condition in a region where it is not common and can contribute to the existing literature on this disease by demonstrating its clinical presentation, radiological findings, and treatment options in a specific geographical and cultural context. In addition, it can also raise awareness in Jazan among healthcare workers and patients about the possibility of CS endometriosis in women with pelvic pain and inconclusive ultrasound results.

CASE PRESENTATION

We present the case of a 43-year-old female with a medical history of previous C-sections who presented to the hospital with complaints of pelvic pain. The patient had undergone two C-sections in the past, with the most recent one being seven years ago.

Figure 1: MRI T2 sagittal image



She reported experiencing severe, cyclic pelvic pain dysmenorrhea, dyspareunia pain during and after sexual intercourse that was affecting her quality of life. On examination, the patient appeared uncomfortable, and there was tenderness on palpation of the lower abdomen.

Initial ultrasound results were inconclusive, and the patient was subsequently referred for further assessment. Clinical and radiological assessments using several modalities were carried out, including MRI with contrast and without contrast. The MRI revealed a about 4 x 6 cm grape-like vesicular mass that was fungating out of the assumed CS scar. Some high vesicular intensities were also seen on the MRI, which was suggestive of endometriosis (Figure 1 and 2).

Figure 2: MRI T2 axial image showing the endometriosis.



The differential diagnosis included inflammatory pelvis disease, post-cesarean adhesions and ectopic pregnancy. The patient was diagnosed with deep abdominal endometriosis and was started on hormonal therapy that suppress ovulation as contraceptive method (injectable medroxyprogesterone& levonorgestrel intrauterine device) to manage her symptoms. She was also given pain medication to alleviate her pain. The patient's response to treatment was monitored through follow-up appointments. She reported a significant improvement in her symptoms, with a reduction in pain and an improvement in her quality of life.

DISCUSSION

This case report illustrates a non-common among women in Jazan but possible complication of C-section, which is the development of endometriosis in the surgical scar. Endometriosis is a chronic inflammatory condition characterized by the presence of endometrial-like tissue outside the uterus, which can cause pelvic pain, infertility, and reduced quality of life [2,5,18,24]. The exact pathogenesis of endometriosis is not fully understood [12,13], but several theories have been proposed, such as retrograde menstruation,

coelomic metaplasia, lymphatic or hematogenous dissemination, and iatrogenic implantation [1]. The latter mechanism is likely to be responsible for the occurrence of endometriosis in the C-section scar, as endometrial tissue can be transferred to the abdominal wall during the surgery [25-28].

The diagnosis of CS endometriosis can be challenging, as it can mimic other conditions, such as hematoma, abscess, suture granuloma, hernia, or neoplasm [16,23]. The clinical presentation can vary, but the most common symptoms are cyclic pain and swelling at the site of the scar during menstruation [29,30]. The diagnosis can be confirmed by histopathological examination of the excised lesion, which shows endometrial glands and stroma surrounded by fibrous tissue [30,31].

Imaging modalities, such as ultrasound, computed tomography (CT), and MRI can also aid in the diagnosis by showing characteristic features of endometriosis, such as heterogeneous hypoechoic nodules with internal hyperechoic foci on ultrasound, soft tissue nodules with heterogeneous post-contrast enhancement and streaky appearance on CT, and high T1 signal (with and without fat suppression) with T2 shading and thin hypointense walls on MRI [17-19,31].

Ultrasound is often used as the first-line imaging modality to diagnose endometriosis. However, it has limitations in detecting deep infiltrating endometriosis, particularly in the presence of bowel involvement. MRI is a useful imaging modality in cases where ultrasound findings are inconclusive or to assess the extent of deep infiltrating endometriosis. In this case, the MRI with contrast revealed a 4x6 cm grape-like vesicular mass is seen fungating out of the assumed CS scar with some high vesicular intensities suggestive of endometriosis.

The treatment of scar endometriosis depends on the size and location of the lesion, the severity of symptoms, and the patient's preference. The main options are surgical excision and medical therapy. Surgical excision is considered the definitive treatment, as it provides histological confirmation and complete removal of the lesion with clear margins [25,27,29]. However, surgery may also carry some risks, such as recurrence, infection, bleeding, or damage to adjacent structures [32,33]. Medical therapy with hormonal agents, such as oral contraceptives, progestins, danazol, or GnRH analogs can offer symptomatic relief by suppressing ovarian function and reducing endometrial

proliferation [11,34]. However, medical therapy may also have some limitations, such as side effects, lack of efficacy in some cases, or recurrence after discontinuation [32]. Pain medication, such as nonsteroidal anti-inflammatory drugs, can also be used to manage the pain associated with endometriosis. In this case, the patient's treatment involved hormonal and pain medication to manage the symptoms.

Conclusion

This case report highlights an important complication of C-section that can cause significant morbidity and distress to patients. It also emphasizes the need for a high index of suspicion and a multidisciplinary approach to diagnose and treat scar endometriosis effectively. Furthermore, it underscores the importance of preventive measures during C-section to minimize the risk of endometrial implantation in the surgical site. These measures may include meticulous hemostasis, careful handling of tissues, avoidance of spillage of blood or amniotic fluid into the abdominal cavity or wound site, thorough irrigation and cleansing of the wound site before closure, and use of barrier methods to separate the uterine incision from the abdominal wall. Hormonal therapy and pain medication can be effective in

managing the symptoms of endometriosis. Early recognition and management of endometriosis can improve the quality of life of affected women and prevent potential complications such as infertility.

Ethical Statement: No institutional approval was required to publish the case details. The patient has provided consent to publish the case report and accompanying images.

Conflict of interest: The author declares that there is no conflict of interest.

References

1. Arafah, M.; Rashid, S.; Akhtar, M. Endometriosis: A Comprehensive Review. *Adv Anat Pathol* **2021**, *28*, 30-43, doi:10.1097/PAP.0000000000000288.
2. Zondervan, K.T.; Becker, C.M.; Koga, K.; Missmer, S.A.; Taylor, R.N.; Vigano, P. Endometriosis. *Nat Rev Dis Primers* **2018**, *4*, 9, doi:10.1038/s41572-018-0008-5.
3. Alimi, Y.; Iwanaga, J.; Loukas, M.; Tubbs, R.S. The Clinical Anatomy of Endometriosis: A Review. *Cureus* **2018**, *10*, e3361, doi:10.7759/cureus.3361.

Funding statement: The author received no financial support for the research authorship and publication of this article.

Consent to publish: The author affirms that patient provided informed consent for publication of the images in Figures 1 and 2. The patient has consented to the submission of the case report to the journal. Patients signed informed consent regarding publishing their data.

4. Chapron, C.; Marcellin, L.; Borghese, B.; Santulli, P. "Rethinking mechanisms, diagnosis and management of endometriosis". *Nature Reviews Endocrinology* **2019**.
5. Blamble, T.; Dickerson, L. Recognizing and treating endometriosis. *JAAPA* **2021**, *34*, 14-19, doi:10.1097/01.JAA.0000750940.47126.58.
6. Samimi, M.; Pourhanifeh, M.H.; Mehdizadehkashi, A.; Eftekhari, T.; Asemi, Z. The role of inflammation, oxidative stress, angiogenesis, and apoptosis in the pathophysiology of endometriosis: Basic science and new insights based on gene

- expression. *Journal of Cellular Physiology* **2019**.
7. Borghese, B.; Santulli, P.; Marcellin, L.; Chapron, C. Definition, description, clinicopathological features, pathogenesis and natural history of endometriosis: CNGOF-HAS Endometriosis Guidelines. *Gynecol Obstet Fertil Senol* **2018**, *46*, 156-167, doi:10.1016/j.gofs.2018.02.017.
 8. Asghari, S.; Valizadeh, A.; Aghebati-Maleki, L.; Nouri, M.; Yousefi, M. Endometriosis: Perspective, lights, and shadows of etiology. *Biomed Pharmacother* **2018**, *106*, 163-174, doi:10.1016/j.biopha.2018.06.109.
 9. Smolarz, B.; Szyłło, K.; Romanowicz, H. The Genetic Background of Endometriosis: Can ESR2 and CYP19A1 Genes Be a Potential Risk Factor for Its Development? *International Journal of Molecular Sciences* **2020**, *21*, 8235.
 10. Pejovic, T.; Thisted, S.; White, M.; Nezhat, F.R. Endometriosis and Endometriosis-Associated Ovarian Cancer (EAOC). *Adv Exp Med Biol* **2020**, *1242*, 73-87, doi:10.1007/978-3-030-38474-6_5.
 11. Donnez, J.; Dolmans, M.-M. Endometriosis and medical therapy: from progestogens to progesterone resistance to GnRH antagonists: a review. *Journal of Clinical Medicine* **2021**, *10*, 1085.
 12. Stephens, V.R.; Rumph, J.T.; Ameli, S.; Bruner-Tran, K.L.; Osteen, K.G. The Potential Relationship Between Environmental Endocrine Disruptor Exposure and the Development of Endometriosis and Adenomyosis. *Frontiers in Physiology* **2022**, *12*, doi:10.3389/fphys.2021.807685.
 13. Moghaddam, M.Z.; Ansariniya, H.; Seifati, S.M.; Zare, F.; Fesahat, F. Immunopathogenesis of endometriosis: An overview of the role of innate and adaptive immune cells and their mediators. *Am J Reprod Immunol* **2022**, *87*, e13537, doi:10.1111/aji.13537.
 14. Chauhan, S.; More, A.; Chauhan, V.; Kathane, A. "Endometriosis: A Review of Clinical Diagnosis, Treatment, and Pathogenesis". *Cureus* **2022**.

15. Bulun, S.E.; Yilmaz, B.D.; Sison, C.; Miyazaki, K.; Bernardi, L.; Liu, S.; Kohlmeier, A.; Yin, P.; Milad, M.; Wei, J. Endometriosis. *Endocr Rev* **2019**, *40*, 1048-1079, doi:10.1210/er.2018-00242.
16. Gonzalez, A.; Artazcoz, S.; Elorriaga, F.; Timmons, D.; Carugno, J. Endometriosis Presenting as Recurrent Haemorrhagic Ascites: A Case Report and Literature Review. *Int J Fertil Steril* **2020**, *14*, 72-75, doi:10.22074/ijfs.2020.5895.
17. Jha, P.; Sakala, M.; Chamie, L.P.; Feldman, M.; Hindman, N.; Huang, C.; Kilcoyne, A.; Laifer-Narin, S.; Nicola, R.; Poder, L.; et al. Endometriosis MRI lexicon: consensus statement from the society of abdominal radiology endometriosis disease-focused panel. *Abdom Radiol (NY)* **2020**, *45*, 1552-1568, doi:10.1007/s00261-019-02291-x.
18. Shah, R.; Jagani, R.P. Review of Endometriosis Diagnosis through Advances in Biomedical Engineering. *Crit Rev Biomed Eng* **2018**, *46*, 277-288, doi:10.1615/CritRevBiomedEng.2018027414.
19. Saar, T.D.; Pacquee, S.; Conrad, D.H.; Sarofim, M.; Rosnay, P.; Rosen, D.; Cario, G.; Chou, D. Endometriosis Involving the Sciatic Nerve: A Case Report of Isolated Endometriosis of the Sciatic Nerve and Review of the Literature. *Gynecol Minim Invasive Ther* **2018**, *7*, 81-85, doi:10.4103/GMIT.GMIT-24-18.
20. Secosan, C.; Balulescu, L.; Brasoveanu, S.; Balint, O.; Pirtea, P.; Dorin, G.; Pirtea, L. Endometriosis in Menopause-Renewed Attention on a Controversial Disease. *Diagnostics (Basel)* **2020**, *10*, doi:10.3390/diagnostics10030134.
21. Bougie, O.; Nwosu, I.; Warshafsky, C. Revisiting the impact of race/ethnicity in endometriosis. *Reprod Fertil* **2022**, *3*, R34-r41, doi:10.1530/raf-21-0106.
22. Zhang, P.; Sun, Y.; Zhang, C.; Yang, Y.; Zhang, L.; Wang, N.; Xu, H. Cesarean scar endometriosis: presentation of 198 cases and literature review. *BMC Womens*

- Health* **2019**, *19*, 14, doi:10.1186/s12905-019-0711-8.
23. Vural, B.; Vural, F.; Muezzinoglu, B. An Abdominal Wall Desmoid Tumour Mimicking Cesarean Scar Endometriomas: A Case Report and Review of the Literature. *J Clin Diagn Res* **2015**, *9*, QD14-16, doi:10.7860/JCDR/2015/14512.6533
24. Toczek, J.; Jastrzebska-Stojko, Z.; Stojko, R.; Droszol-Cop, A. Endometriosis: New Perspective for the Diagnosis of Certain Cytokines in Women and Adolescent Girls, as Well as the Progression of Disease Outgrowth: A Systematic Review. *Int J Environ Res Public Health* **2021**, *18*, doi:10.3390/ijerph18094726.
25. Alnafisah, F.; Dawa, S.K.; Alalfy, S. Skin Endometriosis at the Caesarean Section Scar: A Case Report and Review of the Literature. *Cureus* **2018**, *10*, e2063, doi:10.7759/cureus.2063.
26. Bartlomiej, B.; Malgorzata, S.; Karolina, F.; Anna, S. Caesarean Scar Endometriosis May Require Abdominoplasty. *Clin Med Insights Case Rep* **2021**, *14*, 11795476211027666, doi:10.1177/11795476211027666.
27. Sedhain, N.; Dangal, G.; Karki, A.; Pradhan, H.K.; Shrestha, R.; Bhattachan, K.; Poudel, R.; Bajracharya, N. Caesarean Scar Endometriosis. *J Nepal Health Res Counc* **2018**, *15*, 292-294, doi:10.3126/jnhrc.v15i3.18859.
28. T. Wasfie, E.G., Silvia Seon, B. Zado. Abdominal wall endometrioma after cesarean section: a preventable complication. *International surgery* **2002**.
29. Francica, G.; Giardiello, C.; Angelone, G.; Cristiano, S.; Finelli, R.; Tramontano, G. Abdominal wall endometriomas near cesarean delivery scars: sonographic and color doppler findings in a series of 12 patients. *J Ultrasound Med* **2003**, *22*, 1041-1047, doi:10.7863/jum.2003.22.10.1041.
30. Ozel, L.; Sagiroglu, J.; Unal, A.; Unal, E.; Gunes, P.; Baskent, E.; Aka, N.; Titiz, M.I.; Tufekci, E.C. Abdominal wall endometriosis in the cesarean section surgical scar: a potential diagnostic pitfall. *J Obstet Gynaecol Res* **2012**, *38*, 526-530,

- doi:10.1111/j.14470756.2011.01739.x.
31. Kocher, M.; Hardie, A.; Schaefer, A.; McLaren, T.; Kovacs, M. Cesarean-Section Scar Endometrioma: A Case Report and Review of the Literature. *J Radiol Case Rep* **2017**, *11*, 16-26, doi:10.3941/jrcr.v11i12.3178.
32. Falcone, T.; Flyckt, R. Clinical Management of Endometriosis. *Obstet Gynecol* **2018**, *131*, 557-571, doi:10.1097/AOG.0000000000002469.
33. Saunders, P.T.K.; Horne, A.W. Endometriosis: Etiology, pathobiology, and therapeutic prospects. *Cell* **2021**, *184*, 2807-2824, doi:10.1016/j.cell.2021.04.041.
34. Samy, A.; Taher, A.; Sileem, S.A.; Abdelhakim, A.M.; Fathi, M.; Haggag, H.; Ashour, K.; Ahmed, S.A.; Shareef, M.A.; AlAmodi, A.A. Medical therapy options for endometriosis related pain, which is better? A systematic review and network meta-analysis of randomized controlled trials. *Journal of gynecology obstetrics and human reproduction* **2021**, *50*, 101798.

تشخيص الانتباز البطاني الرحمي من ندبة قيصرية بواسطة الرنين المغناطيسي: تقرير حالة

ساره علي^١

^١ قسم تقنيه الأشعة التشخيصية، كلية العلوم الطبية التطبيقية، جامعه جازان، جازان ٤٥١٤٢، المملكة العربية السعودية

ملخص

يقدم هذا التقرير حالة امرأة تبلغ من العمر ٤٣ عامًا سبق لها اجراء عدة عمليات قيصرية سابقة قدمت إلى المستشفى وهي تعاني من آلام مبرحه في الحوض كما ان نتائج الموجات فوق الصوتية غير حاسمة. بعد التقييم السريري والإشعاعي باستخدام عدة طرق، اظهرت صور التصوير بالرنين المغناطيسي كتلة حويصلية شبيهة بالعنب ٤×٦ سم تظهر خارج الندبة القيصرية المفترضة مع بعض الشدة الحويصلية العالية التي توحى بالانتباز البطاني الرحمي. يُعد الانتباز البطاني الرحمي تشخيصًا صعبًا، حيث إن أعراضه غالبًا ما تكون غير محددة ويمكن أن يشابه الحالات الأخرى. في هذه الحالة، تم تشخيص الانتباز البطاني الرحمي باستخدام التصوير بالرنين المغناطيسي، والذي يعتبر المعيار الذهبي لتصوير الحوض في حالات الانتباز البطاني الرحمي. يتكون علاج المريض من العلاج الهرموني وإدارة الألم لإدارة الأعراض. يسلط تقرير الحالة هذا الضوء على أهمية اعتبار الانتباز البطاني الرحمي تشخيصًا تفريقي في المرضى الذين لديهم تاريخ سابق في الولادة القيصرية يعانون من ألم في الحوض. يعتبر التشخيص المبكر وعلاج الانتباز البطاني الرحمي ضروريا لتحسين نوعية الحياة للأفراد المصابين. يجب أن يكون مقدمو الرعاية الصحية على دراية بالأعراض النمطية وعوامل الخطر وطرق التشخيص لانتباز بطانة الرحم لتوفير الرعاية المثلى لمرضاهم.

الكلمات المفتاحية: الانتباز البطاني الرحمي، التصوير بالرنين المغناطيسي، الجراحة القيصرية، الموجات فوق الصوتية.

Prevalence of malaria, human T lymphotropic virus, and syphilis in healthy blood donors from Jazan region, Saudi Arabia during 2019-2020

Aymen M Madkhali

Department of Medical Laboratory Technology, Faculty of Applied Medical Sciences, Jazan University, Saudi Arabia

Abstract

Background

Transfusion-transmitted infections (TTIs) are a major concern for global health. Screening for TTIs in the blood donors is critical. This study was designed with the main crux of providing valuable data regarding the prevalence of malaria, human T lymphotropic virus (HTLV), and syphilis from Samtah, Jazan; an area located in the southwestern region of Saudi Arabia.

Methods

This retrospective study, on reviewing the blood donation records in Samtah General Hospital, was conducted from January 2019 to August 2020. Only those blood bank and donation registries that contained the results of malaria, HTLV -1/2, and syphilis, were reviewed.

Results

Data of 4977 blood donors were analyzed. Among the 4977 blood donors, only 11 (0.2%) donors were confirmed HTLV 1/2 reactive. Eight (0.16%) blood donors were reported to be positive for syphilis, while the malaria tests of 0.04% (n=2) of the blood donors were found to be positive.

Conclusion

It is concluded that malaria, HTLV, and syphilis are rarely found among blood donors in this area. Although rare, their lethality is beyond description. Hence, strategies should be sorted out to minimize the cost of screening for these infections without compromising the safety of blood and its components.

Keywords: HTLV, syphilis, malaria, transfusion-transmitted infections.

Introduction

The importance of blood in sustaining life in health and disease is a reality beyond

dispute. Just as the loss of blood can result in loss of life, giving blood can save many lives. Because of the strict species

specificity, the only source of blood for human consumption is Man himself. Trans-species blood transfusion is an impossibility and synthetic blood substitutes are still a dream. Hence, for all clinical purposes, human blood must be supplied for human utilization. However, transfusion of blood and /or its components is considered a two-edged sword. It is estimated that nearly 10% of all blood /and or blood component transfusions are accompanied by one or the other adverse effect. (Andreu et al., 2002) Among these adverse effects are transfusion-transmitted infections (TTIs), which are still a global concern, therefore the screening of TTIs in blood donors is crucial. The collected blood is screened for TTIs including hepatitis B virus (HBV), hepatitis C virus (HCV), human immunodeficiency virus (HIV), human T lymphotropic virus (HTLV), malaria, and syphilis. (Bihl et al., 2007; Busch et al., 2019) Here, it is noteworthy to mention that malaria screening is carried out only in malaria-endemic countries, while in non-endemic areas, donors are deferred based on risk group assessment (Bihl et al., 2007).

Geographically, the prevalence of TTIs among blood donors varies from one region to another (Fong & Fong, 2020; Stramer & Dodd, 2013). In Saudi Arabia, several publications have reported the prevalence of TTIs among blood donors in different regions, including Central (Abdo et al., 2012; Alabdulmonem et al., 2020; Alaidarous et al., 2018; El-Hazmi, 2004; Shobokshi et al., 2003), Western (Bamaga et al., 2009; Elbjeirami et al., 2015; Fageeh, 2010; Shobokshi et al., 2003), and Eastern regions (Alzahrani et al., 2018; Bashawri et

al., 2004; Morsi, 2011). In the Jazan region (Southwestern region of Saudi Arabia), the prevalence of TTIs reported in the literature is limited to HBV and HCV among blood donors (Abdullah, 2013a).

Malaria is still endemic in the Southern region of Saudi Arabia, particularly in Asir and Jazan. It is caused by *Plasmodium spp* which invade the red blood cells (RBCs). Malarial parasite transmission occurs mainly through the female *Anopheles* mosquito. However, it can be transmitted by the transfusion of malarial parasite-infected blood (Kitchen & Chiodini, 2006). A study has shown that malaria is highly prevalent in Jazan (66.3%) as compared to five other cities i.e., Al-Baha (1.0%), Asir (7.4%), Madinah (8.7%), and Makkah (16.6%) (Amer et al., 2020). *Plasmodium* species withstand cold temperatures and can survive in stored blood at 4°C (Larison & Gilman, 1983). In general practice, malarial parasites are detected by screening thick and thin blood smears. However, blood smears are used to be positive only in active cases with parasitemia. Hence, this method is not used for the screening of blood units in many countries. Both blood smears and Rapid diagnostic tests (RDT) are used for the diagnosis of suspected clinical cases in Jazan (Madkhali et al., 2022). However, detection of *Plasmodium spp* in blood units is mainly carried out by RDT (Simon et al., 2019).

HTLV 1/2

HTLV 1/2 belongs to the retrovirus family. Persistent infection with HTLV 1 causes T cell proliferation. HTLV genome being RNA is transcribed into DNA with the help of reverse transcriptase found in the virus

and integrates into the host cell's genome. HTLV 1 is considered one of the major risk factors in the development of adult T cell lymphoma/ leukaemia (ATL) (Mozhgani et al., 2018). In addition, patients with ATL develop immunodeficiency that resembles that of in AIDS patients. This virus can also cause HTLV 1-associated myelopathy or tropical spastic paraparesis (HAM/TSP); a progressive neurological disorder. (Nozuma et al., 2020; Nozuma & Jacobson, 2019). Other secondary clinical conditions that develop after primary HTLV1 infection include pneumonia, bronchitis, urinary tract infections, uveitis, and infective dermatitis in children. (Caskey et al., 2007) Predisposition to strongyloidiasis is one of the clinical manifestations of HTLV 1. Known means of the transmission of HTLV 1/2 include vertical transmission (breastfeeding or perinatal exposure), sexual contact or exposure to blood/ blood products, and intravenous drug users through sharing of contaminated needles. The incubation period of HTLV usually ranges from 30–90 days after exposure to HTLV. Following the incubation, an infected person becomes seroconverted. Once seroconversion occurs, anti-HTLV antibodies can be detected in the serum of the infected person that persists for life. (Simon et al., 2019). Globally, 15–20 million people are infected with HTLV 1/2. It is highly prevalent in Japan, Africa, the Caribbean, the Middle East (Iran), Melanesia, the Solomon Islands, Papua New Guinea, as well as the Australian aborigines. (Gessain et al., 2015).

Syphilis: *Treponema pallidum* is an extremely motile, flexible, helical wall

spirochete that can cause syphilis affecting 18 to 56 million people across the globe (Edmondson et al., 2018). After initial infection, syphilis passes through the primary, secondary, and tertiary stages. Chancre or primary lesion, which is comprised of a significantly high number of treponemes, appears at the primary site of infection. Usually, this lesion heals. However, treponemes may be present in the lymph nodes that could lead to secondary and later on tertiary stages of the infection, if left untreated (Hicks & Clement, 2016). The life cycle of treponemes completes when they pass through the bloodstream. During this phase, the blood-containing treponemes could lead to the transmission of treponemes into the recipient. Individuals infected with *T. pallidum* are tested by using serological methods that have the drawback of false negative results if the infected individual is not in the seroconverted stage. It is an interesting fact that *T. pallidum* is a heat-sensitive organism that dies (within 72 hours) after storing the blood at 4°C. VDRL test and RPR are nonspecific tests used for the detection of recent infections. While fluorescent treponemal antibody absorption (FTA-ABS), *T. pallidum* immobilization (TPI), *T. pallidum* hemagglutination (TPHA) are the immunoassays used for the detection of antibodies to *T. pallidum*. Southern blot and polymerase chain reaction (PCR) are confirmatory tests that detect treponemal antigens. The initially reactive blood units are not used until confirmed by FTA or Southern blot (Kilany et al., 2015). The availability of rudimentary information regarding the frequency and understanding of the current epidemiological status of TTIs

among blood donors contributes to blood transfusion safety. Therefore, this study was designed to provide data regarding the prevalence of HTLV 1/2, malaria, and syphilis from a remote area located in the far Southwestern part of Saudi Arabia.

1. Materials and methods

1.1. Sample size and sampling technique

This was a retrospective, cross-sectional study of blood donation records during the period from January 2019 to August 2020. The records of all donors recruited during this period were included in data acquisition and only blood bank and donation registries were reviewed. A brief description of the blood donation process was followed in the blood bank of Samtah General Hospital is given. Routinely, a standard protocol of donor requirements is followed that contains counselling and evaluation of the blood donor before the blood donation. Demographic data and clinical history are recorded, and high-risk donors are deferred (if any). Physically, healthy-looking blood donors with normal hemoglobin (more than 13.5 g/dl for males and 12.5 g/dl for females) are recruited for blood donation. After blood collection and before transfusion, blood units are screened for TTIs.

1.2. Detection of HTLV 1/2 and Syphilis

Chemiluminescent Microparticle Immunoassay (CMIA) utilizing Abbott (n=1033) had no gender records. The distribution of nationality of all donors is summarized in Table 1.

The findings of this study showed that 11 blood donors' units (0.2%) were found to be

ARCHITECT I-2000 SR analyzer (Abbott laboratories, IL) was used for the initial screening of antibodies against HTLV 1/2, and *T. pallidum* (Syphilis). Initial positive samples were labelled as initially reactive (IR) and were run in duplicates during retesting.

1.3. Detection of Malaria

Malarial antigens (Pf/PAN) were detected using Care Start™ Malaria Pf/PAN (HRP2/pLDH) Ag Combo RDT rapid test (Access BIO, Somerset, NJ, USA) in the donor samples.

1.4. Ethical Consideration

The current study was ethically approved by the Jazan Health Ethics Committee, Ministry of Health, Saudi Arabia (No. 2034).

1.5. Statistical analysis

Donor data were entered into a Microsoft excel sheet; the collected data were analyzed and the frequencies were subsequently calculated using Microsoft Excel software.

2. Results

All blood samples obtained from blood donors were tested for anti-HTLV-I/II, syphilis, and malaria in Saudi Arabia, as per national guidelines. Data of 4, 977 blood donors who donated blood in Samtah General Hospital during 2019 and 2020 were evaluated. Among the 4,977 blood donors, the gender of 79.24% (n = 3,944) of the participants was recorded (99.3% males and 0.7% females), whereas 20.76%

reactive for HTLV 1/2. (Table 2). A review of data for syphilis showed that reactive blood units were 8

representing 0.16% (Table 2). In addition, 0.04% (n=2)

of the blood donors had positive malaria tests (Table 2).

Table 1: Distribution of blood donors according to nationality.

Nationality	Number of donors	Percentage
Saudi	2,770	55.66
Yemeni	841	16.89
Egypt	89	1.78
Pakistani	75	1.50
Indian	55	1.10
Sudani	49	0.98
Bangladeshi	25	0.50
Syrian	13	0.26
Philippine	10	0.20
Afghani	7	0.14
Moroccan	6	0.12
Ethiopian	1	0.02
Jordanian	1	0.02
Sir Lanka	1	0.02
Turkey	1	0.02
Not mentioned	1033	20.75
Total	4977	100

Table 2: Frequencies of HTLV, syphilis, and malaria among the study participants.

Blood units	HTLV I & II	Syphilis	Malaria	
			Count	Percentage
Negative	4935 (99.2%)	4938 (99.22%)	4944	99.34%
Positive	11 (0.2%)	8 (0.16%)	2	0.04%
Discarded	31 (0.6%)			

Table 3. The reported prevalence of HTLV, malaria, and syphilis in different cities/ regions of Saudi Arabia.

City/Region	Study period	Sample size (n)	HTLV (%)	MP (%)	Syphilis (%)	Reference
Riyadh	2017–2019	114,638	0.002	NR	NR	(Al-Hababi et al., 2020)
Buraidah / Qassim	2017–2018	4590	0.0	NR	0.043	(Alabdulmonem et al., 2020)
Riyadh	2016–2018	38,621	0.002	NR	0.02	(F, 2020)
Majmaah	2015–2017	3028	0.20	00	0.53	(Alaidarous et al., 2018)
Riyadh	2006 – 2015	239,330	NR	NR	0.025	(Elyamany G, Al Amro M, Pereira WC, 2016)
Hail	2014–2015	361	2.2	NR	4.7	(Sarah et al., 2016)
Hail	2013–2015	11,162	0.07	0.02	0.2	(Alcantara et al., 2018)
Aseer	2012 – 2103	7, 267	00	NR	0.028	(Kilany et al., 2015)
Jazan	2004–2009	29,949	NR	NR	NR	(Abdullah, 2013)
Al-Hofuf, Al-Hasa	1997–2003	47,426	0.06	NR	NR	(Ul-Hassan Z, Al-Bahrani AT, 2004)
Riyadh	2000 –2002	24173	0	NR	NR	(El-Hazmi, 2004)
Al-Khobar	1995–2001	23,493	0.2	NR	NR	(Taha et al., 2003)

NR; not reported

3. Discussion

Transfusion of blood is one of the major routes of transmission of HTLV 1/2. Hence, the screening of blood units for HTLV 1/2 is made mandatory in many countries, including Saudi Arabia. Prevalence of HTLV 1/2 reported in Saudi Arabia ranges from 0% to 2.2% in different studies (Alcantara et al., 2018; F, 2020; Ul-Hassan Z, Al-Bahrani AT, 2004) as shown in Table 3. A total of 11 (0.2%) blood donors' units were reactive for HTLV1/2 during the study period. The findings of this study showed a similar frequency of HTLV 1/2 in Samtah in comparison to Majmaah and Al-Khobar, while it was lower than Hail as shown in Table 3 (Alaidarous et al., 2018; Sarah et al., 2016; Taha et al., 2003). Furthermore, HTLV 1/2 was less prevalent in Riyadh, Hail, and Al-Hasa as compared to the current study as shown in Table 4 (Alcantara et al., 2018; F, 2020; Ul-Hassan Z, Al-Bahrani AT, 2004).

Notably, studies have shown zero prevalence of HTLV 1/2 in Riyadh, Asir, and Qasim (Alabdulmonem et al., 2020; El-Hazmi, 2004b; Kilany et al., 2015b). Furthermore, the two studies conducted in Riyadh with a difference of a decade did not show any increase in the prevalence of HTLV1/2, proving it to be an uncommon infectious agent in the country. Another study recently conducted, showed that among more than 100,000 blood donors, initially, 95 (0.088%) blood units were positive for HTLV antibodies when tested; however, none of these donors were positive when tested for HTLV by the western blot (Hindawi et al., 2018). Based on the findings of the current study as well as previous

studies, it is a well-established fact that HTLV 1/2 are non-endemic in Saudi Arabia. The limited threat of the HTLV1/2 to the safety of blood and blood product questions the of the testing cost of blood units. Strategies should be adopted to screen the blood donors who are at high risk. It has also been suggested that either HTLV 1/2 testing could be carried out on pooled samples or could be only conducted for expatriate donors, who are more infected by HTLV (Arif & Ramia, 1998; Kawashti et al., 2005). The practice of testing the pooled samples (pooling 48 samples) by enzyme immunoassay has been implemented in England which makes this method very cost-effective. Alternatively, the transfusion of leuko-reduced blood units shall be made mandatory to reduce the risk of HTLV 1/2. Keeping in view the high costs of the screening better strategies are needed to screen or exclude the HTLV 1/2 from the screening blood donation process.

A surveillance study, published in 2006, has shown the prevalence of syphilis to be 8.7% of the reported cases of sexually transmitted infections in Saudi Arabia. A study by Madani revealed the prevalence of syphilis to be 0.16% among the blood donor screened over the study period (Madani, 2006). Some other studies, conducted in Saudi Arabia, showed a variable frequency of syphilis among blood donors i.e. Hail 0.2% (Alcantara et al., 2018), Buraidah 0.043% (Alabdulmonem et al., 2020), Riyadh 0.025% (Elyamany et al., 2016). As compared to the findings of the current study, the prevalence of syphilis was found to be higher (0.53%) in Majmaah (Alaidarous et al., 2018). Both the current

and previous studies indicated the low prevalence of syphilis in Saudi Arabia. However, a study conducted in Hail by Sarah et al. (2016) reported a high prevalence of syphilis (4.7%) despite their low study sample size (361 blood donors; Table 4). It is noteworthy here to mention that the majority (55.656%) of blood donors were Saudis. Only one of these cases was found to be positive conveying a message of low prevalence in the Saudi population. Secondly, both donors were male. Studies have shown the high prevalence of syphilis in males. (Kilany et al., 2015).

The findings of this study showed only two (0.04%) positive cases of malaria. The donors who found positive were Saudis, thereby revealing the indigenous nature of the case. Alcantara et al (2018) finding is in the agreement with the observations of our study (Alcantara et al., 2018). While a report published by Alaidarous et al., 2018 did not find any case of malaria in their studied population.

It is concluded that HTLV, syphilis, and malaria are rarely detected among blood donors in Jazan region. Although rare their lethality is beyond description. Hence, strategies shall be sorted out to minimize the cost of screening for these infections without compromising the safety of blood and its components.

References

- Abdo, A. A., Sanai, F. M., & Al-Faleh, F. Z. (2012). Epidemiology of viral hepatitis in Saudi Arabia: Are we off the hook. *Saudi Journal of Gastroenterology*, 18(6), 349–357. <https://doi.org/10.4103/1319-3767.103425>
- Abdullah, S. M. (2013). Prevalence of hepatitis B and C in donated blood from the Jazan region of Saudi Arabia. *Malaysian Journal of Medical Sciences*, 20(2), 42–47.
- Alabdulmonem, W., Shariq, A., Alqossayir, F., AbaAlkhalil, F. M., Al-Musallam, A. Y., Alzaaqui, F. O., Aloqla, A. A., Alodhaylah, S. A., Alsugayyir, A. H., Aldoubiab, R. K., Alsamaany, A. N., Alhammad, S. H., & Rasheed, Z. (2020). Sero-prevalence ABO and Rh blood groups and their associated Transfusion-Transmissible Infections among Blood Donors in the Central Region of Saudi Arabia. *Journal of Infection and Public Health*. <https://doi.org/10.1016/j.jiph.2019.12.004>
- Alaidarous, M., Choudhary, R. K., Waly, M. I., Mir, S., Bin Dukhyil, A., Banawas, S. S., & Alshehri, B. M. (2018). The prevalence of transfusion-transmitted infections and nucleic acid testing among blood donors in Majmaah, Saudi Arabia. *Journal of Infection and Public Health*, 11(5), 702–706. <https://doi.org/10.1016/j.jiph.2018.04.008>
- Alcantara, J. C., Alenezi, F. K. M., & Haj Ali, O. H. (2018). Seroprevalence and trends of markers of transfusion transmissible infections among blood donors: a 3-year hospital based-study. *International Journal Of Community Medicine And Public Health*, 5(12), 5031. <https://doi.org/10.18203/2394-6040.ijcmph20184773>
- Al-Hababi, F., Al-Deailej, I., Al-Sulatan, H., Al-Ghamdi, Y., & Al-Dossari, K. (2020). Human T lymphotropic virus antibodies seroprevalence among healthy blood donors and high risk groups at Riyadh regional laboratory in Riyadh, Saudi Arabia. *Saudi Critical Care Journal*, 4(2), 73. https://doi.org/10.4103/sccj.sccj_13_20

- Alzahrani, F. M., Muzaaheed, Shaikh, S. S., Alomar, A. I., Acharya, S., & Elhadi, N. (2018). Prevalence of Hepatitis B Virus (HBV) among blood donors in eastern Saudi Arabia: Results from a five-year retrospective study of HBV seromarkers. *Annals of Laboratory Medicine*, 39(1), 81–85. <https://doi.org/10.3343/alm.2019.39.1.81>
- Amer, O. S. O., Waly, M. I., Burhan, I. W., Al-Malki, E. S., Smida, A., & Al-Benasy, K. S. (2020). Epidemiological trends of malaria in the Western regions of Saudi Arabia: A cross sectional study. *Journal of Infection in Developing Countries*, 14(11), 1332–1337. <https://doi.org/10.3855/jidc.13246>
- Andreu, G., Morel, P., Forestier, F., Debeir, J., Rebibo, D., Janvier, G., & Hervé, P. (2002). Hemovigilance network in France: Organization and analysis of immediate transfusion incident reports from 1994 to 1998. *Transfusion*, 42(10), 1356–1364. <https://doi.org/10.1046/j.1537-2995.2002.00202.x>
- Arif, M., & Ramia, S. (1998). Seroprevalence of human T-lymphotropic virus type I (HTLV-I) in Saudi Arabia. *Annals of Tropical Medicine & Parasitology*, 92(3), 305–309. <https://doi.org/10.1080/00034983.1998.11813294>
- Bamaga, M. S., Azahar, E. I., Al-Ghamdi, A. K., Alenzi, F. Q., & Farahat, F. M. (2009). Nucleic acid amplification technology for hepatitis B virus, and its role in blood donation screening in blood banks.[Erratum appears in Saudi Med J. 2009 Dec;30(12):1616 Note: Al-Enzi, Faris Q [corrected to Alenzi, Faris Q]]. *Saudi Medical Journal*, 30(11), 1416–1421.
- Bashawri, L. A. M., Fawaz, N. A., Ahmad, M. S., Qadi, A. A., & Almawi, W. Y. (2004). Prevalence of seromarkers of HBV and HCV among blood donors in eastern Saudi Arabia, 1998-2001. *Clinical and Laboratory Haematology*, 26(3), 225–228. <https://doi.org/10.1111/j.1365-2257.2004.00601.x>
- Bihl, F., Castelli, D., Marincola, F., Dodd, R. Y., & Brander, C. (2007). Transfusion-transmitted infections. *Journal of Translational Medicine*, 5(Table 1), 1–11. <https://doi.org/10.1186/1479-5876-5-25>
- Busch, M. P., Bloch, E. M., & Kleinman, S. (2019). Prevention of transfusion-transmitted infections. *Blood*, 133(17), 1854–1864. <https://doi.org/10.1182/blood-2018-11-833996>
- Caskey, M. F., Morgan, D. J., Porto, A. F., Giozza, S. P., Muniz, A. L., Orge, G. O., Travassos, M. J., Barrón, Y., Carvalho, E. M., & Glesby, M. J. (2007). Clinical manifestations associated with HTLV type I infection: A cross-sectional study. *AIDS Research and Human Retroviruses*, 23(3). <https://doi.org/10.1089/aid.2006.0140>
- D, H. (2019). Modern Blood Banking & Transfusion Practices. In *F.A. Davis* (Vol. 7).
- Edmondson, D. G., Hu, B., & Norris, S. J. (2018). Long-term in vitro culture of the syphilis spirochete *treponema pallidum* subsp. *Pallidum*. *MBio*, 9(3). <https://doi.org/10.1128/mBio.01153-18>
- Elbjeirami, W. M., Arsheed, N. M., Al-Jedani, H. M., Elnagdy, N., Abou Eisha, H. M., Abdulwahab, A., Abdulateef, N. A., Hezam, E., Al-Allaf, F. A., & Elbjeirami, W. (2015). Prevalence and Trends of HBV, HCV, and HIV Serological and NAT Markers and Profiles in Saudi Blood Donors. *J Blood*

- Disord Transfus*, 6, 3. <https://doi.org/10.4172/2155-9864.1000280>
- El-Hazmi, M. M. (2004). Prevalence of HBV, HCV, HIV-1, 2 and HTLV-I/II infections among blood donors in a teaching hospital in the Central region of Saudi Arabia. In *undefined*.
- Elyamany G, Al Amro M, Pereira WC, A. O. (2016). Prevalence of syphilis among blood and stem cell donors in Saudi Arabia: An institutional experience. *Electronic Physician*, 8(8), 2747–2751.
- F, A. M. (2020). Prevalence of Transfusion-Transmissible Infections among Blood Donors in Riyadh: A Tertiary Care Hospital- Based Experience. *Journal of Nature and Science of Medicine*, 3, 247–251. <https://doi.org/10.4103/JNSM.JNSM>
- Fageeh, W. M. (2010). Should We Screen for HIV in Saudi Arabia? *JKAU: Med. Sci*, 17(3), 45–54. <https://doi.org/10.4197/Med>
- Fong, I. W., & Fong, I. W. (2020). Blood Transfusion-Associated Infections in the Twenty-First Century: New Challenges. In *Current Trends and Concerns in Infectious Diseases* (pp. 191–215). Springer International Publishing. https://doi.org/10.1007/978-3-030-36966-8_8
- Gessain, A., Cassar, O., Grossi, P., & Taylor, G. (2015). Geographical distribution of areas with a high prevalence of HTLV-1 infection. In *European Centre for Disease Prevention and Control*.
- Hicks, C., & Clement, M. (2016). Syphilis: Epidemiology, pathophysiology, and clinical manifestations in HIV-uninfected patients. *UpToDate*.
- Hindawi, S., Badawi, M., Fouda, F., Mallah, B., Mallah, B., Rajab, H., & Madani, T. A. (2018). Testing for HTLV 1 and HTLV 2 among blood donors in Western Saudi Arabia: prevalence and cost considerations. *Transfusion Medicine (Oxford, England)*, 28(1), 60–64. <https://doi.org/10.1111/tme.12440>
- Kawashti, M. I. S., Hindawi, S. I., Damanhour, G. A., Rowehey, N. G., Bawazeer, M. M., & Alshawa, M. (2005). Serological screening of human T cell lymphotropic virus I and II (HTLV I/II) in blood banks by immunoblotting and enzyme-immunoassays: to demand or to defeat? *The Egyptian Journal of Immunology*, 12(2), 137–142.
- Kilany, M., Bin Dajem, S. M., Ibrahim, Y. M., Alshehri, A., Aljamelani, A. A., & Ibrahim, E. H. (2015). Seroprevalence of anti-Treponemapallidum antibodies (Syphilis) in blood donors in the southern area of Saudi Arabia. *Research Journal of Pharmaceutical, Biological and Chemical Sciences*, 6(1), 549–556.
- Kitchen, A. D., & Chiodini, P. L. (2006). Malaria and blood transfusion. In *Vox Sanguinis* (Vol. 90, Issue 2). <https://doi.org/10.1111/j.1423-0410.2006.00733.x>
- Larison, J., & Gilman, J. G. (1983). Modern blood banking and transfusion practices. In *Hemoglobin* (Vol. 7, Issue 6). <https://doi.org/10.3109/03630268309027947>
- Madani, T. A. (2006). Sexually transmitted infections in Saudi Arabia. *BMC Infectious Diseases*, 6(3), 1–6. <https://doi.org/10.1186/1471-2334-6-3>
- Madkhali, A. M., Ghzwani, A. H., & Al-Mekhlafi, H. M. (2022). Comparison of Rapid Diagnostic Test, Microscopy, and Polymerase Chain Reaction for the

- Detection of Plasmodium falciparum Malaria in a Low-Transmission Area, Jazan Region, Southwestern Saudi Arabia. *Diagnostics*, 12(6). <https://doi.org/10.3390/diagnostics12061485>
- Morsi, H. A. (2011). *Routine Use of Mini-Pool Nucleic Acid Testing (MP-NAT) Multiplex Assay for Sero-Negative Blood Donors*. J. Egypt. Soc. of Haemat & Res.
- Mozhgani, S. H., Zarei-Ghobadi, M., Teymoori-Rad, M., Mokhtari-Azad, T., Mirzaie, M., Sheikhi, M., Jazayeri, S. M., Shahbahrami, R., Ghourchian, H., Jafari, M., Rezaee, S. A., & Norouzi, M. (2018). Human T-lymphotropic virus 1 (HTLV-1) pathogenesis: A systems virology study. *Journal of Cellular Biochemistry*, 119(5). <https://doi.org/10.1002/jcb.26546>
- Nozuma, S., & Jacobson, S. (2019). Neuroimmunology of human T-lymphotropic virus type 1-associated myelopathy/tropical spastic paraparesis. *Frontiers in Microbiology*, 10(APR), 1–11. <https://doi.org/10.3389/fmicb.2019.00885>
- Nozuma, S., Kubota, R., & Jacobson, S. (2020). Human T-lymphotropic virus type 1 (HTLV-1) and cellular immune response in HTLV-1-associated myelopathy/tropical spastic paraparesis. In *Journal of NeuroVirology* (Vol. 26, Issue 5, pp. 1–11). <https://doi.org/10.1007/s13365-020-00881-w>
- Sarah, Y. A. E. G. A., Sabry, A. E. G. A. E. H. E. S., & Maryam, A. A. S. (2016). Seropositivity of TTIs among blood donors in Hail, Saudi Arabia, from 2014 to 2015. *Asian Pacific Journal of Tropical Disease*, 6(2), 141–146. [https://doi.org/10.1016/S2222-1808\(15\)61000-3](https://doi.org/10.1016/S2222-1808(15)61000-3)
- Shobokshi, O. A., Serebour, F. E., Al-Drees, A. Z., Mitwalli, A. H., Qahtani, A., & Skakni, L. I. (2003). Hepatitis C virus seroprevalence rate among Saudis. *Saudi Medical Journal*.
- Simon T, Snyder E, Solheim B, Stowell C, Strauss R, P. M. (2019). *Rossi's Principles of Transfusion Medicine* (Vol. 53, Issue 9). <https://doi.org/10.1017/CBO9781107415324.004>
- Stramer, S. L., & Dodd, R. Y. (2013). Transfusion-transmitted emerging infectious diseases: 30 years of challenges and progress. In *Transfusion* (Vol. 53, Issue 10 PART 2, pp. 2375–2383). Wiley-Blackwell. <https://doi.org/10.1111/trf.12371>
- Taha, M. A., Bashawri, L. A. M., Ahmed, M. S., & Ahmed, M. A. (2003). Prevalence of antibodies to human T-lymphotropic viruses types I and II among healthy blood donors. *Saudi Medical Journal*, 24(6), 637–640.
- Ul-Hassan Z, Al-Bahrani AT, P. B. (2004). Prevalence of human T-lymphotropic virus type I and type II antibody among blood donors in Eastern Saudi Arabia. *Saudi Medical Journal*, 25(10), 1419–1422.

انتشار الملاريا وفيروس تي اللفاوي البشري والزهري في المتبرعين بالدم من الأصحاء بمنطقة جازان بالمملكة العربية السعودية خلال الفترة ٢٠١٩-٢٠٢٠

أيمن محمد مدخلي

قسم تقنية المختبرات الطبية، كلية العلوم الطبية التطبيقية، جامعة جازان، المملكة العربية السعودية

الملخص

تعد الأمراض المنقولة عن طريق نقل الدم مصدر قلق كبير للصحة العامة. ويعد فحص الأمراض المنقولة عن طريق الدم للمتبرعين بالدم أمرًا بالغ الأهمية. وهدف هذه الدراسة توفير بيانات حول انتشار الملاريا وفيروس تي اللفاوي البشري والزهري من مستشفى صامطة العام بجازان في المملكة العربية السعودية. أجريت هذه الدراسة من خلال مراجعة سجلات التبرع بالدم في مستشفى صامطة العام، في الفترة من يناير ٢٠١٩ إلى أغسطس ٢٠٢٠. تم مراجعة سجلات بنك الدم وسجلات وحدة التبرع التي تحتوي على نتائج الملاريا، وفيروس تي اللفاوي البشري، والزهري فقط وعليه فقد تم تحليل سجلات ٤٩٧٧ متبرع بالدم. من بين ٤٩٧٧ متبرعًا بالدم، تم تأكيد إصابة ١١ متبرعًا فقط (٠,٢٪) من فيروس تي اللفاوي البشري. كما تم الكشف عن ثمانية متبرعين بالدم (٠,١٦٪) إيجابيين للزهري بينما تم رصد حالتين إيجابية للملاريا بنسبة (٠,٠٤٪، $n =$). وقد خلصت الدراسة إلى أن الملاريا وفيروس تي اللفاوي والزهري نادرًا ما توجد بين المتبرعين بالدم في هذا المجال. وعلى الرغم من ندرتها، إلا أن إصابات ذات خطورة عالية. وبالتالي، يجب ترتيب استراتيجيات لتقليل تكلفة فحص هذه العدوى دون المساس بسلامة الدم ومكوناته.

الكلمات المفتاحية: فيروس تي اللفاوي البشري، الزهري، الملاريا، الأمراض المنقولة عن طريق نقل الدم.

مجلة جامعة جازان

للعلوم التطبيقية

دورية علمية محكمة

المشرف العام

أ.د. مرعي بن حسين القحطاني

نائب المشرف العام

أ.د. محمد بن حسن أبو راسين

مدير إدارة المجلة

أ.عبدالرحمن بن حسن حوياتي

رئيس هيئة التحرير

أ.د. أحمد بن عبدالرحمن الحسين البراق

هيئة التحرير

أ.د. محمد بن علي خلوفة مباركي

أ.د. قاسم بن محمد عبدالله ابوظويل

د. محمد بن عبدالرحيم محمد عقيل

د. زكي بن ولي محمد حكمي

د. باسم بن إبراهيم علي عسيري

د. نواف بنت حسين محمد أبوهادي

الكادر الإداري

أ. أحمد بن محمد الحازمي

أ. علي بن محمد أحمد قبي

أ. بندر بن علي عبده واصلي

المراسلات

توجه جميع المراسلات إلى:

رئيس هيئة التحرير مجلة جامعة جازان للعلوم التطبيقية جازان - المدينة الجامعية - البرج الإداري - ص ب ١١٤ - الرمز البريدي ٤٥١٤
المملكة العربية السعودية أو على البريد الإلكتروني jas@jazanu.edu.sa

جامعة جازان (١٤٤٥)

جميع حقوق الطبع محفوظة . لا يسمح بإعادة طبع أي جزء من المجلة أو نسخه بأي شكل وبأي وسيلة سواء كانت إلكترونية أو آلية بما في ذلك التصوير والتسجيل أو الإدخال في أي نظام حفظ معلومات أو إستعادتها بدون الحصول على موافقة كتابة من رئيس تحرير المجلة .



المملكة العربية السعودية

وزارة التعليم

جامعة جازان

مجلة

جامعة جازان

للعلوم التطبيقية

دورية علمية محكمة

ملحق المجلد ١١ العدد ٢ (جماد الأول ١٤٤٥ هـ - نوفمبر ٢٠٢٣ م)

رمد : ٦٩١٣-١٦٥٨

- ٤- نقد الكتاب
٥- الخطابات الموجهة إلى المحرر، والملاحظات والردود،
والنتائج الأولية.

تقوم هيئة التحرير، بالنظر في نشر المواد المعرفية ذات الصلة بذلك الفرع، وتقدم البحوث الأصلية، التي لم يسبق نشرها، وفي حال قبول البحث للنشر تؤول كل حقوق النشر للمجلة و لا يجوز نشره في أي منفذ نشر آخر ورقيا أو إلكترونيا، دون إذن كتابي من رئيس هيئة التحرير .

مجلة جامعة جازان للعلوم التطبيقية دورية علمية محكمة تنشرها الجامعة، وهي تهدف إلى إتاحة الفرصة للباحثين لنشر إنتاجهم العلمي وتقوم المجلة بنشر المواد الآتية :

- ١- البحث : ويندرج تحت تخصص الباحث ويجب أن يحتوي على إضافة للمعرفة في مجاله .
٢- المقالة الاستعراضية التي تتضمن عرضاً نقدياً لبحوث سبق إجراؤها في مجال معين أو أجريت في خلال فترة زمنية محددة.
٣- البحث المختصر.

تعليمات النشر في المجلة

مثال : هادي، أحمد بن جابر. (٢٠١١م)، " استخدام تقنية النانو لتعريف الشفرات الوراثية "مجلة جامعة جازان، ١، ١ : ٢٠٠-٢٢٠.

ب- يشار إلى الكتب في المتن داخل قوسين بالاسم والتاريخ . أما في قائمة المراجع، فيكتب الاسم الأخير للمؤلف، ثم الاسم الأول، ثم الأسماء الأخرى أو اختصارا لها، ثم سنة النشر بين قوسين، فعنوان الكتاب بين علامتي تنصيص، ثم بيان الطبعة، فناشر، فمدينة النشر : ثم صفحات الكتاب إن وجدت.
مثال :

١- تقديم المواد : يقدم أصل البحث مخرجا في صورته النهائية متضمنا الإشارة إلى أماكن الجداول والأشكال داخل المتن و مطبوع على هيئة صفحات مرقمة ترقيما متسلسلا، مع ضرورة إرفاق قرص ممتط مطبوع عليه البحث على برنامج Ms Word باستخدام النظام المتوافق مع IBM ، وسيعتبر عن قبول أي بحث لا يلتزم مؤلفه بهذه التعليمات.

٢- الملخصات: يرفق ملخصان بالعربية والإنجليزية للبحوث و المقالات الاستعراضية والبحوث المختصرة على ألا يزيد عدد كلمات كل منهما على ٢٠٠ كلمة، وعلى عمود واحد بعرض كتابة ١٣ سم.

٣- لا بد من احتواء كل بحث على كلمات مفتاحية (Key Words)توضع أسفل الملخصين العربي والانجليزي على ألا تزيد عن عشر كلمات.

٤- الجداول والمواد التوضيحية: يجب أن تكون الجداول والرسومات واللوحات مناسبة لمساحة الصف في صفحة المجلة ١٦ ٢٤ سم بالحواشي، ويتم إعداد الأشكال الخطية على برامج الحاسب الآلي، ولا تقبل إلا أصول الأشكال. كما يجب أن تكون الخطوط واضحة ومحددة ومنتظمة من حيث كثافة الحبر وتناسب سمكها مع حجم الرسم، ويراعى أن تكون الصور الفوتوغرافية (الضوئية) الملونة وغير الملونة مطبوعة على ورق لماع، أو محملة على برنامج (Adobe Photoshop)مع كتابة عنوان لكل جدول، وتطبيق لكل شكل وصورة، والإشارة إلى مصدر المادة إن كانت مقتبسة.

٥- الاختصارات: يجب استخدام الاختصارات المقبنة دولية مثل : سم، م، كم، سم، مل، مجم، كجم...إلخ.

٦- المراجع :يشار إلى المراجع داخل المتن بنظام الاسم والتاريخ، وتوضع المراجع جميعها في قائمة المراجع بنهاية المادة مرقمة ومتباعدة نظام ترتيب البيانات البيولوجرافية التالي :

أ- يشار إلى الدوريات في المتن بنظام الاسم والتاريخ بين قوسين على مستوى السطر، أما في قائمة المراجع فيبدأ المرجع بنكر الاسم الأخير للمؤلف، ثم الاسم الأول، ثم الأسماء الأخرى أو اختصاراتها بالخط الأسود، ثم سنة النشر بين قوسين، فعنوان البحث كاملا بين علامتي تنصيص " " ، فاسم الدورية، فرقم المجلد، ثم رقم العدد : ثم أرقام الصفحات تفصل بشرطة .

عبدالهادي، محمد علي، (١٤٣٣هـ)، " مقدمة في التقية الحيوية"، جامعة جازان، جازان.

ويجب عدم استخدام الاختصارات المرجعية مثل :المرجع نفسه . المرجع السابق...إلخ.

٧- أ- الحواشي: تستخدم لتزويد القارئ بمعلومات توضيحية، ويشار إليها في المتن بأرقام مرتفعة عن السطر. وترقيم التعليقات متسلسلة داخل المتن. وفي حال الضرورة؛ يمكن الإشارة إلى مرجع داخل الحاشية عن طريق استخدام كتابة الاسم والتاريخ بين قوسين وبنفس طريقة استخدامها في المتن، وتوضع الحواشي أسفل الصفحة التي تخصها والتي ذكرت بها وتفصل بخط عن المتن وبخط أصغر.

ب- يستخدم في تخريج الأحاديث والآثار الطريقة المنهجية المعتمدة في هذا الفن وهي كالتالي : اسم المؤلف - اسم الكتاب - رقم الجزء والصفحة والحديث.

٨- المواد المنشورة في المجلة تعبر عن وجهة نظر صاحبها، ولا تعبر بالضرورة، عن رأي مجلة جامعة جازان.

٩- يتأكد الباحث من صحة اللفظ وسلامة لغة البحث، وخلوه من الأخطاء اللغوية والنحوية.

١٠- للمجلة الحق في تحديد أولويات نشر البحوث.

١١- المجلة غير ملزمة بإعادة البحوث التي تصل إليها سواء أحيزت للنشر أم لم تجز.

١٢- يتم إخضاع جميع البحوث المستلمة لفحص مبدئي، من قبل هيئة التحرير، لتقرير أهليتها للتحكيم، ويحق لها أن تعتنر عن قبول البحث دون إبداء الأسباب.

١٣- تصدر المجلة مرتين في العام.

المملكة العربية السعودية

وزارة التعليم

جامعة جازان



مجلة

جامعة جازان

للعلوم التطبيقية

جامعة جازان

دورية علمية محكمة

ملحق المجلد ١١ العدد ٢ (جماد الأول ١٤٤٥ هـ - نوفمبر ٢٠٢٣ م)

رمد: ١٦٥٨-٦٩١٣